UNIVERSITY OF CALIFORNIA,
IRVINE

# Non-receptors, Feedback, and Robust Signaling Gradients in Biological Tissue Patterning

DISSERTATION

submitted in partial satisfaction of the requirements
for the degree of

DOCTOR OF PHILOSOPHY

in Mathematics

by

Aghavni Simonyan

Dissertation Committee:
Professor Frederic Y. M. Wan, Chair
Professor Long Chen
Professor Qing Nie

2017

# DEDICATION

To my family, with special dedication to
the memory of my grandfather Harutyun Avetisyan

# TABLE OF CONTENTS

# LIST OF FIGURES

# ACKNOWLEDGMENTS

I would like to express my sincere gratitude to my advisor Professor Frederic Wan. Without his encouragement, patience, and constant guidance, this work would have never been complete.

I would also like to thank my committee members Professor Long Chen and Professor Qing Nie for their advising, support and encouragement.

Special thanks go to Professor Alessandra Pantano for introducing me to the Math Community Educational Outreach program and for hosting Women in Mathematics gatherings. I have enjoyed every single one of them.

I would like to thank my friends at UCI, especially Mary Lee and Ani Asatryan for all the help in the graduate program, Cynthia Sanchez for many stimulating discussions and for being the best officemate, for all the late night office pizza parties and more.

Last, but not least, I am extremely grateful to my family; my wonderful parents Rafik and Gohar for instilling the love for education in me, for always believing in me and encouraging to do my best in everything, for their unconditional love and support, my sister Varduhi and my brother Andranik for always helping me with everything and being my best friends for life, my husband Cesar for his constant encouragement, confidence in me, and always being by my side, my daughter Tsovinar and my son Harutyun for being my source of inspiration. You give a new meaning to my life.

# CURRICULUM VITAE

## Aghavni Simonyan

### EDUCATION

**Doctor of Philosophy in Mathematics** **2017**
University of California, Irvine *Irvine, California*

**Master of Science in Mathematics** **2012**
University of California, Irvine *Irvine, California*

**Bachelor of Science in Mathematics** **2009**
University of California, Los Angeles *Los Angeles, California*

# ABSTRACT OF THE DISSERTATION

Non-receptors, Feedback, and Robust Signaling Gradients in Biological Tissue Patterning

By

Aghavni Simonyan

Doctor of Philosophy in Mathematics

University of California, Irvine, 2017

Professor Frederic Y. M. Wan, Chair

The present dissertation is concerned with robust signaling gradients in biological tissue patterning. The patterning of many developing tissues is orchestrated by gradients of morphogens through a variety of elaborate regulatory interactions. Such interactions are thought to make gradients robust, that is, resistant to changes induced by genetic or environmental perturbations. A variety of inhibitors for reducing ectopic signaling activities are known to exist and their specific role in down-regulating the undesirable ectopic activities reasonably well established. However, how a developing organism manages to adjust inhibition/stimulation in response to genetic and/or environmental changes is still not understood. The need to adjust for ectopic signaling activities requires the presence of one or more feedback mechanisms to stimulate the needed adjustment.

Recently extensive numerical simulations suggest that robustness of the signaling gradient cannot be attained by negative feedback (of the Hill's function type) on signaling receptors; magnitude reduction of signaling gradients achieved through adequate non-signaling receptors mediated degradation is accompanied by gradient shape distortion rendering development non-robust; adequate nonreceptor-mediated degradation and commensurate negative feedback on receptor synthesis lead to robustness, but with robustness sensitive to additional up- or down-regulations of non-receptors.

Since the ultimate effect of many inhibitors (including those of the non-receptor type) is generally to reduce the availability of signaling morphogens for binding with signaling receptors, we begin our examination of possible mechanisms for achieving robust development by investigating a spatially uniform negative feedback on signaling morphogen synthesis rate. Our findings on the effectiveness of such feedback adjustments as well as similar feedback mechanisms on receptor and non-receptor syntheses both in steady state and during transient development will be discussed to provide a simpler theoretical explanation of the results from numerical simulations.

# Chapter 1

# Introduction

At the beginning (in the early stages of embryonic development), all the cells of a biological organism have the same potential. However, those cells have to become what is the final shape and pattern. Morphogen gradients are responsible for cell differentiation and hence pattern formation. Morphogens or ligands are proteins that are synthesized and transported away from their sources to bind to relevant cell (signaling) receptors at different locations to form a spatial gradient of signaling morphogen-receptor complexes (or a *signaling gradient* for brevity). Such signaling gradients convey positional information for cells to adopt differential fates to result in tissue patterning. This process of cell differentiation is well established in developmental biology. For example, the morphogen *Decapentaplegic* (Dpp) which is a member of the BMP gene family is one of the key morphogens required for Drosophila's (fruit fly) wing patterning. Dpp is involved in the development of the Drosophila wing imaginal disc and is synthesized in a narrow region of about two-cell width at the boundary between the anterior and posterior compartments of the disc. Dpp molecules produced are transported away from the localized source and degrade upon reaching the edge of the disc. As they are transported downstream toward the wing imaginal disc edge, some of the Dpp molecules bind reversibly with the cell-surface signaling receptor *Thickvein* (Tkv) to form

a spatial gradient of signaling morphogen concentration over the span of the wing imaginal disc. Graded differences in receptor occupancy at different locations underlie the signaling differences that ultimately lead cells down different paths of development [10, 13, 39, 47]. Simple models of this simple process of gradient formation have been shown to produce a unique signaling gradient that is monotone and stable with respect to small perturbations (see [22, 23] for example).

For normal biological development, it is important that signaling morphogen gradients not be easily altered by genetic or epigenetic (such as environmental) fluctuations that affect the constitution of the biological organism. For example, experimental results (carried out by S. Zhou in A.D. Lander's lab (see also [47]) show that Dpp synthesis rate doubles when the ambient temperature is increased by $6°C$. With such an increase in Dpp synthesis rate, the simple models developed in [22, 23, 24] would predict an enhanced (or, more commonly, "ectopic") signaling gradient quantitatively and qualitatively different from that for the lower ambient temperature. However, the development of the wing imaginal disc generally does not change significantly with temperature changes of such magnitude. The insensitivity of system output to sustained alterations in input or system characteristics so necessary for normal development is often termed *robustness* of biological development. How this robustness requirement is met has been the subject of a number of recent studies.

An attempt to determine mechanisms for attaining robust development (after the self-enhanced ligand degradation proposed in [8]) was to consider a negative feedback on receptor synthesis rate in [26]. A Hill function type negative feedback was incorporated into the basic morphogen gradient model of [23] to reduce the synthesis rate of Tkv by an amount that depends on the ectopic signaling morphogen concentration at the spatial location. It was found that robustness (as measured by an "induced relative error $E$" defined in [26]) was not achieved for any of the $10^6$ combinations of system parameter values in a parameter space of 6-dimensions. A subsequent theoretical analysis delineated and confirmed theoretically

the ineffectiveness of this negative feedback mechanism [17]. Briefly, a Hill type of negative feedback reduces the receptor synthesis rate nonuniformly, disproportionately more so at locations of high signaling morphogen concentration. Such reduction generally leads to a modified gradient of different slope and convexity from the original gradient. The theoretical results suggest that a spatially uniform negative feedback responding to some overall measure of ectopicity (such as the average impact of the local changes on the system) may be more effective [17]. This suggestion has led to the initiation of a new general approach to attain robustness by way of a feedback mechanism that is spatially uniform.

Thus in Chapter 2, we initiate a proof-of-concept investigation of a spatially uniform feedback mechanism. With a view that most feedback mechanisms have the ultimate effect of reducing the morphogen available for binding with signaling receptors, a proof-of-concept prototype model for a spatially uniform negative feedback on morphogen synthesis rate is investigated. The findings of this preliminary effort can also be found in [19].

Then in Chapter 3, we complement the implementation of this new spatially uniform feedback mechanism in the steady state with feedback adjustments occurring in the transient phase of biological development. The findings on Chapter 3 investigation can also be found in [37].

In Chapter 4, we study a set of models that are the counterparts of those investigated in [26] but now with our new feedback instrument instead of the Hill function type previously employed. One significant feature of our approach is that the new models may be analyzed theoretically so that our results are mathematically conclusive. Our new model with its spatially uniform negative feedback on receptor synthesis rate leads to modified ectopic signaling gradient that is generally similar in shape as the wild-type gradient and any change in gradient slope and convexity does not cause as severe a distortion of the signaling gradient as a Hill function type feedback. However, the new negative feedback on receptor synthesis rate generally does not reduce the unacceptable ectopic signaling gradient magnitude resulting from the enhanced morphogen synthesis rate. The new spatially uniform negative feedback

approach has the advantage of allowing us to see explicitly the reason for the ineffectiveness of a feedback on receptor syntheis rate in addition to reinforcing a similar finding in [26] with a theoretical underpin that does not involve the kind of sophisticate mathematical analyses of [28, 29, 31].

To seek a more effective feedback mechanism to achieve robustness, it was noted that signaling gradients are known to be affected by other existing molecular/protein activities. Signaling ligands such as Dpp regularly bind with other kinds of molecular entities to form molecular complexes that do not signal for cell differentiation [4]. Such non-signaling entities are known to exist for Dpp and other BMP family ligands; they include Nog (noggin) [30, 45, 48], Chd (chordin) [35, 46], Dally (*division abnormally delayed*) [18, 1], FST (*follistatin (FST)* [3, 15, 44, 33], Sog (*short gastrulation*) [5, 31], and various heparan sulfate proteoglycans. Collectively, they are called *nonreceptors* since they bind with morphogens but the resulting complexes have no role in cell differentiation. As such, the presence of non-receptors reduces the amount of morphogens available for binding with signaling receptors and thereby down-regulates the signaling gradients. Effects of nonreceptors was first modeled and analyzed in [25] where the simple wing disc morphogen model of [22, 23] was extended to include the possibility of morphogens binding with a fixed concentration of cell-surface nonreceptor. This simplest model offered the first theoretical glimpse into the inhibiting effects of nonreceptors on the formation and properties of steady state signaling gradients.

Subsequently, large scale computational studies of non-receptors synthesized at a prescribed rate to absorb excessive Dpp concentration was carried out concurrently in [26]. Extensive numerical simulations there showed that robustness can be achieved in some region of the 6-dimensional parameter space but most of the corresponding gradients are not biologically realistic for cell differentiation for reasons such as high receptor occupancy due to a very low receptor synthesis rate. The simulation results were validated theoretically in [28] (see also

[42]). Adding a negative feedback (of the Hill function type) on receptor synthesis rate to an adequate concentration of nonreceptors was found in [26] to enhance the range of robust gradients that are biologically useful. On the other hand, the addition of (a positive Hill's function type) feedback on nonreceptor synthesis rate was found by numerical simulations to actually work against robustness.

Given the findings of [26, 25, 28, 29, 31] on non-receptors (with and without Hill function type feedback) as an instrument for promoting signaling gradient robustness, we undertake a similar investigation of nonreceptors with feedback but now of the spatially uniform type investigated in Chapter 2 and Chapter 3 to show the efficacy of our new approach.

Finally, our findings are summarized and other feedback mechanisms are proposed in the last chapter.

# Chapter 2

# Feedback for Robust Signaling Gradients: A Novel Approach

## 2.1 Introduction

In this chapter, we initiate a different approach to the role of feedback in ensuring robust signaling gradients. Our goal is to investigate the effectiveness of feedback mechanisms other than a negative feedback of the Hill's function type. Since the ultimate effect of many inhibitors is generally to reduce the availability of signaling morphogens for binding with signaling receptors, as a first step, we begin our examination of possible mechanisms for achieving robust development by investigating a spatially uniform negative feedback (distinctly different from the conventional spatially nonuniform Hill function approach) on signaling morphogen synthesis rate. Drosophila is one of the best researched insects in the world, and extensive biological data is available for the processes in its imaginal wing disc. Thus, we focus on *Dpp* gradients in Drosophila wing imaginal disc as our model. Our findings

and discussions, with some modifications, can be generalized and applied to other morphogen systems.

## 2.2 A Model of Drosophila Wing Imaginal Disc

We concentrate our investigation on *Dpp* gradients. Only the extracellular space of the posterior compartment of a Drosophila wing imaginal disc will be regarded. We can do so since it has been shown in [24] that the inclusion of transcytosis leads only to a re-interpretation of the system parameters in the steady state results. Also, we may simplify the morphogen activities in the wing imaginal disc as a one-dimensional reaction-diffusion problem in which morphogen is introduced at the rate $V_L$ locally adjacent (and symmetric with respect) to the border, $X = -X_m$, between the *anterior* and *posterior* compartments of the disc, and absorbed at the other end, $X = X_{\max}$, the edge of the posterior compartment. We take the biological development to be uniform in the direction along the compartment border (except possibly for a layer phenomenon at each end of the compartment) to reflect the fact that the ligand synthesis rate is taken to be uniform in that direction.

### 2.2.1 A Basic Extracellular Model

In the one-dimensional reaction-diffusion model, let $[L(X,T)]$ be the concentration of a diffusing ligand (such as *Dpp*) at time $T$ and distance $X$ toward wing disc edge normal to the compartment boundary with the localized source spanning $-X_m < X < 0$. As in [22], we take the diffusion of the ligand to be governed by $\partial[L]/\partial T = D\partial^2[L]/\partial X^2$, $D$ being the constant diffusion coefficient. We add to this reversible binding and degradation of ligands and receptors as well as degradation of ligand-receptor complexes with the binding rate $k_{on}[L][R]$, dissociation rate $k_{off}[LR]$, degradation rate $k_{\deg}[LR]$ for the bound ligands along

with the degradation rates for the free ligands and receptors $k_L[L]$ and $k_R[R]$, respectively. In these expressions, $[R]$ is the concentration of signaling receptors (e.g., *Tkv* for *Dpp*) synthesized at the spatially distributed rate of $V_R(X,T)$, and $[LR]$ is the concentration of ligand-receptor (*Dpp-Tkv*) complexes. The parameters $k_{on},\ k_R,\ k_L,\ k_{\deg}$ and $k_{off}$ are the the various binding, degradation and dissociation rate constants which may not be known (or constant) due to possible feedback phenomena. Except for $k_{on}$, all the other rate constants are in units of $1/\sec.$ while the "binding rate constant" $k_{on}$ is in units of $1/\sec./mole$.

There is no endocytosis prior to degradation in this formulation. The omission of receptor internalization results in no loss of generality for the purpose of our investigation; it has already been established in [24] that the boundary value problem (BVP) governing the steady state behavior of a more general system with transcytosis can be reduced to the same BVP for our simpler system.

Thus, we have the following nonlinear reaction-diffusion model governing the evolution of the three unknown concentrations $[L],\ [R]$ and $[LR]$ which generally vary in space and time:

$$\frac{\partial[L]}{\partial T} = D\frac{\partial^2[L]}{\partial X^2} - k_{on}[L][R] + k_{off}[LR] - k_L[L] + V_L \tag{2.1}$$

$$\frac{\partial[LR]}{\partial T} = k_{on}[L][R] - (k_{off} + k_{\deg})[LR], \tag{2.2}$$

$$\frac{\partial[R]}{\partial T} = -k_{on}[L][R] + k_{off}[LR] - k_R[R] + V_R, \tag{2.3}$$

where $V_L(X,T)$ is the localized morphogen synthesis rate (centered at and) spanning symmetrically with respect to the border $X = -X_{\min}$ between the two wing disc compartments. Below is a typical form of such synthesis rate relevant to our investigation:

$$V_L(X,T) = \bar{V}_L H(-X) = \begin{cases} \bar{V}_L & (-X_m < X < 0) \\ 0 & (0 < X < X_{\max}) \end{cases} \tag{2.4}$$

The receptor synthesis rate is typically taken to be uniform in space and time with $V_R(X,T) = \bar{V}_R > 0$ for $-X_{\min} < X < X_{\max}$ and all $T > 0$.

With the early stage of the anterior compartment and posterior compartment developing more or less similarly, we consider here only the ligand activities in the posterior compartment for which we have the following idealized boundary conditions:

$$X = -X_{\min}: \qquad \frac{\partial [L]}{\partial X} = 0, \qquad X = X_{\max}: \qquad [L] = 0, \tag{2.5}$$

for all $T > 0$, where the no flux condition at the compartment border being a consequence of symmetry, and the kill end condition at the distal edge, $X = X_{\max}$, of the compartment reflects the assumption of an absorbing edge.

Until morphogens being generated starting at $T = 0$, ligand activities are expected to be in quiescence so that we have as initial conditions

$$T = 0: \qquad [L] = [LR] = 0, \qquad [R] = R_0 \tag{2.6}$$

for $-X_m \leq X \leq X_{\max}$. For the case of a uniform receptor synthesis rate, we have from (2.2)

$$R_0 = \frac{\bar{V}_R}{k_R}. \tag{2.7}$$

by steady state consideration prior to the onset of morphogen synthesis. With $k_L = 0$, the initial-boundary value problem (IBVP) defined by (2.1)-(2.6) corresponds to the model investigated in [23].

### 2.2.2 Dimensionless Form

To non-dimensionalize the system, we introduce the normalized quantities

$$t = \frac{D}{X_0^2}T, \qquad x = \frac{X}{X_0}, \qquad \ell_M = \frac{X_{\max}}{X_0}, \quad x_m = \frac{X_{\min}}{X_0} \tag{2.8}$$

$$\{a, b, r\} = \frac{1}{R_0}\{[L], [LR], [R]\}, \tag{2.9}$$

$$\{f_0, g_0, h_0, g_R, g_L\} = \frac{X_0^2}{D}\{k_{off}, k_{deg}, k_{on}R_0, k_R, k_L\}, \tag{2.10}$$

$$\{v_L(x,t), v_R(x,t)\} = \frac{X_0^2}{D}\left\{\frac{V_L}{R_0}, \frac{V_R}{R_0}\right\}, \qquad \{\bar{v}_L, \bar{v}_R\} = \frac{X_0^2}{D}\left\{\frac{\bar{V}_L}{R_0}, \frac{\bar{V}_R}{R_0}\right\} \tag{2.11}$$

where $X_0$ is some typical scale length, taken to be $X_{\max}$ for the finite domain case so that $\ell_M = X_{\max}/X_0 = 1$. With these normalized quantities, we rewrite the IBVP for the three unknowns $[L]$, $[LR]$ and $[R]$ in the following normalized form

$$\frac{\partial a}{\partial t} = \frac{\partial^2 a}{\partial x^2} - h_0 ar + f_0 b - g_L a + v_L(x,t), \tag{2.12}$$

$$\frac{\partial b}{\partial t} = h_0 ar - (f_0 + g_0)b, \qquad \frac{\partial r}{\partial t} = v_R(x,t) - h_0 ar + f_0 b - g_R r, \tag{2.13}$$

with the boundary conditions

$$x = -x_m: \quad \frac{\partial a}{\partial x} = 0, \qquad x = \ell_M: \quad a = 0, \tag{2.14}$$

all for $t > 0$, and the initial conditions

$$t = 0 : \qquad a = b = 0, \qquad r = 1. \tag{2.15}$$

### 2.2.3 Time Independent Steady State Behavior

**Reduction to a Well-Posed Boundary Value Problem for $\bar{a}(x)$**

Given that both the ligand and receptor synthesis rates are time independent, it can be shown [23] that the extracellular model system has a unique steady state given by

$$\{\bar{a}(x), \bar{b}(x), \bar{r}(x)\} = \lim_{t\to\infty} \{a(x,t), b(x,t), r(x,t)\}, \tag{2.16}$$

that is linearly stable with respect to a small perturbation. It was shown in [23] that the three governing equations may be reduced to a well-posed two-point boundary value problem (BVP) for $\bar{a}(x)$:

$$\bar{a}'' - \frac{g_0 \bar{a}}{\alpha_0 + \zeta_0 \bar{a}} - g_L \bar{a} + \bar{v}_L H(-x) = 0, \tag{2.17}$$

$$\bar{a}'(-x_m) = 0, \qquad \bar{a}(\ell_M) = 0. \tag{2.18}$$

with

$$\bar{b}(x) = \frac{\bar{a}(x)}{\alpha_0 + \zeta_0 \bar{a}(x)}, \qquad \bar{r}(x) = \frac{\alpha_0}{\alpha_0 + \zeta_0 \bar{a}(x)} \tag{2.19}$$

where

$$\alpha_0 = \frac{f_0 + g_0}{h_0}, \qquad \zeta_0 = \frac{k_{\rm deg}}{k_R}. \tag{2.20}$$

For a finite domain, $X_0$ would normally be $X_{\rm max}$ so that $\ell_M = 1$.

**Low Receptor Occupancy**

The morphogen system is said to be in a state of *low receptor occupancy* (LRO) if

$$\zeta_0 a = k_{\rm deg} a / k_R \ll \alpha_0. \tag{2.21}$$

For such a system, we may neglect terms involving $\zeta_0 a$ in (2.17)-(2.19) to get an approximate set of solutions $\{a_0(x), b_0(x), r_0(x)\}$ determined by

$$a_0'' - \mu_L^2 a_0 + \bar{v}_L H(-x) = 0, \qquad \mu_L^2 = \frac{g_0}{\alpha_0} + g_L \tag{2.22}$$

$$a_0'(-x_m) = 0, \qquad a_0(\ell_M) = 0. \tag{2.23}$$

with

$$b_0(x) = \frac{a_0(x)}{\alpha_0}, \qquad r_0(x) = 1. \tag{2.24}$$

We limit our discussion to a finite positive $X_{\rm max}$ so that the exact solution for $\bar{a}_0(x)$ is

$$a_0(x) = \begin{cases} \frac{\bar{\nu}_L}{\mu_L^2}\{1 - \frac{\cosh(\mu_L)}{\cosh(\mu_L(1+x_m))}\cosh(\mu_L(x+x_m))\} & (-x_m \le x \le 0) \\ \frac{\bar{\nu}_L}{\mu_L^2}\frac{\sinh(\mu_L x_m)}{\cosh(\mu_L(1+x_m))}\sinh(\mu_L(1-x)) & (0 \le x \le 1) \end{cases}, \tag{2.25}$$

with

$$\bar{b}(x) \simeq \frac{a_0(x)}{\alpha_0}, \qquad \bar{r}(x) \simeq 1. \tag{2.26}$$

## 2.3 Robustness of Signaling Gradient

We use the extracellular model summarized earlier to investigate the effectiveness of feedback processes for achieving robust signaling gradients with respect to a significant change in the morphogen synthesis rate. We do this in a broader context than the conventional Hill function approach. In particular, the results for gradient systems in a state of low receptor occupancy will be useful in later developments for at least two reasons. Biological gradients that are differentiating tend to be suitably convex which is typically achieved through a state of low receptor occupancy. The mathematical model for systems in a low receptor occupancy state may be linearized to yield explicit solutions for the relevant BVP and IBVP and thereby offering clearer insight to the system behavior. In the subsections below, we recall certain aspects of robustness of signaling gradients with respect to significant changes in the morphogen synthesis rate first formulated in [26] and further developed in [20, 28, 29, 42]. While other measures of robustness have also been considered and analyzed (see [21]), our main purpose is to introduce a global measure of robustness to provide a key ingredient for a new approach to effective feedback mechanisms for achieving stable biological developments.

### 2.3.1 Perturbation due to Enhanced Morphogen Synthesis

Normal development of wing imaginal disc and other biological organisms may be altered by an enhanced morphogen synthesis rate stimulated by genetic or epigenetic changes. As we have already mentioned, *Dpp* synthesis rate in Drosophila imaginal disc doubles when the

ambient temperature is increased by $6°C$ (shown by S. Zhou while in A.D. Lander's Lab, see also [47]). At a state of lower receptor occupancy, a significant increase in morphogen synthesis rate has been shown to increase the steady state signaling gradient magnitude proportionately and change the slope and convexity of the gradient as well. As such, the cell fate at each spatial location would be altered [20, 23, 42]. Without the restriction of low receptor occupancy, the steady state signaling gradient has also been shown to be an increasing function of synthesis rate, though not necessarily proportionately [20, 23].

Even if the difference between the normal and enhanced signaling gradients is small at a particular location $x$ as it would be for a system in a state of high receptor occupancy (except for a narrow region near the edge of wing disc), the pattern developed would still be significantly different since the cell type that was at $\bar{x}$ is now at some distance away at $\tilde{x}$. However, the development of biological organisms are generally not particularly sensitive to a significant change in the ambient temperature that leads to significant signaling morphogen synthesis rate change. Some kind of feedback control process must be at work to minimize the effects of such changes on the biological developments. First attempts in finding such feedback control mechanisms focused on a Hill function type negative feedback on receptor synthesis rate. It was found by numerical simulations [26] that such a feedback process does not lead to robustness. That conclusion was proved mathematically in [17] where some insight was gained on the reason for the ineffectiveness of such feedback. Briefly, the effect of a Hill function type negative feedback on receptor synthesis rate tends to reduce the convexity of the gradient leading to significant qualitative difference in the convexity between normal and enhanced signaling gradients even if the difference in their magnitude along much of the spatial span may have improved by the feedback.

It was suggested in [17] that a different kind of feedback process would be more appropriate for safeguarding against such unwanted enhanced signaling gradient. Two robustness indices have been introduced in [20, 26, 42] to provide global measures of the deviation from normal

signaling gradient after synthesis rate enhancement. We describe one of these in the next subsection to be used in our proof-of-concept development of a new approach to feedback for robustness.

### 2.3.2 Root-Mean-Square Signaling Differential

Let $b(x,t)$ be the normalized signaling morphogen concentration $[LR]/R_0$ for a normal (wild type) ligand synthesis rate $V_L(X,T) = \bar{V}_L H(-X)$ (or $v_L(x,t) = \bar{v}_L H(-x)$ after normalization). Let $b_e(x,t)$ be same quantity for an enhanced (ectopic) synthesis rate $e\bar{V}_L H(-X)$ (or $e\bar{v}_L H(-x)$ after normalization) for some amplification factor $e$. A rather natural global measure of signaling gradient robustness is the following *signal robustness index* $R_b$ corresponding to the root mean square of the deviation between $b_e(x,t)$ and $b(x,t)$:

$$R_b(t) = \frac{1}{b_h - b_\ell}\sqrt{\frac{1}{x_\ell - x_h}\int_{x_h}^{x_\ell}[b_e(x,t) - b(x,t)]^2 dx} \tag{2.27}$$

where $0 \le b_\ell(t) < b_h(t) \le b(-x_m, t)$ and $-x_m \le x_h < x_\ell \le \ell_M = 1$. The quantities $x_\ell$, $x_h$, $b_\ell$ and $b_h$ may be chosen away from the extremities to minimize the exaggerated effects of outliers.

For a system in steady state with

$$\bar{b}(x) = \lim_{t\to\infty} b(x,t), \qquad \tilde{b}(x) = \lim_{t\to\infty} b_e(x,t), \tag{2.28}$$

the robustness index $R_b(t)$ tends to a constant $\bar{R}_b$:

$$\bar{R}_b = \lim_{t\to\infty} R_b(t) = \frac{1}{b_h - b_\ell}\sqrt{\frac{1}{x_\ell - x_h}\int_{x_h}^{x_\ell}[\tilde{b}(x) - \bar{b}(x)]^2 dx} \tag{2.29}$$

We set $x_h = 0$ in part because signaling is irrelevant in the interval of ligand synthesis. We also take $b_\ell = b(1,t) = 0$ for simplicity. For the case of low receptor occupancy, we take $b_h$ to be the explicit (approximate) steady state value for $\bar{b}(0)$ known from (2.25) and (2.26) to be

$$b_h = \frac{\bar{v}_L}{\alpha_0 \mu_L^2} \frac{\sinh(\mu_L x_m)\sinh(\mu_L \ell_M)}{\cosh(\mu_L(\ell_M + x_m))} \;\sim\; \bar{b}(0), \tag{2.30}$$

For the case of high receptor occupancy (which is usually not biologically useful), it would be more appropriate to take $b_h = g_r/g_0$ corresponding to receptor saturation.

The signal robustness index $R_b(t)$ is not the only measure of the deviation of the modified signaling gradient from the one prior to morphogen synthesis rate enhancement. Given an existing genetic program for individual cells, a more relevant measure of robustness may be the displacement of the same level of morphogen-receptor complex concentration due to an ectopic morphogen synthesis rate. Such a robustness index, denoted by $R_x(t)$, was first introduced in [26] and investigated in [42] and references cited therein. We will be working with $R_b(t)$ and $\bar{R}_b$ only and leave the discussion on $R_x(t)$ and $\bar{R}_x$ to an investigation in future work.

### 2.3.3 Approximate Solution for Low Receptor Occupancy

For a morphogen system in a state of low occupancy so that $g_0 a/g_R \ll \alpha_0$, we have from [23] the following approximate steady state solutions for the signaling gradients of the normal (wild type) and (environmentally or genetically) perturbed system:

$$\tilde{b}(x) \;\sim\; e\bar{b}(x) = \frac{e\bar{v}_L}{\alpha_0 \mu_L^2} \frac{\sinh(\mu_L x_m)\sinh(\mu_L(1-x))}{\cosh(\mu_L(1+x_m))}, \quad (0 \le x \le \ell_M) \tag{2.31}$$

where $\mu_L^2 = g_L + g_0/\alpha_0$ with $\mu_L^2 \simeq h_0 + g_L$ whenever $f_0 \ll g_0$ (assuming that the perturbed system is also in a state of low receptor occupancy). In the absence of any feedback, the parameter $e$ is the amplification factor of the ligand synthesis rate. In particular, for $e = 2$, $x_\ell = 1$, $x_h = 0$, we have

$$\begin{aligned}\bar{R}_b &\sim \frac{1}{\sinh(\mu_L)}\sqrt{\int_0^1 [\sinh(\mu_L(1-x))]^2 dx} \\ &= \frac{1}{\sinh(\mu_L)}\sqrt{\frac{1}{2}\left(\frac{\sinh(2\mu_L)}{2\mu_L} - 1\right)}. \end{aligned} \tag{2.32}$$

For a gradient system with $g_0 = 0.2,\ f_0 = 0.001,\ g_r = 1,\ h_0 = 10,\ \ell_M = 1,\ x_m = 0.1$ and $\bar{v}_L = 0.05$ (together with $\bar{V}_L = 0.002\ \mu M,\ \bar{V}_R = 0.04\ \mu M,\ D = 10^{-7} cm^2/\sec.,\ X_{\max} = 0.01cm$ ) corresponding to $\beta = 0.25$ in Table 2 of [23], the steady state is in low receptor occupancy. For this case, the approximate solution for $\bar{R}_b$ given by (2.32) is $0.3938\cdots$ while accurate numerical solutions of the BVP for $\bar{a}(x)$ gives 0.3939... for a percentage error of less than 0.01%.

If ligand synthesis rate is increased 20 times to $\bar{V}_L = 0.04\ \mu M$, the accurate numerical solution for $\bar{R}_b$ is found to be $0.37486\cdots$ The percentage error of the low receptor occupancy approximate is still less than 1% . These comparisons serve to validate the numerical simulation code developed for exact numerical solutions of our model.

Our main interest however is in the use of $\bar{R}_b$, or more generally $R_b(t)$, in an appropriate feedback mechanism for attaining robustness of signaling morphogen gradients. To the extent that some enhanced ligand systems may only be *near* low receptor occupancy (and still sufficiently differentiating), the use of the approximate signaling robustness index based on the approximate solution (2.31) may not be sufficiently accurate. For these cases, it is necessary to obtain numerical solutions for $\bar{a}(x)$ and $\tilde{a}_e(x)$ and the corresponding value for $\bar{R}_b$.

## 2.4 Feedback on Ligand Synthesis Rate

### 2.4.1 A Non-local Feedback with Delay

Down-regulation of signaling activities are known to be accomplished in different ways. Whether it is through more nonreceptors or higher degradation rate of free or bound ligands, the net effect is equivalent to a lower concentration of free ligand available for binding with signaling receptors. Thus, for our proof-of-concept investigation, we focus on direct feedback on the ligand synthesis rate. To initiate our new approach to feedback, we consider in this first effort the effect of a negative feedback stimulated by a higher than normal signaling ligand concentration to be simply a reduction of the ligand synthesis rate $V_L$. To implement this approach, we take the normalized synthesis rate $v_L(x,t)$ to include a negative feedback factor using the signaling robustness index $R_b(t)$ as an instrument for down-regulating the synthesis rate:

$$v_L(x,t) = \kappa(t;\tau)\bar{v}_L H(-x) \equiv \frac{e\bar{v}_L H(-x)}{1 + c\,[R_b(t-\tau)]^n} \tag{2.33}$$

where the *amplification factor* $e$ is as previously defined and where $c$ and $n$ are two parameters to be chosen for appropriate feedback strength similar to those for a Hill's function. We should note two features of the feedback process in (2.33). First, with $c = n = 1$, the feedback mechanism reduces the synthesis rate by a fraction that depends on the average deviation over an appropriate spatial span (e.g., the distal span of the posterior compartment of the wing imaginal disc of the Drosophila). Second, the feedback may not be instantaneous as a delay of $\tau$ unit of dimensionless time is allowed for the feedback to become effective.

With $\tau > 0$ (and $v_R(x,t) = \bar{v}_R$ uniformly throughout the entire distal-proximal span of the wing imaginal disc), the IBVP for the three normalized concentration may be computed as we would for the problem without feedback except that the ligand synthesis rate changes

with time. In particular, for the period $[0, \tau]$, the problem is identical to the one without feedback. For the interval $[k\tau, (k+1)\tau]$ and with $t = k\tau + \eta$, the synthesis rate is modified to

$$v_L(x,t) = \frac{e\bar{v}_L H(-x)}{1 + c\left[R_b((k-1)\tau + \eta)\right]^n} \qquad (0 < \eta < \tau) \tag{2.34}$$

with all concentrations continuous at the junctions between the time intervals. We will implement this solution process and analyze the results in the next chapter.

### 2.4.2 Time Independent Steady State with Feedback

It has been shown in [23] that the extracellular model system without feedback has a unique steady state that is linearly stable with respect to small perturbations from the steady state. We show here that the same is true for our model with feedback on the ligand synthesis rate. Suppose $\{a(x,t),\, b(x,t), r(x,t)\}$ of (2.12) - (2.15) tend to the time independent states $\{\tilde{a}(x), \tilde{b}(x), \tilde{r}(x)\}$ and therewith $R_b(t) \to \bar{R}_b$ (see (2.27) and (2.29)). In that case, we have $v_L(x,t)$ of (2.34) tends to $\bar{\kappa}(\bar{R}_b)\bar{v}_L H(-x)$ , where

$$\bar{\kappa}(\bar{R}_b) = \lim_{t\to\infty} \kappa(t;\tau) = \frac{e}{1 + c\left(\bar{R}_b\right)^n}. \tag{2.35}$$

Note that we have used $\bar{\kappa}(\bar{R}_b)$ for $\kappa(t;\tau)$ in the steady state case since the *amplitude factor* $\kappa(t;\tau)$ is no longer time dependent and is only a function of $\bar{R}_b$ (and of course of $e, n$ and $c$ in both cases).

For the steady state solution $\{\tilde{a}(x), \tilde{b}(x), \tilde{r}(x)\}$, we have $\partial(\ )/\partial t = 0$ so that the governing partial differential equations and boundary conditions become

$$\tilde{a}'' - h_0\tilde{a}\tilde{r} + f_0\tilde{b} - g_L\tilde{a} + \bar{\kappa}(\bar{R}_b)\bar{v}_L H(-x) = 0 \tag{2.36}$$

$$h_0\tilde{a}\tilde{r} - (f_0 + g_0)\tilde{b} = 0, \qquad (g_r + h_0\tilde{a})\tilde{r} - f_0\tilde{b} = \bar{v}_R, \tag{2.37}$$

with

$$\tilde{a}'(-x_m) = 0, \qquad \tilde{a}(1) = 0, \tag{2.38}$$

where a prime indicates differentiation with respect to $x$, i.e., $(\ \ )' = d(\ \ )/dx$.

As in the case without feedback, we can solve (2.37) for $\tilde{b}$ and $\tilde{r}$ in terms of $\tilde{a}$ (analogous to (2.19) and (2.20))

$$\tilde{b}(x) = \frac{\tilde{a}(x)}{\alpha_0 + \zeta_0\tilde{a}(x)}, \qquad \tilde{r}(x) = \frac{\alpha_0}{\alpha_0 + \zeta_0\tilde{a}(x)} \tag{2.39}$$

with

$$\alpha_0 = \frac{f_0 + g_0}{h_0}, \qquad \zeta_0 = \frac{k_{\text{deg}}}{k_R}. \tag{2.40}$$

and use the results to eliminate these two quantities from the only ordinary differential equation (ODE) (2.36) to get a BVP for $\tilde{a}$ alone:

$$\tilde{a}'' - \frac{g_0\tilde{a}}{\alpha_0 + \zeta_0\tilde{a}} - g_L\tilde{a} + \bar{\kappa}(\bar{R}_b)\bar{v}_L H(-x) = 0, \tag{2.41}$$

$$\tilde{a}'(-x_m) = 0, \qquad \tilde{a}(1) = 0. \tag{2.42}$$

where $\bar{\kappa}(\bar{R}_b)$ is given by (2.35).

The following theorem, similar to the one in [23], ensures the BVP for the steady state concentration $\bar{a}(x)$ above is well-posed, nonnegative and monotone decreasing:

**Theorem 2.1.** *For positive values of the parameters $g_0, f_0, h_0, \bar{\nu}_L$ and $\bar{\nu}_R$, there exists a unique, nonnegative solution $\bar{a}(x)$ of the BVP (2.41) and (2.42). The corresponding concentrations $\bar{b}(x)$ and $\bar{r}(x)$ can then be calculated from (2.39).*

*Proof.* The existence proof is similar to that in [23] for the case without feedback. It suffices to produce an upper solution and a lower solution for the problem in order to apply the known monotone method of [36] (see also [2], [38]).

Evidently, $a_\ell(x) \equiv 0$ is a *lower* solution since

$$\begin{aligned} &-[a_\ell]'' + \frac{g_0 a_\ell}{\alpha_0 + \zeta_0 a_\ell} + g_L a_\ell - \frac{e\bar{v}_L}{1 + c\left(\bar{R}_b\right)^n} H(-x) \\ &= -\frac{e\bar{v}_L}{1 + c\left(\bar{R}_b\right)^n} H(-x) \le 0 \qquad (-x_m < x < 1), \end{aligned} \tag{2.43}$$

with

$$a_\ell'(-x_m) = 0, \qquad a_\ell(1) = 0.$$

For an *upper* solution, we note that

$$\tilde{a}'' + e\bar{v}_L \ge \tilde{a}'' - \frac{g_0 \tilde{a}}{\alpha_0 + \zeta_0 \tilde{a}} - g_L \tilde{a} + \frac{e\bar{v}_L}{1 + c\left(\bar{R}_b\right)^n} H(-x) = 0$$

The exact solution for $\tilde{a}'' + e\bar{v}_L = 0$ is

$$a_u(x) = e\bar{v}_L \left\{ \left( x_m + \frac{1}{2} \right) - x_m x - \frac{1}{2} x^2 \right\}$$

with $a_u'(-x_m) = 0$ and $a_u(1) = 0$. From $(i)$ $a_u(-x_m) = \frac{\bar{v}_L}{2}(1 + x_m)^2 > 0$, $(ii)$ $a_u'(x) = -\bar{v}_L(x + x_m) < 0$ for $x > -x_m$, and $(iii)$ $a_u(1) = 0$, we have

$$a_u(x) > 0 \qquad (-x_m \le x < 1).$$

It follows that

$$
\begin{aligned}
&-[a_u]'' + \frac{g_0 a_u}{\alpha_0 + \zeta_0 a_u} + g_L a_u - e\bar{v}_L H(-x) \qquad (2.44)\\
&= e\bar{v}_L + \frac{g_0 a_u}{\alpha_0 + \zeta_0 a_u} + g_L a_u - e\bar{v}_L H(-x) > e\bar{v}_L - e\bar{v}_L H(-x) \geq 0
\end{aligned}
$$

for $-x_m < x < 1$ so that $a_u(x)$ is an upper solution for the BVP for $\bar{a}(x)$. The monotone method assures us that there exists a solution $\tilde{a}(x)$ of the BVP (2.41) and (2.42) with

$$0 = a_\ell(x) \leq \tilde{a}(x) \leq a_u(x).$$

Since $a_u(x)$ is already known to be positive for $-x_m \leq x < 1$, $\tilde{a}(x)$ must be nonnegative in the whole solution domain.

To prove uniqueness, let $a^{(1)}(x)$ and $a^{(2)}(x)$ be two (nonnegative) solutions and $a(x) = a^{(1)}(x) - a^{(2)}(x)$ . Then as a consequence of the differential equation (2.41) for $a^{(1)}(x)$ and $a^{(2)}(x)$, the difference $a(x)$ satisfies the following differential equation:

$$-a'' + \frac{g_0 \zeta_0 \alpha_0 a}{(\alpha_0 + \zeta_0 a^{(1)})(\alpha_0 + \zeta_0 a^{(2)})} + g_L a = 0.$$

Multiplying by $a$ and integrating gives

$$\int_{-x_m}^{1} \left[ -a'' + \frac{g_0 \zeta_0 \alpha_0 a}{(\alpha_0 + \zeta_0 a^{(1)})(\alpha_0 + \zeta_0 a^{(2)})} + g_L a \right] a dx = 0,$$

then we integrate by parts. Upon observing continuity of $\tilde{a}(x)$ and $\tilde{a}'(x)$, and application of the boundary conditions in (2.42), the relation above may be transformed into

$$\int_{-x_m}^{1} [a'(x)]^2 dx + \int_{-x_m}^{1} \left\{ \frac{g_0 \zeta_0 \alpha_0 [a(x)]^2}{(\alpha_0 + \zeta_0 a^{(1)}(x))(\alpha_0 + \zeta_0 a^{(2)}(x))} + g_L [a(x)]^2 \right\} dx = 0.$$

Since both integrands are non-negative and not identically zero; we must have $a(x) \equiv 0$ thus proving the uniqueness. □

### 2.4.3 Monotonicity

We follow the analysis of the model in [23] to show that the free morphogen concentration $\tilde{a}(x)$ and the corresponding signaling morphogen gradient $\tilde{b}(x)$ are (positive and) monotone decreasing in the open interval $(-x_m, 1)$. First, we show that there are not any extremum in that interval.

**Proposition 2.2.** *Under the same hypotheses as those in Theorem 2.1, the nonnegative steady state concentration $\tilde{a}(x)$ does not attain a maximum or minimum in $(0, 1)$ and hence is monotone decreasing in that interval..*

*Proof.* First, it is easy to see that the nonnegative $\tilde{a}(x)$ does not have an interior maximum in the interval $0 < x < 1$. If it should have a local maximum at some interior point $x_0$, then we must have ($\tilde{a}'(x_0) = 0$ and) $\tilde{a}''(x_0) \leq 0$. But since $\tilde{a}(x) \geq 0$ and $v_L(x) = 0$ in $x > 0$, we have

$$\tilde{a}'' = \frac{g_0 \tilde{a}}{\alpha_0 + \varsigma_0 \tilde{a}} + g_L \tilde{a} \geq 0.$$

It follows that we must have $\tilde{a}''(x_0) = 0$ and therewith $\tilde{a}(x_0) = 0$. Since $x_0$ is a maximum point, we must have $\tilde{a}(x) = 0$ in $0 < x < 1$. The continuity requirements imply $\tilde{a}(0) = \tilde{a}'(0) = 0$. But it is impossible for any nontrivial solution of the ODE (2.41) to satisfy both of these conditions unless $\tilde{a}(x) = 0$ for all $x$ in $[-x_m, 0]$ as well. Such a free morphogen concentration does not satisfy (2.41) in the interval $(-x_m, 0)$ where the normalized *Dpp* synthesis rate is a positive constant $\bar{v}_L$. Hence $\tilde{a}(x)$ does not have a maximum in $(-x_m, \infty)$.

Also, $\tilde{a}(x)$ does not have a positive interior minimum. If it should have one at $x_0$ (with $\tilde{a}(x_0) > 0$), then it must have an interior maximum at some $x_1 > x_0$ in order for $\tilde{a}(x)$ to decrease from $\tilde{a}(x_1) > 0$ to $\tilde{a}(1) = 0$. However, this contradicts the fact that $\tilde{a}(x)$ does not have an interior maximum. There is still the possibility of a local interior minimum $\tilde{a}(x_0) = 0$. With $\tilde{a}'(x_0) = 0$ at the local minimum, we have $\tilde{a}(x) \equiv 0$ which does not satisfy the ODE (2.41) in the interval $(-x_m, 0)$. Altogether, the solution $\tilde{a}(x)$ of the BVP must be (nonnegative and) monotone decreasing from $\tilde{a}(-x_m) > 0$ to $\tilde{a}(\ell_M) = 0$. □

We can actually prove that the relevant morphogen concentrations are positive for $x < 1$ which we will need in subsequent development.

**Corollary 2.3.** *Under the hypotheses of Theorem 2.1, the concentrations* $\tilde{a}(x), \tilde{b}(x)$, *and* $\tilde{r}(x)$ *do not vanish in* $(-x_m, 1)$.

*Proof.* Suppose $\tilde{a}$ vanishes at $x_0$ in $(-x_m, 1)$ and hence attains a local minimum there (since $\tilde{a}(x)$ is nonnegative). This contradicts Proposition 2.2 which asserts that $\tilde{a}(x)$ does not have an interior minimum. That the remaining quantities do not vanish follows from (2.39) and (2.40). □

### 2.4.4 Low Receptor Occupancy

If the morphogen system is in a state of *low receptor occupancy* prior to and after ligand synthesis enhancement so that (2.21) is met generally by the present feedback model (including the special case where $c = 0$ and $e = 1$ so that $\tilde{a}(x; \bar{R}_b)$ reduces to $\bar{a}(x)$), we may use the linearized model

$$a_0'' = \mu_L^2 a_0 - \bar{\kappa}(\bar{R}_b)\bar{v}_L H(-x), \tag{2.45}$$

$$a_0'(-x_m) = 0, \quad a_0(1) = 0 \tag{2.46}$$

with

$$\mu_L^2 = g_L + \frac{g_0}{\alpha_0}. \tag{2.47}$$

for an approximate solution of our problem. The exact solution of (2.45)-(2.46), denoted by $a_0(x; \bar{R}_b)$ for its dependence on $\bar{R}_b$, is expected to be an accurate approximation of the exact solution $\tilde{a}(x; \bar{R}_b)$. It reduces to the (approximate) wild-type ligand concentration when $c = 0$ and $e = 1$. For a finite positive $X_{\max}$, the exact solution for $a_0(x)$ is

$$a_0(x) = \begin{cases} \frac{\bar{\kappa}\bar{\nu}_L}{\mu_L^2}\{1 - \frac{\cosh(\mu_L \ell_m)}{\cosh(\mu_L(1+x_m))}\cosh(\mu_L(x+x_m))\} & (-x_m \le x \le 0) \\ \frac{\bar{\kappa}\bar{\nu}_L}{\mu_L^2}\frac{\sinh(\mu_L x_m)}{\cosh(\mu_L(1+x_m))}\sinh(\mu_L(1-x)) & (0 \le x \le 1) \end{cases}, \tag{2.48}$$

with

$$\tilde{b}(x) \simeq \frac{a_0(x)}{\alpha_0}, \qquad \alpha_0 \tilde{b}(0) \simeq \tilde{a}(0) \simeq a_0(0) = \frac{\bar{\kappa}\bar{\nu}_L}{\mu_L^2}\frac{\sinh(\mu_L x_m)}{\cosh(\mu_L(1+x_m))}\sinh(\mu_L). \tag{2.49}$$

For $\mu_L \gg 1$, the expression for $a_0(x)$ in the signaling range of $0 \le x < 1$ is asymptotically

$$a_0(x) \sim \frac{\bar{\kappa}\bar{\nu}_L}{\mu_L^2} e^{-\mu_L x} \qquad (0 \le x < 1),$$

so that the gradient is effectively a boundary layer adjacent to $x = 0$, steep near $x = 0$ and dropping sharply to near zero away from $x = 0$. The discussion above leads to the following observation:

**Proposition 2.4.** *Even if a morphogen system is in a steady state of low receptor occupancy (so that the condition (2.21) is satisfied), its signaling gradient may not be a biologically meaningful gradient for the intended tissue patterning if the condition $\mu_L = O(1)$ is not met.*

## 2.5 Numerical Algorithms for Steady State Solutions

### 2.5.1 A Single Pass Solution Scheme

The presence of the factor $\bar{R}_b$ in the ODE for $\tilde{a}$ makes the solution of the BVP (2.41)-(2.42) much less straightforward. As $\bar{R}_b$ encapsulates the unknown concentrations of normal and enhanced signaling ligand-receptor complexes, it depends on the solutions of two BVPs over the entire span of the solution domain through the integrated condition (2.29). To the extent that there are reliable software for solving BVP in ODE, we may make use of these tools by re-configuring the integro-differential equation problem for $\tilde{a}$ to a BVP for a system of ODEs.

For this purpose, we let $\bar{a}(x)$ and $\tilde{a}(x)$ be the unknown free (unbound) ligand concentration for a wild type ligand synthesis rate $\bar{\nu}_L H(-x)$ and an ectopic synthesis rate $\bar{\kappa}\bar{\nu}_L H(-x)$, respectively, with the amplification factor $\bar{\kappa}$ to be specified. The wild type concentration $\bar{a}(x)$ is determined by the BVP (2.41)-(2.42) with $e = 1$ and $c = 0$ so that

$$\bar{a}'' - \frac{g_0 \bar{a}}{\alpha_0 + \zeta_0 \bar{a}} - g_L \bar{a} + \bar{v}_L H(-x) = 0, \tag{2.50}$$

$$\bar{a}'(-x_m) = 0, \qquad \bar{a}(1) = 0. \tag{2.51}$$

Correspondingly, $\tilde{a}$ is determined by the BVP (2.41)-(2.42) and the integral condition (2.29) with $x_\ell = 1$, $x_h = 0$, and $b_\ell = 0$ so that

$$\bar{R}_b = \frac{1}{b_h}\sqrt{\int_0^1 [\tilde{b}(x;\bar{R}_b) - \bar{b}(x)]^2 dx}. \tag{2.52}$$

where

$$\tilde{b}(x;\bar{R}_b) = \frac{\tilde{a}(x;\bar{R}_b)}{\alpha_0 + \zeta_0\tilde{a}(x;\bar{R}_b)}, \qquad \bar{b}(x) = \frac{\bar{a}(x)}{\alpha_0 + \zeta_0\bar{a}(x)}. \tag{2.53}$$

As indicated previously, we take $b_h$ to be given by (2.30) for systems of low receptor occupancy (and $b_h = k_R/k_{\rm deg}$ for less likely systems of high receptor occupancy).

For a single pass algorithm for the solution of our problem where the nonlinear relation (2.29) involves the unknown $\tilde{a}(x;\bar{\kappa}(R_b))$, we introduce two new functions to replace the integral relation (2.29). The first is the function $R_2(x)$ defined by

$$R_2' = \frac{1}{b_h^2}[\tilde{b}(x) - \bar{b}(x)]^2 = \frac{1}{b_h^2}\left(\frac{\tilde{a}(x)}{\alpha_0 + \zeta_0\tilde{a}(x)} - \frac{\bar{a}(x)}{\alpha_0 + \zeta_0\bar{a}(x)}\right)^2 H(x), \tag{2.54}$$

and the initial condition

$$R_2(-x_m) = 0. \tag{2.55}$$

With the Heaviside function $H(x)$ on the right hand side of (2.54), we may stipulate $R_2(x)$ to be continuous $x = 0$.

The second new function is $R_b(x)$ defined by

$$R_b' = 0 \tag{2.56}$$

specifying that it does not change with location and is therefore some (unknown) constant $\bar{R}_b$, i.e., $R_b(x) = \bar{R}_b$. The two new functions are related by the integral condition (2.52) taken in the form

$$R_2(1) = \bar{R}_b^2. \tag{2.57}$$

In terms of the two new functions, we may rewrite (without altering the content of the ODE (2.36)) the BVP for $\tilde{a}$ as

$$\tilde{a}'' - \frac{g_0\tilde{a}}{\alpha_0 + \zeta_0\tilde{a}} - g_L\tilde{a} + \bar{\kappa}(R_b)\bar{v}_L H(-x) = 0, \tag{2.58}$$

$$\tilde{a}'(-x_m) = 0, \qquad \tilde{a}(1) = 0, \tag{2.59}$$

with

$$\bar{\kappa}(R_b) = \frac{2}{1 + cR_b}, \tag{2.60}$$

where we have taken $e = 2$ and $n = 1$ to be concrete (with $c$ still to be specified). In this form, $R_b$ is treated as a function of position $R_b(x)$.

Note that (2.58), (2.54) and (2.56) are now three coupled ODE for the three unknowns $\tilde{a}(x), R_2(x)$ and $R_b(x)$ to be solved simultaneously. It is a fourth order system with four auxiliary conditions given in (2.59), (2.55) and (2.57) with the latter taken in the form

$$R_2(1) = [R_b(1)]^2. \tag{2.61}$$

Together, the BVP for the fourth order system defined by (2.58), (2.54), (2.56), (2.59), (2.55) and (2.61) enables us to avoid having the global parameter $\bar{R}_b$ as an unknown to be

determined by an integral on the yet unknown solutions of the two principal ODE over the entire solution domain.

Adding to this the BVP defined by (2.50) and (2.51), we have a sixth order system for the four unknowns $\bar{a}(x)$, $\tilde{a}(x)$, $R_b(x)$ and $R_2(x)$. Such a BVP can be solved by computing software generally available on *MatLab*, *Mathematica* and *Maple*. It should be noted however that a single pass solution algorithm for this problem requires the software to have the capability of handling a vanishing Jacobian in the linearization of the nonlinear BVP by some form of Newton's method.

### 2.5.2 An Iterative Algorithm

It is possible to avoid computing with vanishing Jacobians. Given the dependence of $\tilde{a}(x)$ (and hence $\tilde{b}(x)$) on $\bar{R}_b$, the relation (2.52) may be written abstractly as

$$\bar{R}_b = C(\bar{R}_b), \tag{2.62}$$

where

$$C(\bar{R}_b) = \frac{1}{b_h}\sqrt{\int_0^1 [\tilde{b}(x;\bar{R}_b) - \bar{b}(x)]^2 dx} \tag{2.63}$$

Observe that $0 \leq C(0) < 1$ and, for $0 \leq c < 1$,

$$0 \leq C(\bar{R}_b) < 1 \tag{2.64}$$

given $\left[\tilde{b}(x;\bar{R}_b) - \bar{b}(x)\right]/b_h < 1$ for $x > 0$.

A typical iterative solution scheme would start with some initial estimate $\bar{R}_0$ and calculate successive iterates $\bar{R}_k$ by the simple iteration

$$\bar{R}_{k+1} = C(\bar{R}_k) = \frac{1}{b_h}\sqrt{\int_0^1 [\tilde{b}(x;\bar{R}_k) - \bar{b}(x)]^2 dx}, \qquad k = 0, 1, 2, 3, .... \tag{2.65}$$

where $\tilde{b}(x;\bar{R}_k)$ is determined from the solution $\tilde{a}(x;\bar{R}_k)$ of the BVP (2.58)-(2.60) with $\bar{R}_b = \bar{R}_k$ in

$$\bar{\kappa}(\bar{R}_b) = \frac{2}{1 + c\bar{R}_k}. \tag{2.66}$$

We first show that $\tilde{a}(x;\bar{R}_b)$ and $\tilde{b}(x;\bar{R}_b)$ are both decreasing functions of $\bar{R}_b$. The non-positivity of the marginal change of $\tilde{b}(x;\bar{R}_b)$ with $\bar{R}_b$ is then used in

$$\frac{dC}{d\bar{R}_b} = \frac{1}{b_h^2 C}\int_0^1 [\tilde{b}(x;\bar{R}_b) - \bar{b}(x)]\frac{\partial\tilde{b}(x;\bar{R}_b)}{\partial\bar{R}_b}dx \tag{2.67}$$

to analyze the convergence of the iterative process (2.65).

Upon differentiating all relations in the BVP for $\tilde{a}(x;\bar{R}_b)$ partially with respect to $\bar{R}_b$, we obtain

$$-w'' + \left(\frac{\alpha_0}{\alpha_0 + \zeta_0\tilde{a}} + g_L\right) w - \frac{2\bar{v}_L}{\left(1 + \bar{R}_b\right)^2} H(-x) = 0, \tag{2.68}$$

$$w'(-x_m;\bar{R}_b) = 0, \qquad w(1;\bar{R}_b) = 0. \tag{2.69}$$

where

$$w(x;\bar{R}_b) = -\frac{\partial\tilde{a}(x;\bar{R}_b)}{\partial\bar{R}_b}$$

Clearly, $w_\ell(x;\bar{R}_b) \equiv 0$ is a lower solution of the BVP for $u(x;\bar{R}_b)$ given

$$\begin{aligned} &-w_\ell'' + \frac{\alpha_0(1+g_L)+g_L\zeta_0\tilde{a}}{\alpha_0+\zeta_0\tilde{a}} w_\ell - \frac{2\bar{v}_L}{\left(1+\bar{R}_b\right)^2} H(-x) \\ =& -\frac{2\bar{v}_L}{\left(1+\bar{R}_b\right)^2} H(-x) \le 0 \qquad (0 \le x \le 1). \end{aligned} \tag{2.70}$$

As an upper solution, we have

$$w_u(x;\bar{R}_b) = \frac{2\bar{v}_L}{\left(1+\bar{R}_b\right)^2}\left\{\left(x_m+\frac{1}{2}\right) - x_m x - \frac{1}{2}x^2\right\}$$

with

$$-w_u'' - \frac{2\bar{v}_L}{\left(1+\bar{R}_b\right)^2} = 0.$$

Note that

$$\begin{aligned} &-w_u'' + \left(\frac{\alpha_0}{\alpha_0+\zeta_0\tilde{a}} + g_L\right) w_u - \frac{2\bar{v}_L}{\left(1+\bar{R}_b\right)^2} H(-x) \\ \ge& -w_u'' - \frac{2\bar{v}_L}{\left(1+\bar{R}_b\right)^2} H(-x) = \frac{2\bar{v}_L}{\left(1+\bar{R}_b\right)^2}\left[1-H(-x)\right] \ge 0, \end{aligned} \tag{2.71}$$

and

$$w_u'(-x_m;\bar{R}_b) = 0, \qquad w_u(1;\bar{R}_b) = 0.$$

The monotone method of in [36] implies that $w(x;\bar{R}_b)$ exists, is unique and non-negative so that

$$-w_u(x;\bar{R}_b) \le \frac{\partial\tilde{a}(x;\bar{R}_b)}{\partial\bar{R}_b} \le 0$$

This leads to the following proposition on the non-positivity of the marginal value $\partial\tilde{b}(x;\bar{R}_b)/\partial\bar{R}_b$:

**Proposition 2.5.** $\partial\tilde{b}(x;\bar{R}_b)/\partial\bar{R}_b \leq 0.$

*Proof.* Upon differentiating the expression for $\tilde{b}(x;\bar{R}_b)$ in (2.53) partially with respect to $\bar{R}_b$, we obtain

$$\frac{\partial\tilde{b}(x;\bar{R}_b)}{\partial\bar{R}_b} = \frac{\alpha_0}{(\alpha_0+\zeta_0\tilde{a})^2}\frac{\partial\tilde{a}(x;\bar{R}_b)}{\partial\bar{R}_b} \leq 0.$$

□

Together with (2.64) and $\tilde{b}(x;\bar{R}_b) > 0$, Proposition 2.5 implies $dC/d\bar{R}_b \leq 0$ as long as $[\tilde{b}(x;\bar{R}_b) - \bar{b}(x)] \geq 0$ (which is the case at the start of the iterative scheme). However, this does not make $\{\bar{R}_k\}$ a non-increasing sequence (though bounded below by 0). If $\bar{R}_{k+1} < \bar{R}_k$, we would have $\tilde{a}(x;\bar{R}_{k+1}) > \tilde{a}(x;\bar{R}_k)$ and therewith $\bar{R}_{k+2} > \bar{R}_{k+1}$ (consistent with $dC/d\bar{R}_b \leq 0$). As such, we have a non-negative sequence $\{\bar{R}_k\}$ alternately increasing and decreasing with successive iterations bounded below (by 0) and above (by $\bar{R}_b(c=0)$ offering the prospect of convergence. As we shall see from an illustrative example in the next section, the iterative scheme converges rapidly for $c = 1$ but the steady state value found is unstable for $c \gg 1$.

### 2.5.3 An Illustrative Example

To gain some insight to the iterative algorithm for the steady state value $\bar{R}_b$ of the robustness index, we apply it to the system characterized by the parameter values shown in Table 2.1. This system meets the condition (2.21) for a state of low receptor occupancy and is further confirmed to be so by comparison of the exact numerical solution with that of the linearized model. The steady state robustness index $\bar{R}_b$ is found after less than 10 iterations with less than 0.2% discrepancy between the $8^{th}$ and $9^{th}$ iterations as shown on the line for $c = 1$ in Table 2.1 below:

Table 2.1 Numerical Solutions by the Iterative Algorithm

$$X_{\max} = 0.01\ cm, \quad X_{\min} = 0.001\ cm, \quad k_{on}R_0 = 0.01 \sec./\mu M,$$
$$k_{deg} = 2 \times 10^{-4}/\sec., \quad k_R = 0.001/\sec., \quad k_{off} = 10^{-6}/\sec., \quad k_L = 0,$$
$$D = 10^{-7}\ cm^2/\sec., \quad \bar{V}_L = 0.002\ \mu M/\sec., \quad \bar{V}_R = 0.04\ \mu M/\sec.$$

| $c$ | $\bar{R}_k$ | $\bar{R}_{k+1}$ | $\bar{b}(0)$ | $\tilde{b}(0;\bar{R}_k)$ | $\tilde{b}(0;\bar{R}_{k+1})$ | $\tilde{b}(0;0)$ |
|---|---|---|---|---|---|---|
| 0 | 0.39380 | 0.39380 | 0.05798 | 0.11533 | 0.11533 | 0.11533 |
| 1 | 0.24190 | 0.24051 | 0.05798 | 0.09327 | 0.09306 | 0.11533 |
| 2 | 0.18177 | 0.18296 | 0.05798 | 0.08451 | 0.08469 | 0.11533 |
| 4 | 0.11114 | 0.11163 | 0.05798 | 0.07422 | 0.07431 | 0.11533 |

The quick convergence of the scheme for the particular example is gratifying. However, the biological implication is not as satisfying. Taking the average of the two iterates for $\bar{R}_k$ shown in the Table gives a rather accurate numerical solution of $\bar{R}_b \simeq 0.24121...$ for the steady state robustness index. This is above the acceptable threshold of $\bar{R}_b \leq 0.2$ set (arbitrarily) in [26] for robustness. While there is some flexibility in setting the reference value $b_h$ and reinterpreting the new definition, a more serious issue is the magnitude and shape of the resulting steady state signaling gradient.

Comparing the values of $\bar{b}(0)$ and $\tilde{b}(0;0)$ with the accurate numerical solution $\tilde{b}(0;\bar{R}_k)$ associated with the final acceptable iterate $\bar{R}_k$ shows that the solution with feedback is reduced but still closer to the corresponding enhanced concentration $\tilde{b}(0;0)$ than the concentration for the wild type system. The same is true for the entire signaling region of the solution domain. Two questions arise: Is this the best we can do by the new feedback mechanism in the form (2.33) (and consequently robustness cannot be attained by such a mechanism)? If so, are there modifications that would lead to robustness? We examine possible answers to these questions in the following subsections.

### Wild Type and Perturbed Systems at Low Receptor Occupancy

For our example, the model system is in a state of low receptor occupancy before and after ligand synthesis enhancement. In that case, accurate approximate solutions for $\tilde{a}(x)$ and $\bar{a}(x)$ can be obtained similar to the model without feedback. In particular, the ODE for $\tilde{a}(x)$ is linearized to give a linear equation for the approximate solution $a_0(x)$:

$$a_0'' - \mu_L^2 a_0 + \bar{\kappa}(\bar{r}_b)\bar{\nu}_L H(-x) = 0,$$

$$a_0'(-x_m) = 0, \qquad a_0(1) = 0.$$

where $\mu_L^2$ is as given by (2.47) and where $\bar{R}_b$ in the expression (2.66) for $\bar{\kappa}$ is now replaced by the corresponding approximate expression $\bar{r}_b$ using the low receptor occupancy approximate solution $b_0(x;\bar{r}_b)$ for $\tilde{b}(x;\bar{R}_b)$. The exact solution for this problem is given by (2.48) with

$$\alpha_0\tilde{b}(x;\bar{R}_b) \simeq a_0(x;\bar{r}_b) = \frac{\bar{\kappa}(\bar{r}_b)\bar{\nu}_L}{\mu_L^2}\frac{\sinh(\mu_L x_m)}{\cosh(\mu_L(1+x_m))}\sinh(\mu_L(1-x)), \tag{2.72}$$

$$\alpha_0\bar{b}(x) \simeq [a_0(x)]_{\bar{\kappa}=1} = \frac{\bar{\nu}_L}{\mu_L^2}\frac{\sinh(\mu_L x_m)}{\cosh(\mu_L(1+x_m))}\sinh(\mu_L(1-x)), \tag{2.73}$$

for the signaling region $0 \le x \le 1$.

### $\bar{R}_b$ at Low Receptor Occupancy

The expressions (2.72) and (2.73) for the enhanced and wild-type normalized signaling morphogen gradients, $\tilde{b}(x;\bar{R}_b)$ and $\bar{b}(x)$, in the range relevant for cell signaling are to be used, respectively, in the expression (2.52) as was done in (2.32) to obtain for a low receptor occupancy system

$$\bar{R}_b \simeq \bar{r}_b(c) = \gamma(\mu_L)\left[\frac{2}{1+c\bar{r}_b} - 1\right] \tag{2.74}$$

with

$$\gamma(\mu_L) = \frac{1}{\sqrt{2}\sinh(\mu_L)}\sqrt{\left(\frac{\sinh(2\mu_L)}{2\mu_L} - 1\right)}. \tag{2.75}$$

For $c = 0$ (corresponding the case of no feedback), we have immediately

$$\left[\bar{R}_b\right]_{c=0} \simeq \bar{r}_b(0) = \gamma(\mu_L),$$

which is 0.3938..... for our example (as already reported in the discussion following (2.32)) while accurate numerical solution by the iterative algorithm of the previous section gives $\bar{R}_b = 0.3939...$

For $0 < c < \infty$, the relation (2.74) may be written as the quadratic equation

$$c\bar{r}_b^2 + (1 + c\gamma)\bar{r}_b - \gamma = 0 \tag{2.76}$$

for $\bar{r}_b$ with one positive solution

$$\bar{R}_b \simeq \bar{r}_b = \frac{1}{2c}\left[-(1 + c\gamma) + \sqrt{(1 + c\gamma)^2 + 4\gamma}\right] > 0. \tag{2.77}$$

For the problem specified by the parameter values in Table 2.1 and $c = 1$, such a feedback process gives

$$\left[\bar{R}_b\right]_{c=1} \simeq \bar{r}_b(1) = 0.24108... \tag{2.78}$$

which is almost the same as the average 0.24160... of the $8^{th}$ and $9^{th}$ iterates found earlier for $\bar{R}_b(c = 1)$. As such, $\bar{R}_b(c = 1) \simeq 0.24121...$ (together with a corrected signaling gradient that is closer to the perturbed gradient than the unperturbed one) is the best the feedback (2.33) with $c = 1$ can attain.

**Modification for a More Effective Feedback Process**

To improve on the feedback mechanism toward robustness of signaling gradients, we note that a larger value of $c$ in the expression (2.33) would reduce the enhanced synthesis rate to result in a lower concentration level of $\tilde{a}(x;\bar{R}_b)$ and $\tilde{b}(x;\bar{R}_b)$. This in turn should lead to a smaller robustness index $\bar{R}_b(c)$ as we would like to have. This expectation is easily proved for systems in a state of low receptor occupancy by differentiating the relation (2.76) with respect to $c$ to get for $c > 0$:

$$\frac{d\bar{r}_b}{dc} = -\frac{\gamma - \bar{r}_b}{c(1 + c\gamma + 2c\bar{r}_b)} < 0,$$

given $\bar{r}_b > 0$ for $c > 0$. The same result can be established for gradient systems of more general receptor occupancy:

**Proposition 2.6.** $d\bar{R}_b/dc < 0 \quad for \quad c > 0.$

*Proof.* We first prove

$$\partial\tilde{a}(x;\bar{R}_b(c))/\partial c < 0, \qquad \partial\tilde{b}(x;\bar{R}_b(c))/\partial c < 0,$$

using the approach for proving

$$\partial\tilde{b}(x;\bar{R}_b)/\partial\bar{R}_b < 0$$

when $c$ was set equal to 1. The proposition follows from

$$\frac{d\bar{R}_b}{dc} = \frac{1}{b_h^2\bar{R}_b(c)}\int_0^1 [\tilde{b}(x;\bar{R}_b(c)) - \bar{b}(x)]\frac{\partial\tilde{b}(x;\bar{R}_b(c))}{\partial c}dx,$$

given $[\tilde{b}(x;\bar{R}_b(c)) - \bar{b}(x)] > 0$ for $0 < c < \infty$. □

From (2.77), we have

$$\lim_{c\to\infty} \bar{R}_b(c) = 0.$$

Thus by choosing $c$ large enough, we should be able to reduce the robustness index and scale down $\tilde{b}(x;\bar{R}_b(c))$ to be close to $\bar{b}(x)$. The results for such an effort for $c = 2$ and $c = 4$ are reported in the last two rows of Table 2.1. For $c = 4$, not only is $\bar{R}_b$ ($\simeq 0.111385..$ ) well below the robustness threshold of 0.2, the feedback adjusted normalized signaling ligand concentration ($\simeq 0.074265...$) at $x = 0$ is now much closer to the wild type concentration ($\simeq 0.05798...$) than the enhanced concentration ($\simeq 0.11533...$) without feedback. In fact, the feedback adjusted gradient $\tilde{b}(x;\bar{R}_b(c))$ is also closer to $\bar{b}(x)$ than $\tilde{b}(x;0)$ for all $x > 0$.

Note that a large $c$ value also has the effect of changing $\bar{R}_b(c)$, and therewith $\tilde{b}(x;\bar{R}_b(c))$, more drastically from iteration to iteration.

**A Hill Function Type Modification**

For comparison, we consider here a different kind of feedback process on the synthesis rate for the steady state behavior of the form

$$\hat{\kappa} = \frac{2}{1+[\phi(x)]^2}, \qquad \phi = \frac{1}{b_h}\left[\tilde{b}(x;0) - \bar{b}(x)\right] \tag{2.79}$$

This Hill function type feedback is spatially nonuniform and provides a crude model for a delay feedback with effects quickly reaching a steady state. The steady state solution of the morphogen system with such a feedback correction gives $\hat{R}_b = 0.2050885...$ and $\hat{b}(0) \simeq 0.0879065....$

While the results are slight better than those by the spatially uniform feedback (2.60), the two corresponding signaling gradients $\tilde{b}(x;\bar{R}_k)$ and $\hat{b}(x)$ are not significantly different. More

importantly, the comparison would favor the spatially uniform feedback if the enhanced synthesis rate should induce a receptor saturated state. For then, the signaling gradient resulting from (2.79) would be more concave and biologically less differentiating for the purpose of differential cell fates similar to the results found in [17].

## 2.6 Concluding Remarks

Robustness with respect to an ectopic signaling gradient resulting from genetic or epigenetic perturbations requires one or more signaling inhibiting agents to be stimulated (by the enhanced signaling morphogen concentration) and up-regulated above their normal level. This means the existence of some kind of feedback process in order to promote robustness. Feedback has long been seen as a mechanism for maintaining stable developments and specific feedback loops have been identified in the morphogen literature, for example, [8, 12, 32, 11, 34]. Though the conventional Hill function type negative feedback on receptor synthesis rate proves to be ineffective for this purpose [26, 17, 28], we have shown in this chapter that a spatially uniform feedback process based on a spanwise average of excess signaling can play such a role. With the two algorithms developed for the solution of specific integro-differential equation system for such a feedback mechanism, the results obtained confirm that at least one such feedback mechanism can be effective for ensuring robustness and suggest that many other effective feedback mechanisms are also possible and should be investigated.

# Chapter 3

# Feedback During the Transient Phase of the Biological Development

## 3.1 Introduction

In Chapter 2, we initiated a different approach to the role of feedback in ensuring robust signaling gradients. Our goal is to investigate the effectiveness of feedback mechanisms other than a negative feedback of the Hill's function type on signaling receptor synthesis (which is known to be ineffective [17, 28, 26]). With the ultimate effect of many inhibitors (of the non-receptor type) being a reduction of the availability for signaling morphogens for binding with signaling receptors, we embark a proof-of-concept investigation of a new spatially uniform nonlocal feedback process (distinctly different from the conventional (spatially nonuniform) Hill function feedback) on the morphogen synthesis rate. The negative feedback on signaling morphogen synthesis rate based on a root-mean-square measure of the spatial distribution of signaling concentration offers a simple approach to robustness and we have shown for it to be effective for a signaling gradient in steady state. In this chapter, we examine the

corresponding transient problem with repeated feedback adjustments taking effect during the transient phase of the development.

## 3.2 Signaling Gradients and Pattern Formation

### 3.2.1 The Initial-Boundary Value Problem for the Basic Model

As in Chapter 2, we work with the basic model of Drosophila wing imaginal disc. Let us recall the system of the differential equations in dimensionless form:

$$\frac{\partial a}{\partial t} = \frac{\partial^2 a}{\partial x^2} - h_0 ar + f_0 b - g_L a + v_L(x,t), \tag{3.1}$$

$$\frac{\partial b}{\partial t} = h_0 ar - (f_0 + g_0)b, \qquad \frac{\partial r}{\partial t} = v_R(x,t) - h_0 ar + f_0 b - g_R r, \tag{3.2}$$

for the concentrations, $a$, $b$ and $r$, of free morphogen (e.g., *Dpp* in the Drosophila wing disc), bound morphogen (or the ligand-receptor complex) and unoccupied receptors (e.g., *Tkv* for *Dpp* in Drosophila wing disc), respectively. As before, all three concentrations are normalized by the steady state receptor concentration $R_0$ prior to the onset of the normalized ligand synthesis $v_L(x,t)$. Receptors are synthesized by a time independent synthesis rate (normalized to $v_R(x)$) long before the onset of ligand production. The dimensionless space and time variable $x$ and $t$ are normalized by $X_{\max}$ (the span of the wing imaginal disc in the distal direction from the boundary of the anterior and posterior compartment in the case of the wing imaginal disc) and the time constant $X_{\max}^2/D$ with $D$ being the diffusion coefficient for the diffusive ligand molecules, respectively. The various rate constants $\{k_{on}R_0, k_{off}, k_L, k_{\deg}, k_R\}$ for binding, dissociation, free ligand degradation, bound ligand degradation and unoccupied

receptor degradation are also normalized by the same time constant,

$$\{h_0, f_0, g_L, g_0, g_R\} = \frac{X_{\max}^2}{D}\{k_{on}R_0, k_{off}, k_L, k_{\deg}, k_R\}. \tag{3.3}$$

We normalize the synthesis rate $V_L$ (setting $v_L(x,t) = (V_L/R_0)/(D/X_{\max}^2)$) to get

$$v_L(x,t) = e\bar{v}_L H(-x) = \frac{e\bar{V}_L/R_0}{D/X_{\max}^2}H(-x) = \begin{cases} e\bar{v}_L & (-x_m \le x < 0) \\ 0 & (0 < x \le 1) \end{cases} \tag{3.4}$$

where $\bar{V}_L$ is the uniform (wild-type) synthesis rate in the narrow production region, $x_m = X_{\min}/X_{\max}$. Here $e$ is a constant, an *enhancement factor*; for wild-type systems it is normally 1. However, $e$ may assume other values due to environmental changes. We have receptor synthesis rate $\bar{V}_R$ uniform in both time and space (throughout the spatial domain) with

$$v_R(x,t) = v_R(x) = \bar{v}_R = \frac{\bar{V}_R/R_0}{D/X_{\max}^2}. \tag{3.5}$$

Prior to the onset of ligand synthesis, unoccupied receptors should be in a steady state concentration determined by the second equation in (3.2) to be

$$R_0 = \frac{\bar{V}_R}{k_R} = \frac{\bar{v}_R}{g_R}R_0 \tag{3.6}$$

with

$$\bar{v}_R = \frac{\bar{V}_R/R_0}{D/X_0^2} = \frac{k_R}{D/X_0^2} = g_R. \tag{3.7}$$

For the (normalized) boundary conditions we have:

$$x = -x_m: \quad \frac{\partial a}{\partial x} = 0, \qquad x = 1: \quad a = 0, \tag{3.8}$$

all for $t > 0$. And for the (normalized) initial conditions we have:

$$t = 0 : \qquad a = b = 0, \quad r = 1. \tag{3.9}$$

### 3.2.2 A Steady State Particular Solution

Let's denote the unique time independent particular solution by

$$\{\bar{a}_e(x), \bar{b}_e(x), \bar{r}_e(x)\} = \lim_{t\to\infty}\{a(x,t), b(x,t), r(x,t)\}. \tag{3.10}$$

Note that the subscript $e$ in these steady state quantities indicates the level of synthesis rate enhancement (ectopicity). $e = 1$ corresponds to normal (wild-type) development, and $e > 1$ corresponds to ectopic signaling gradients.

The steady state solution may be determined by the well-posed two-point boundary value problem (BVP) for $\bar{a}_e(x)$:

$$\bar{a}_e'' - \frac{g_0\bar{a}_e}{\alpha_0 + \zeta_0\bar{a}_e} - g_L\bar{a}_e + e\bar{v}_L H(-x) = 0, \tag{3.11}$$

$$\bar{a}_e'(-x_m) = 0, \qquad \bar{a}_e(1) = 0. \tag{3.12}$$

with

$$\bar{b}_e(x) = \frac{\bar{a}_e(x)}{\alpha_0 + \zeta_0\bar{a}_e(x)}, \qquad \bar{r}_e(x) = \frac{\alpha_0}{\alpha_0 + \zeta_0\bar{a}_e(x)} \tag{3.13}$$

where

$$\alpha_0 = \frac{f_0 + g_0}{h_0}, \qquad \zeta_0 = \frac{k_{\text{deg}}}{k_R} = \frac{g_0}{g_R}, \tag{3.14}$$

keeping in mind $\bar{v}_R = g_R$ (see (3.7)).

### 3.2.3 A State of Low Receptor Occupancy

For the state of *low receptor occupancy* (LRO), we get an approximate set of solutions $\{\bar{A}_e(x), \bar{B}_e(x), \bar{R}_e(x)\}$ to be determined by

$$\bar{A}_e'' - \mu_L^2 \bar{A}_e + e\bar{v}_L H(-x) = 0, \qquad \mu_L^2 = \frac{g_0}{\alpha_0} + g_L \tag{3.15}$$

$$\bar{A}_e'(-x_m) = 0, \qquad \bar{A}_e(1) = 0. \tag{3.16}$$

The exact solution for $\bar{A}_e(x)$ is

$$\bar{A}_e(x) = \begin{cases} \frac{e\bar{\nu}_L}{\mu_L^2}\{1 - \frac{\cosh(\mu_L)}{\cosh(\mu_L(1+x_m))}\cosh(\mu_L(x+x_m))\} & (-x_m \le x \le 0) \\ \frac{e\bar{\nu}_L}{\mu_L^2}\frac{\sinh(\mu_L x_m)}{\cosh(\mu_L(1+x_m))}\sinh(\mu_L(1-x)) & (0 \le x \le 1) \end{cases}, \tag{3.17}$$

with

$$\bar{b}_e(x) \simeq \bar{B}_e(x) = \frac{\bar{A}_e(x)}{\alpha_0}, \qquad \bar{r}_e(x) \simeq \bar{R}_e(x) = 1. \tag{3.18}$$

The following result is of some general interest:

**Proposition 3.1.** *$\bar{a}_e(x) > \bar{A}_e(x)$ for all $x$ in $[-x_m, 1)$.*

*Proof.* We compare the steady state solutions $\bar{a}_e(x)$ and $\bar{A}_e(x)$ determined by

$$\bar{a}_e'' = \frac{g_0 \bar{a}_e}{\alpha_0 + \zeta_0 \bar{a}_e} + g_L \bar{a}_e - e\bar{v}_L H(-x), \qquad \bar{a}_e'(-x_m) = \bar{a}_e(1) = 0$$

and

$$\bar{A}_e'' = \frac{g_0}{\alpha_0}\bar{A}_e + g_L\bar{A}_e - e\bar{v}_L H(-x), \qquad \bar{A}_e'(-x_m) = \bar{A}_e(1) = 0,$$

respectively. We see that starting from the same end point $\bar{a}_e(1) = \bar{A}_e(1) = 0$, $\bar{a}_e(x)$ is less convex than $\bar{A}_e(x)$ and hence increases faster as $x$ decreases. With the denominator $\alpha_0 + \zeta_0\bar{a}_e$ also increasing with decreasing $x$, the difference in curvature increases with decreasing $x$ which further exaggerates the difference $\bar{a}_e(x) - \bar{A}_e(x)$ as $x$ moves away from the disc edge. Hence, we have $\bar{a}_e(x) > \bar{A}_e(x)$ for all $x$ in $[0, 1)$. The addition of the same negative source term reduces the curvature of both by the same amount and hence does not affect the expected differential of the two concentrations. □

## 3.3 Robustness of Signaling Gradient

### 3.3.1 Ectopic Gradients

As we have already mentioned, *Dpp* synthesis rate in Drosophila imaginal wing disc doubles when the ambient temperature is increased by $6°C$. From (3.17)-(3.18) we see that at a state of low receptor occupancy (LRO), a significant increase in morphogen synthesis rate will increase proportionately the magnitude of the steady state signaling morphogen concentration. That, in turn, will change the cell fate at each spatial location. Without the restriction of LRO, the steady state free and signaling morphogen gradients are expected to be an increasing function of synthesis rate (but not necessarily proportionately and now also with some gradient shape distortion) as shown below.

**Proposition 3.2.** *$\bar{a}_e(x; e)$ is a non-decreasing function of $e$ and increasing at least for some segment(s) of the solution domain $[-x_m, 1]$.*

Let $w(x,e) = \partial \bar{a}_e/\partial e$. After doing partial differentiation of the BVP for $\bar{a}_e(x,e)$ with respect to $e$, we get

$$w'' - \frac{\alpha_0 g_0 w}{(\alpha_0 + \zeta_0 \bar{a}_e)^2} - g_L w + v_L H(-x) = 0,$$

$$w'(-x_m, e) = 0, \qquad w(1,e) = 0$$

We see that $w_\ell(x,e) = 0$ is a lower solution (but not an exact solution) of the BVP for $w(x,e)$ and $w_u(x,e) = v_L\{(x_m(1-x) + (1-x^2)/2\}$ is an upper solution (again not an exact solution). The monotone method of [36, 2, 38] affirms that $w(x,e)$ exists with

$$0 = w_\ell(x,e) \le w(x,e) \le w_u(x,e),$$

and $w(x,e)$ is not identically zero (since $w_\ell(x,e) = 0$ is not the solution of the BVP for $w(x,e)$).

**Corollary 3.3.** *$\bar{b}_e(x,e)$ is a non-decreasing function of $e$ and increasing in some segment(s) of $[-x_m, 1]$.*

*Proof.* Upon differentiating $\bar{b}_e(x,e)$ partially with respect to $e$, we obtain

$$\frac{\partial \bar{b}_e}{\partial e} = \frac{\partial}{\partial e}\left[\frac{\bar{a}_e(x)}{\alpha_0 + \zeta_0 \bar{a}_e(x)}\right] = \frac{\alpha_0 g_0 w}{(\alpha_0 + \zeta_0 \bar{a}_e)^2} \ge 0$$

and not identically zero in some segment of $[-x_m, 1]$. □

### 3.3.2 A Robustness Index

In Chapter 2 we have introduced a robustness index $R_b(t)$ to measure the deviations of ectopic signaling gradient after ligand synthesis rate enhancement ($e > 1$). Now, to have more

descriptive notation, we let $b_1(x,t)$ be the normalized signaling morphogen concentration for a normal ($e = 1$) ligand synthesis rate $v_L(x,t) = \bar{v}_L H(-x)$ (after normalization) and let $b_e(x,t)$ be the same quantity for an enhanced (ectopic) synthesis rate $e\bar{v}_L H(-x)$ . Then the *signal robustness index* $R_b$ will be:

$$R_b(t) = \frac{1}{b_h - b_\ell}\sqrt{\frac{1}{x_\ell - x_h}\int_{x_h}^{x_\ell}[b_e(x,t) - b_1(x,t)]^2 dx} \tag{3.19}$$

where $0 \le b_\ell(t) < b_h(t) \le b(-x_m, t)$ and $-x_m \le x_h < x_\ell \le 1$.

When a system is in steady state, we have

$$\bar{b}_1(x) = \lim_{t\to\infty} b_1(x,t), \qquad \bar{b}_e(x) = \lim_{t\to\infty} b_e(x,t). \tag{3.20}$$

Then the robustness index $R_b(t)$ tends to a constant $\bar{R}_b$:

$$\bar{R}_b = \lim_{t\to\infty} R_b(t) = \frac{1}{\bar{b}_h - \bar{b}_\ell}\sqrt{\frac{1}{x_\ell - x_h}\int_{x_h}^{x_\ell}[\bar{b}_e(x) - \bar{b}_1(x)]^2 dx} \tag{3.21}$$

As before, we take $x_h = 0$ so that $\bar{b}_h = \bar{b}_1(0)$ for a representative magnitude as a measure of the extent of the root-mean-square deviation. For the other end, we take $x_\ell = 1$ so that $\bar{b}_\ell = \bar{b}_1(1) = 0$. In that case, (3.21) simplifies to

$$\bar{R}_b = \frac{1}{\bar{b}_1(0)}\sqrt{\int_0^1 [\bar{b}_e(x) - \bar{b}_1(x)]^2 dx}. \tag{3.22}$$

### 3.3.3 Approximate Solution for Low Receptor Occupancy

When a morphogen system is in a state of LRO (before and after ligand synthesis rate enhancement) so that $g_0 a_e/g_R \ll \alpha_0$, we have from (3.17)-(3.18) the following approximate steady state expression for the signaling gradients of the normal (wild type) and (environ-

mentally or genetically) perturbed system:

$$\bar{b}_e(x) \;\sim\; \frac{e\bar{v}_L}{\alpha_0\mu_L^2}\frac{\sinh(\mu_L x_m)\sinh(\mu_L(1-x))}{\cosh(\mu_L(1+x_m))} = \frac{\bar{v}_L}{\alpha_0\mu_L^2}\bar{B}_e(x) = \frac{\bar{v}_L}{\alpha_0\mu_L^2}\left[e\bar{B}_1(x)\right], \qquad (3.23)$$

for $0 \le x \le 1$, where $\mu_L^2 = g_L + g_0/\alpha_0$ with $\mu_L^2 \simeq h_0 + g_L$ whenever $f_0 \ll g_0$ (as it is for *Dpp* in Drosophila wing imaginal disc).

When $x_h = 0$, for LRO systems we have from (3.17) and (3.18)

$$\bar{b}_h = \bar{b}_1(0) \simeq \frac{\bar{v}_L}{\alpha_0\mu_L^2}\frac{\sinh(\mu_L x_m)\sinh(\mu_L \ell_M)}{\cosh(\mu_L(\ell_M + x_m))} \;= \frac{e\bar{v}_L}{\alpha_0\mu_L^2}\;\bar{B}_1(0). \qquad (3.24)$$

By taking $x_\ell = 1$ and $\bar{b}_\ell = \bar{b}(1) = 0$ and with $e = 2$ for the enhanced synthesis rate, $\bar{R}_b$, in the absence of any feedback, is approximately given by

$$\begin{aligned}\bar{R}_b \simeq \bar{r}_b &= \frac{1}{\sinh(\mu_L)}\sqrt{\int_0^1 [\sinh(\mu_L(1-x))]^2 dx} \\ &= \frac{1}{\sinh(\mu_L)}\sqrt{\frac{1}{2}\left(\frac{\sinh(2\mu_L)}{2\mu_L} - 1\right)} \equiv \gamma. \end{aligned} \qquad (3.25)$$

## 3.4 Feedback in Transient Phase

For a biological organism a feedback mechanism generally would not become effective until the enhanced signaling reaches a noticeable level of ectopicity. Typically, this occurs during the transient phase of the development (and not when the system is already in a quasi-steady state). Most likely the organism does not react instantaneously, so there might be a delay in sensing the excessive signaling and the actual initiation of the response with the delay time short compared to the time to quasi-steady state. For systems capable of repeated feedbacks, their impact prior to steady state may be cumulative toward eventual patterning

and development. It is important then to investigate feedback effective during the transient phase of the signaling morphogen gradient formation.

In principle, the developing organism may adjust continuously with continuous feedback but is unlikely to function with such sensitivity or efficiency. It is more likely to make feedback adjustments at a few instants or perhaps only once at some threshold ectopicity. As a proof-of-concept investigation, we consider two models of a feedback adjustment after each time interval $\tau$, both for the special case of $n = 1$, to illustrate the method of solution for this class of problems.

Let $t_k = k\tau, k = 0, 1, 2, 3, ....$and suppose feedback adjustments are made only at $t_1, t_2, t_3, t_4, \ .....$ and not in between these instants in time. We designate the time interval $[t_k, t_{k+1})$ as period $k$. For both models, an additional feedback adjustment is made during period $k$ on the enhanced ligand synthesis rate $v_L(x,t) \equiv v_e^{(k-1)}(x,t)$ of the previous time interval. The adjustment is by a factor $(1 + cR_b(\bar{t}_k))^{-1}$ for some constant $c$ and some instant $\bar{t}_k$ (keeping $n = 1$ for this first effort).

In this section, we investigate the *first model* in which feedback adjustment for period $k$ is made at the start time $t_k$ of that time interval on the basis of the robustness index $R_b$ at that moment so that $\bar{t}_k = t_k$. In that case, we have for period $k$

$$v_L(x,t) \equiv v_e^{(k)}(x,t) = \frac{v_e^{(k-1)}(x,t)}{1 + cR_b(t_k)} \equiv e\kappa_k \bar{v}_L H(-x).$$

We now examine the evolution of the signaling gradient with time in successive time intervals $[t_k, t_{k+1})$.

## The Interval $[0, t_1)$

In this initial interval corresponding to $k = 0$, the enhanced ligand synthesis rate with (our nonlocal spatially uniform) feedback is

$$v_L = \frac{e\bar{v}_L H(-x)}{1 + cR_b(t_0)} \;=\; e\bar{v}_L H(-x) \equiv v_e^{(0)}(x,t) \qquad (0 \le t \le t_1 = \tau) \tag{3.26}$$

since

$$\begin{aligned} R_b(t_0) &= \frac{1}{\bar{b}_h}\int_0^1 [b_e(x,t_0) - b_1(x,t_0)]^2 dx \\ &= \frac{1}{\bar{b}_h}\int_0^1 [b_e^{(0)}(x,0) - b_1(x,0)]^2 dx = 0 \end{aligned} \tag{3.27}$$

given $b_e(x,0) = b_1(x,0) = 0$ by the initial conditions. To emphasize that the result applies only to the initial time interval $[0, t_1)$, we adopt the notation

$$R_b(t_0) \equiv R_b^{(0)}(0) = 0.$$

Thus the feedback is not effective in this interval. In that case, the synthesis rate of the ectopic IBVP (3.1), (3.2), (3.8) and (3.9) in this time interval, $v_L = v_e^{(0)}(x,t) = e\bar{v}_L H(-x)$ is the same as the problem without feedback. The solution, to be denoted by $a_e^{(0)}(x,t)$, $b_e^{(0)}(x,t)$ and $r_e^{(0)}(x,t)$ (including the wild type corresponding to $e = 1$ in (3.26)) can be obtained by numerical methods with the initial conditions (3.9) at $t = 0$ (as it has been done in [23] for problems without feedback).

## The Interval $[t_1, t_2)$

In this next interval $\tau = t_1 \leq t < t_2 = 2\tau$ corresponding to $k = 1$, the enhanced ligand synthesis rate with feedback is

$$v_L = \frac{e\bar{v}_L H(-x)}{1 + cR_b(t_1)} \equiv v_e^{(1)}(x,t) \qquad (\tau \leq t < \tau).$$

with

$$\begin{aligned} R_b(t_1) &= \frac{1}{\bar{b}_h}\int_0^1 [b_e(x,t_1) - b_1(x,t_1)]^2 dx \\ &= \frac{1}{\bar{b}_h}\int_0^1 [b_e^{(0)}(x,\tau) - b_1(x,\tau)]^2 dx \equiv R_b^{(1)}(t_1) \end{aligned} \tag{3.28}$$

since, by continuity, $b_e(x,t_1)$ is the same at the junction $t_1$ of the two adjacent intervals. $b_e^{(1)}(x,\tau) = b_e^{(0)}(x,\tau)$ by continuity. With $b_e^{(0)}(x,\tau)$ already known from the solution of the IBVP for the previous interval, the modified synthesis rate for the ectopic IBVP in this time interval,

$$v_L = v_e^{(1)}(x,t) = \frac{e\bar{v}_L H(-x)}{1 + cR_b^{(1)}(t_1)} = e\kappa_1 \bar{v}_L H(-x) \qquad (t_1 \leq t < t_2), \tag{3.29}$$

is a known function. The solution of the IBVP in $[t_1, t_2)$, denoted by $\left\{a_e^{(1)},\ b_e^{(1)},\ r_e^{(1)}\right\}$, can be obtained by numerical methods with the continuity condition

$$\left\{a_e^{(1)}(x,t_1),\ b_e^{(1)}(x,t_1),\ r_e^{(1)}(x,t_1)\right\} = \left\{a_e^{(0)}(x,t_1),\ b_e^{(0)}(x,t_1),\ r_e^{(0)}(x,t_1)\right\}$$

as the initial conditions and with the quantities on the right already known from the solution for the previous interval.

Note that feedback on the synthesis rate is now effective for the interval $[t_1, t_2)$. As such the solution of the IBVP (3.1), (3.2), (3.8) and (3.9) for the ectopic problem in this time

interval is generally different from the corresponding solution without feedback (the special case $c = 0$). Anticipating the subsequent development, we adopt the notation $\kappa_0 = 1$ so that we may write

$$\kappa_1 = \frac{\kappa_0}{1 + cR_b^{(1)}(t_1)}.$$

## The Interval $[t_2, t_3)$

In the next interval $2\tau = t_2 \leq t < t_3 = 3\tau$ corresponding to $k = 2$, the enhanced ligand synthesis rate with feedback is

$$v_L = \frac{v_e^{(1)}(x,t)}{1 + cR_b(t_2)} \equiv v_e^{(2)}(x,t).$$

Similar to the previous interval, $R_b(t_2)$ for the new interval is completely determined from the solution of the previous interval at the junction $t_2$ between the two adjacent intervals:

$$R_b(t_2) = \frac{1}{\bar{b}_h} \int_0^1 [b_e^{(1)}(x,t_2) - b_1(x,t_2)]^2 dx \equiv R_b^{(2)}(t_2).$$

The corresponding solution of the IBVP (3.1), (3.2), (3.8) and (3.9), to be denoted by $\left\{a_e^{(2)},\ b_e^{(2)},\ r_e^{(2)}\right\}$, may be obtained by numerical methods starting from the continuity conditions at $t_2$:

$$\{a_e^{(2)}(x,t_2),\ b_e^{(2)}(x,t_2), r_e^{(2)}(x,t_2)\} = \{a_e^{(1)}(x,t_2),\ b_e^{(1)}(x,t_2), r_e^{(1)}(x,t_2)\} \tag{3.30}$$

with the quantities on the right already obtained in the discussion of the previous interval. The synthesis rate for the ectopic IBVP with feedback in this time interval may be written

as

$$v_L = v_e^{(2)}(x,t) = \ e\bar{v}_L\kappa_2 H(-x) \qquad (t_2 \le t < t_3) \tag{3.31}$$

with

$$\kappa_2 = \frac{\kappa_1}{1 + cR_b^{(2)}(t_2)} = .\frac{\kappa_0}{\left[1 + cR_b^{(2)}(t_2)\right]\left[1 + cR_b^{(1)}(t_1)\right]}. \tag{3.32}$$

## The Interval $[t_k, t_{k+1}),\ k \ge 3$ :

In a general interval $k\tau = t_k \le t < t_{k+1} = (k+1)\tau$ for $k \ge 3$, the enhanced ligand synthesis rate with feedback is

$$v_L = \frac{v_e^{(k-1)}(x,t)}{1 + cR_b(t_k)} \ = \frac{e\bar{v}_L\kappa_{k-1}H(-x)}{\left[1 + cR_b^{(k)}(t_k)\right]} = e\bar{v}_L\kappa_k H(-x) \equiv v_e^{(k)}(x,t) \qquad (t_{k-1} \le t - \tau < t_k) \tag{3.33}$$

with

$$R_b^{(k)}(t_k) = \frac{1}{\bar{b}_h}\int_0^1 [b_e^{(k-1)}(x,t_k) - b_1(x,t_k)]^2 dx. \tag{3.34}$$

Hence, the feedback adjusted synthesis rate of the ectopic IBVP in the interval $t_k \le t < t_{k+1}$ is

$$v_L = v_e^{(k)}(x,t) = \quad e\bar{v}_L\kappa_k H(-x) \quad (t_k \le t < t_{k+1}) \tag{3.35}$$

with

$$\kappa_k(t_1,\ ....,\ t_k) = \frac{1}{\prod_{j=1}^{k}\left[1 + cR_b^{(j)}(t_j)\right]} \tag{3.36}$$

given $\kappa_0 = 1$. In the expression (3.36), the robustness indices $\{R_b^{(j)}(t_j)\}$ are calculated from the formula (3.34) (with $k$ replaced by $j$ ) sequentially with increasing $j$ starting from $j = 1$.

The corresponding solution of the IBVP (3.1), (3.2), (3.8) and (3.9), denoted by $\left\{a_e^{(k)},\ b_e^{(k)},\ r_e^{(k)}\right\}$, may be obtained by numerical methods starting from the continuity conditions at $t_k$:

$$\{a_e^{(k)}(x,t_k),\ b_e^{(k)}(x,t_k), r_e^{(k)}(x,t_k)\} = \{a_e^{(k-1)}(x,t_k),\ b_e^{(k-1)}(x,t_k), r_e^{(k-1)}(x,t_k)\}.$$

### 3.4.1 Numerical Results

We see that $\kappa_k$ decreases with $k$. Thus $R_b^{(k)}$ also decreases with $k$. Then the iterative algorithm above is expected to converge. To compare the effectiveness of cumulative repeated feedback adjustments during the transient phase with that of steady state theory obtained in the previous chapter, we apply the present approach to the illustrative example already examined. With the system parameter values given in Table 2.1, we take $c = 1$, $n = 1$ and $\tau = 4$ in units of $(D/X_{\max}^2)^{-1}$ with the system reaching steady state around $5\tau = 20$. Note that the top curve in the Figure 3.1 is essentially the quasi-steady state $b_e$ (for $e = 2$) without feedback with the signaling gradient reaching steady state around $t = 20$, with the onset of morphogen synthesis at $t = 0$. The expected role of any feedback adjustment is to bring $b_e^{(5)}(x, 20)$ as close as possible to the the bottom steady state wild-type signaling gradient curve in that figure ($e = 1$ and no feedback). After the feedback adjustments become effective (starting with $k = 2$), the cumulative effect of the repeated adjustments continues to reduce the signaling gradient in successive time intervals, leading to a gradient

$b_e^{(5)}(x, 20)$ very close to the wild-type gradient prior to synthesis rate being enhanced from $e = 1$ to $e = 2$.

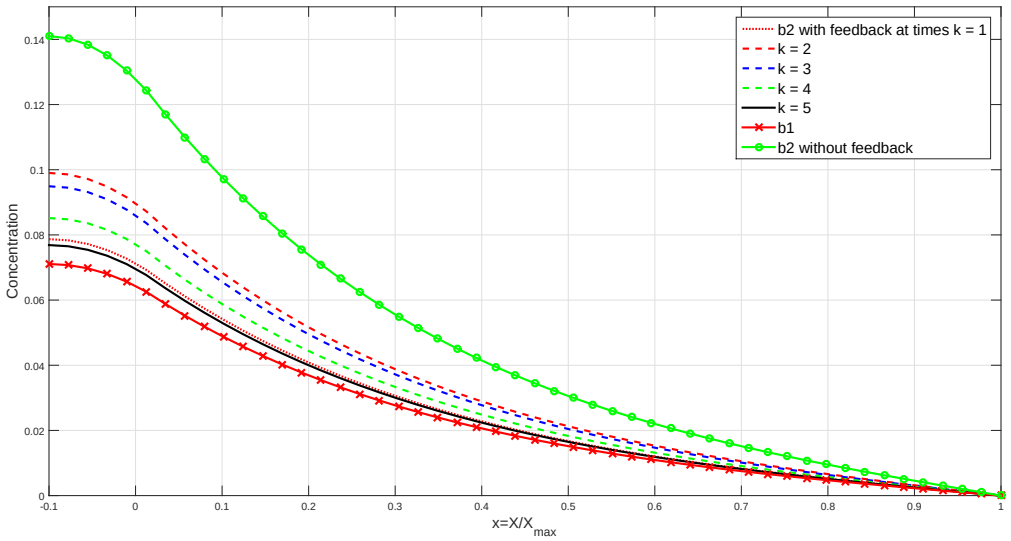


Figure 3.1: Various Signaling Gradients (some with feedback adjustment): Wild-type $b_1(x, 20)$ with ($e = 1$ and $c = 0$) at the bottom; Ectopic $b_e(x, 20)$(with $e = 2$ and $c = 0$) at the top; In between from top down are $b_e(x, t_k)$ at $t = t_2, t_3, t_4, t_1$ and $t_5 = 20$.

Even more important is the shape of the wild-type gradient being maintained by the feedback adjusted ectopic gradient. More specifically, the spatially uniform nonlocal feedback mechanism does not suffer the same fate as the Hill's function type feedback mechanism applied to the signaling receptor synthesis rate first found in [17], see Figure 3.2 (reproduced here for comparison).

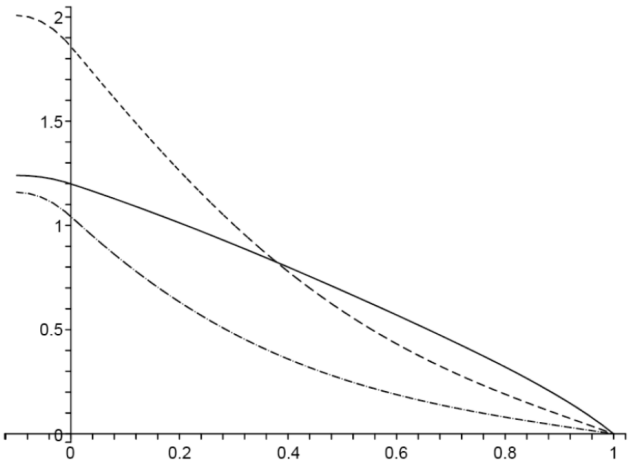


Figure 3.2: Negative feedback of Hill's function type on receptor synthesis rate: Wild-type signaling gradient ($e = 1$, no feedback) - bottom dashed curve; Ectopic signaling gradient ($e = 2$ without feedback) - top dashed curve; Ectopic signaling gradient ($e = 2$) with negative feedback on receptor synthesis

Table 3.1 Comparison of $R_b(x, t_k)$

| Transient ($c = 1$) | | Steady State |
|---|---|---|
| *No Delay* ($k$) | *With Delay* ($k$) | *From* [19] ($c$) |
| 0.24937 (1) | 0.24937 (1) | 0.39379 (0) |
| 0.26524 (2) | 0.36501 (2) | 0.24051 (1) |
| 0.18738 (3) | 0.31731 (3) | 0.18296 (2) |
| 0.10145 (4) | 0.18769 (4) | ..... |
| 0.03769 (5) | 0.05747 (5) | 0.11163 (4) |

In the first column of Table 3.1, we report robustness index values at different instants in time for the feedback mechanism described above. Except for an increase in $R_b^{(2)}(x, t_2)$ over $R_b^{(1)}(x, t_1)$ (because there is no feedback adjustment for the interval $[0, 4)$), modifications of the synthesis stimulated by feedback repeatedly reduce the robustness index to below the acceptable robustness threshold value of 0.2 by $t = 12$ and well below that threshold by $t = 20$ (effectively in steady state). We compare these results to the steady state approach discussed in the previous chapter (also reported in [19]) where the same nonlocal spatially uniform feedback mechanism becomes effective when the system reaches its steady state. The results using that approach are reproduced in the third column of Table 3.1 and show

that $R_b(x,\infty)$ is well above 0.2 for $c = 1$ (the same value of $c$ used for all cases in the first column).

## 3.5 Transient Feedback with Delay

In this section, we investigate the *second model* when the effect of feedback through the robustness index $R_b(\bar{t})$ is recorded at the start of the time interval $t_k$ but reacting with a delayed time $\tau$ so that $\bar{t}_k = t_k - \tau = t_{k-1}$:

$$v_L(x,t) \equiv v_e^{(k)}(x,t) = \frac{v_e^{(k-1)}(x,t)}{1 + cR_b(t_{k-1})} \equiv e\bar{v}_L d_k H(-x)$$

We now examine the evolution of the signaling gradient with time in successive time intervals $[t_k, t_{k+1})$.

### The Interval $[0, t_1)$

In the initial interval $(0 = t_0 \leq t < t_1 = \tau)$ corresponding to $k = 0$, the enhanced ligand synthesis rate with (our spatially uniform) feedback is

$$v_L = \frac{e\bar{v}_L H(-x)}{1 + cR_b(t_0 - \tau)} = \frac{e\bar{v}_L H(-x)}{1 + cR_b(-\tau)} = \quad e\bar{v}_L H(-x) \equiv v_e^{(0)}(x,t) \tag{3.37}$$

(again with the subscript $e$ corresponding the magnitude of ectopicity) since $b_e(x,t) = b_1(x,t) = 0$ for $t$ prior to the onset of morphogen synthesis so that

$$R_b(-\tau) = \frac{1}{\bar{b}_h} \int_0^1 [b_e(x,-\tau) - b_1(x,-\tau)]^2 dx = 0.$$

With

$$R_b(t_0 - \tau) \equiv R_b^{(0)}(-\tau) = 0$$

so that feedback is not effective given the delay, the synthesis rate of the ectopic IBVP (3.1), (3.2), (3.8) and (3.9) in this time interval $v_L = v_e^{(0)}(x,t) = \ e\bar{v}_L H(-x)\ $ is the same as that without feedback. The solution, to be denoted by $a_e^{(0)}(x,t)$, $b_e^{(0)}(x,t)$ and $r_e^{(0)}(x,t)$ (including the wild type corresponding to $e = 1$ in (3.26)) can be obtained by numerical methods with the initial conditions (3.9) at $t = 0$.

## The Interval $[t_1, t_2)$

In this next interval $\tau = t_1 \le t < t_2 = 2\tau$ corresponding to $k = 1$, the enhanced ligand synthesis rate with feedback is

$$v_L = \frac{v_e^{(1)}(x,t)}{1 + cR_b(t_1 - \tau)} = \frac{e\bar{v}_L H(-x)}{1 + cR_b(0)} \ \equiv v_e^{(1)}(x,t) \qquad (0 \le t - \tau < \tau).$$

With

$$\begin{aligned} R_b(t_1 - \tau) &= \frac{1}{\bar{b}_h} \int_0^1 [b_e(x,0) - b_1(x,0)]^2 dx \\ &= \frac{1}{\bar{b}_h} \int_0^1 [b_e^{(0)}(x,0) - b_1(x,0)]^2 dx = 0, \end{aligned} \tag{3.38}$$

given the initial conditions $b_e(x,0) = b_1(x,0) = 0$, we have also

$$R_b(t_1 - \tau) \equiv R_b^{(1)}(0) = 0$$

in the interval $t_1 \leq t < t_2$ . The synthesis rate for the ectopic IBVP in this time interval is

$$v_L = v_e^{(1)}(x,t) = \frac{e\bar{v}_L H(-x)}{1 + cR_b^{(1)}(0)} = e\bar{v}_L H(-x) \qquad (t_1 \leq t < t_2).$$

The solution, denoted by $\left\{a_e^{(1)}(x,t),\ b_e^{(1)}(x,t),\ r_e^{(1)}(x,t)\right\}$ is the same as one without feedback and can be obtained by the usual numerical methods with the continuity condition

$$\left\{a_e^{(1)}(x,t_1),\ b_e^{(1)}(x,t_1),\ r_e^{(1)}(x,t_1)\right\} = \left\{a_e^{(0)}(x,t_1),\ b_e^{(0)}(x,t_1),\ r_e^{(0)}(x,t_1)\right\}$$

as initial conditions. Note that the quantities on the right have already been obtained for the previous interval.

With feedback on the synthesis rate not yet effective for the combined interval $[0, t_2)$, the solution of the IBVP (3.1), (3.2), (3.8) and (3.9) for the ectopic problem in the time interval $t_1 \leq t < t_2$ is merely a continuation of that for the previous interval.

## The Interval $[t_2, t_3)$

In the next interval $2\tau = t_2 \leq t < t_3 = 3\tau$ corresponding to $k = 2$, the enhanced ligand synthesis rate with feedback is

$$v_L = \frac{v_e^{(1)}(x,t)}{1 + cR_b(t_2 - \tau)} = \frac{e\bar{v}_L H(-x)}{1 + cR_b(\tau)} \equiv v_e^{(2)}(x,t)$$

with

$$\begin{aligned} R_b(t_2 - \tau) &= \frac{1}{\bar{b}_h} \int_0^1 [b_e(x,\tau) - b_1(x,\tau)]^2 dx \\ &= \frac{1}{\bar{b}_h} \int_0^1 [b_e^{(1)}(x,\tau) - b_1(x,\tau)]^2 dx = R_b^{(2)}(t_1) \end{aligned} \tag{3.39}$$

given $b_e^{(2)}(x,t_1) = b_e^{(1)}(x,t_1)$ by continuity. For the interval $t_1 \le \bar{t} = t - \tau < t_2$ and feedback adjustment effective only at $t_1$, we have

$$R_b(t_2 - \tau) = R_b^{(2)}(t_1)$$

and the feedback modified synthesis rate for the ectopic IBVP in this time interval is

$$v_L = v_e^{(2)}(x,t) = \frac{e\bar{v}_L H(-x)}{1 + cR_b^{(2)}(t_1)} \equiv e\bar{v}_L d_2 H(-x) \qquad (t_2 \le t < t_3) \tag{3.40}$$

with

$$d_2 = \frac{1}{1 + cR_b^{(2)}(t_1)}. \tag{3.41}$$

With the feedback adjusted synthesis rate completely known for the interval $t_2 \le t < t_3$, the solution of the IBVP (3.1), (3.2), (3.8) and (3.9), denoted by $\left\{a_e^{(2)},\ b_e^{(2)},\ r_e^{(2)}\right\}$, can be obtained by numerical methods starting from the continuity conditions at $t_2$:

$$\{a_e^{(2)}(x,t_2),\ b_e^{(2)}(x,t_2), r_e^{(2)}(x,t_2)\} = \{a_e^{(1)}(x,t_2),\ b_e^{(1)}(x,t_2), r_e^{(1)}(x,t_2)\}. \tag{3.42}$$

with the quantities on the right already obtained for the previous interval.

Given $v_L = v_e^{(2)}(x,t) = e\bar{v}_L d_2(t_1) H(-x)$ which is known but different from $v_e^{(1)}(x,t) = v_e^{(0)}(x,t) = e\bar{v}_L H(-x)$, feedback on the synthesis rate is effective in the interval $[t_2, t_3)$. As such the solution of the IBVP for the transient ligand concentration for the ectopic problem is expected to be different from the correspond solution without feedback in this interval.

## The Interval $[t_k, t_{k+1}),\ k \geq 3$ :

In period $k$, where $k\tau = t_k \leq t < t_{k+1} = (k+1)\tau$ for $k \geq 3$, the enhanced ligand synthesis rate with feedback is

$$v_L = \frac{v_e^{(k-1)}(x,t)}{1 + cR_b(t_k - \tau)} = \frac{e\bar{v}_L d_{k-1} H(-x)}{[1 + cR_b(t_{k-1})]} \equiv v_e^{(k)}(x,t) \qquad (t_{k-1} \leq t - \tau < t_k) \tag{3.43}$$

with

$$\begin{aligned} R_b(t_k - \tau) &= \frac{1}{\bar{b}_h} \int_0^1 [b_e(x, t_{k-1}) - b_1(x, t_{k-1})]^2 dx \\ &= \frac{1}{\bar{b}_h} \int_0^1 [b_e^{(k-1)}(x, t_{k-1}) - b_1(x, t_{k-1})]^2 dx = R_b^{(k)}(t_{k-1}) \end{aligned} \tag{3.44}$$

Hence, the feedback adjusted synthesis rate of the ectopic IBVP in the interval $t_k \leq t < t_{k+1}$ is

$$v_L = v_e^{(k)}(x,t) = \quad e d_k \bar{v}_L H(-x) \tag{3.45}$$

where $d_0 = d_1 = 1$ and

$$d_k(t_1,\ ....,\ t_{k-1}) = \frac{1}{\prod_{j=2}^{k} \left[1 + cR_b^{(j)}(t_{j-1})\right]} \qquad (k \geq 2).$$

The solution of the IBVP, denoted by $\left\{a_e^{(k)},\ b_e^{(k)}, r_e^{(k)}\right\}$, can be obtained by numerical methods starting with the continuity condition:

$$\{a_e^{(k)}(x,t_k),\ b_e^{(k)}(x,t_k), r_e^{(k)}(x,t_k)\} = \{a_e^{(k-1)}(x,t_k),\ b_e^{(k-1)}(x,t_k), r_e^{(k-1)}(x,t_k)\}.$$

### 3.5.1 Numerical Results

To compare the effectiveness of the cumulative effects from repeated (delayed) feedback adjustments during the transient phase with that of steady state theory obtained in the previous chapter, we apply the present approach to the illustrative example already examined. With the system parameter values given in Table 2.1, we take $c = 1$ and $\tau = 4$ in units of $(D/X_{\max}^2)^{-1}$ to obtain a similar set of solutions for delayed feedback modified $b_e(x,t)$ at $t_k = \tau, 2\tau, 3\tau, 4\tau$ and $5\tau = 20$ as well as $b_e(x,t)$ without feedback for $e = 1$ (wild-type) and $e = 2$ (ectopic gradient). The results are shown in Figure 3.3.

As in Figure 3.1, the top curve in the figure is essentially the quasi-steady state $b_e$ (for $e = 2$) without feedback with the signaling gradient reaching steady state around $t = 20$. The expected role of any feedback adjustment is to bring $b_e^{(5)}(x, 20)$ as close as possible to the the bottom steady state wild-type signaling gradient curve in that figure ($e = 1$ and no feedback). After the feedback adjustments become effective (starting with $k = 2$), the cumulative effect of the repeated adjustments continues to reduce the signaling gradient in successive time intervals, leading to a gradient $b_e^{(5)}(x, 20)$ very close to the wild-type gradient prior to synthesis rate being enhanced from $e = 1$ to $e = 2$.

However, there are significant differences between the same nonlocal spatially uniform feedback mechanism without and with delay. For example, the feedback adjusted ectopic signaling gradient is seen to be slightly higher than the ectopic gradient during the early transient phase of $k = 1$; but this relative position is reversed for the same feedback mechanism without delay. The reason for the difference is associated with the unmodified increase in the deviation of the ectopic gradient from the wild-type for a second period so that feedback adjustment of the development actually occurs one period later when the feedback implementation is delayed by one period.

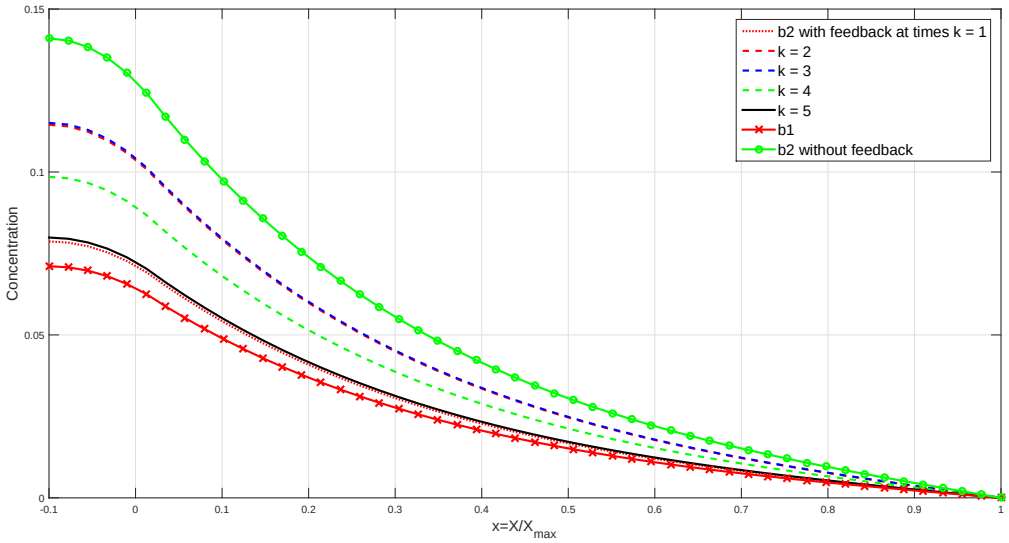


Figure 3.3: Various Signaling Gradients (some with delayed feedback): Wild-type with ($e = 1$ and $c = 0$) at the bottom; Ectopic (with $e = 2$ and $c = 0$) at the top; In between from top down are $b_e^{(k)}(x, t)$ at $t_k = 2\tau, 3\tau, 4\tau, 5\tau = 20$ and $\tau$.

In the second column of Table 3.1, we report robustness index values at different instants in time for the same feedback mechanism as in the previous section but now with a delay in sensing the need for, and in implementing feedback adjustments. Given that modification of the synthesis rate stimulated by feedback only begins to be effective starting with period 2. There is then no effect of feedback in period 0 and period 1 leading to a larger $R_b$ after the initial period. To reach the same robustness index with the delayed feedback would require additional adjustments well into the steady state phase or an increase in the value for $c$ to 2 or higher (or increasing $n$ to a large value than 1).

## 3.6 Time Dependent LRO Problem

### 3.6.1 A Perturbation for the Transient Phase of a LRO State

From the results for our illustrative example, we see that both the wild-type and ectopic steady state behavior meet the requirements for a LRO state. For such cases, we may take during the transient phase the following perturbation expansions in terms of a small dimensionless parameter $\varepsilon$:

$$\{a_e, b_e, r_e\} = \{0, 0, 1\} + \sum_{i=1} \{A_e^{(i)}(x,t), B_e^{(i)}(x,t), R_e^{(i)}(x,t)\}\varepsilon^i$$

with $0 < \varepsilon \ll 1$. (One possible choice of the small parameter $\varepsilon$ is the dimensionless ligand synthesis rate $\bar{v}_L$ which is necessarily small for a state of LRO.) Upon substituting these expansions in to the IBVP (3.1), (3.2), (3.8) and (3.9), the leading terms of the expansions $\{A_e^{(1)}(x,t), B_e^{(1)}(x,t), 1\}$ and the first order correction term $R_e^{(1)}(x,t)$ for receptor concentration are found to be determined by the simpler IBVP:

$$\frac{\partial A_e^{(1)}}{\partial t} = \frac{\partial^2 A_e^{(1)}}{\partial x^2} - (h_0 + g_L)A_e^{(1)} + f_0 B_e^{(1)} + v_L(x,t), \tag{3.46}$$

$$\frac{\partial B_e^{(1)}}{\partial t} = h_0 A_e^{(1)} - (f_0 + g_0)B_e^{(1)}, \qquad \frac{\partial R_e^{(1)}}{\partial t} = -h_0 A_e^{(1)} + f_0 B_e^{(1)} - g_R R_e^{(1)}, \tag{3.47}$$

with

$$x = -x_m : \quad \frac{\partial A_e^{(1)}}{\partial x} = 0, \qquad x = 1 : \quad A_e^{(1)} = 0, \tag{3.48}$$

all for $t > 0$, and

$$t = 0 : \quad A_e^{(1)} = B_e^{(1)} = R_e^{(1)} = 0 \qquad (0 \le x \le 1). \tag{3.49}$$

The two unknowns $A_e^{(1)}(x,t)$ and $B_e^{(1)}(x,t)$ may be solved separately with the solution used in the second ODE of (3.47) and the initial condition $R_e^{(1)}(x,0)=0$ for the determination of $R_e^{(1)}(x,t)$. The first approximation solution $\left\{A_e^{(1)}(x,t),\ B_e^{(1)}(x,t),1\right\}$ is designated as the *low receptor occupancy solution* for the problem.

### 3.6.2 Eigenfunction Expansions

For $t$ in the interval $[t_k,t_{k+1})$, we have

$$v_L(x,t)=e\kappa_k\bar{v}_L H(-x)\equiv v_e^{(k)}(x,t),\qquad \kappa_k=\frac{1}{\prod\limits_{j=2}^{k}\left[1+cR_b^{(j)}(t_{j-1})\right]}, \tag{3.50}$$

which is independent of time except for the constant $\kappa_k$ characterizing the cumulative effect of prior feedback, A particular solution of the linear IBVP for $A_e^{(1)}(x,t)$ and $B_e^{(1)}(x,t)$ for that interval is the steady state LRO solution $\bar{A}_{ek}(x)$ given in (3.17) and

$$\bar{B}_{ek}(x)=\frac{\bar{A}_{ek}(x)}{\alpha_0}, \tag{3.51}$$

for the synthesis rate (3.50) with $e\bar{v}_L$ replaced by $e\kappa_k\bar{v}_L$. It is worth pointing out that the particular solution pair $\{\bar{A}_{ek}(x),\bar{B}_{ek}(x)\}$, though time independent for at least the initial period, generally changes from period to period since the synthesis rate $v_L$ is being adjusted with a new robustness index from period to period. For that reason, we take the LRO solution $A_e^{(1)}(x,t)$ and $B_e^{(1)}(x,t)$ in period $k$ as a sum of the corresponding particular solution and a transient counterpart

$$A_e^{(1)}(x,t)=\bar{A}_{ek}(x)+\hat{A}_{ek}(x,t),\qquad B_e^{(1)}(x,t)=\bar{B}_{ek}(x)+\hat{B}_{ek}(x,t). \tag{3.52}$$

The complementary solutions $\hat{A}_e(x,t)$ and $\hat{B}_e(x,t)$ are determined by the IBVP

$$\frac{\partial \hat{A}_{ek}}{\partial t} = \frac{\partial^2 \hat{A}_{ek}}{\partial x^2} - (h_0 + g_L)\,\hat{A}_{ek} + f_0 \hat{B}_{ek}, \tag{3.53}$$

$$\frac{\partial \hat{B}_{ek}}{\partial t} = h_0 \hat{A}_{ek} - (f_0 + g_0)\hat{B}_{ek}, \tag{3.54}$$

subject to the boundary conditions

$$x = -x_m : \quad \frac{\partial \hat{A}_{ek}}{\partial x} = 0, \qquad\qquad x = 1 : \quad \hat{A}_{ek} = 0, \tag{3.55}$$

for $t_k \leq t < t_{k+1}$ and initial conditions

$$\left\{ \begin{array}{c} \hat{A}_{ek}(x,t_k) + \bar{A}_{ek}(x) \\ \hat{B}_{ek}(x,t_k) + \bar{B}_{ek}(x) \end{array} \right\} = \left\{ \begin{array}{c} \hat{A}_{ek-1}(x,t_k) + \bar{A}_{e(k-1)}(x) \\ \hat{B}_{e(k-1)}(x,t_k) + \bar{B}_{e(k-1)}(x) \end{array} \right\} \tag{3.56}$$

for $0 \leq x \leq 1$.

Given the linearity of the governing PDE and auxiliary conditions, the complementary solution of this IBVP may be obtained by eigenfunction expansions

$$\left\{ \begin{array}{c} \hat{A}_{ek}(x,t) \\ \hat{B}_{ek}(x,t) \end{array} \right\} = \sum_{j=0}^{\infty} \left\{ \begin{array}{c} a_{kj}(t) \\ b_{kj}(t) \end{array} \right\} \phi_j(x) \tag{3.57}$$

with

$$\phi_j(x) = \sin\left(\lambda_j \frac{1-x}{1+x_m}\right), \qquad \lambda_j = \left(j + \frac{1}{2}\right)\pi. \tag{3.58}$$

Once we substitute (3.57) into (3.53)-(3.54), we get

$$\frac{d}{dt}\left( \begin{array}{c} a_{kj}(t) \\ b_{kj}(t) \end{array} \right) = -C(\lambda_j^2) \left( \begin{array}{c} a_{kj}(t) \\ b_{kj}(t) \end{array} \right) \qquad (j = 0, 1, 2, \ ....)$$

where

$$C(\lambda_j^2) = \begin{bmatrix} c_{11} & c_{12} \\ c_{21} & c_{22} \end{bmatrix} = \begin{bmatrix} \lambda_j^2 + h_0 + g_L & -f_0 \\ -h_0 & f_0 + g_0 \end{bmatrix}.$$

The solution of the first order system for $a_{kj}(t)$ and $b_{kj}(t)$

$$\begin{pmatrix} a_{kj}(t) \\ b_{kj}(t) \end{pmatrix} = \begin{pmatrix} a_{kj}^{(1)} e^{-\omega_{kj}^{(1)} t} + a_{kj}^{(2)} e^{-\omega_{kj}^{(2)} t} \\ b_{kj}^{(1)} e^{-\omega_{kj}^{(1)} t} + b_{kj}^{(2)} e^{-\omega_{kj}^{(2)} t} \end{pmatrix} \tag{3.59}$$

where $\omega_{kj}^{(1)}$ and $\omega_{kj}^{(2)}$ are the two roots

$$\begin{pmatrix} \omega_{kj}^{(1)} \\ \omega_{kj}^{(2)} \end{pmatrix} = \frac{1}{2} \left\{ Tr[C] \pm \sqrt{(Tr[C])^2 - 4Det[C]} \right\}$$

of the quadratic equation for $\omega_{kj}$

$$\det \left[ \omega_{kj} I - C(\lambda_j^2) \right] = \omega_{kj}^2 + Tr[C]\omega_{kj} + Det[C] = 0.$$

The coefficients $\{a_{kj}^{(1)}, a_{kj}^{(2)}, b_{kj}^{(1)}, b_{kj}^{(2)}\}$ are related by

$$b_{kj}^{(m)} = \frac{h_0 a_{kj}^{(m)}}{\omega_{kj}^{(m)} + f_0 + g_0}$$

with the two remaining unknowns $a_{kj}^{(1)}$ and $a_{kj}^{(2)}$ found from the two continuity conditions

(3.56) in the form

$$\begin{aligned}
&\left\{ \begin{array}{l} a_{kj}^{(1)} e^{-\omega_{kj}^{(1)} t_k} + a_{kj}^{(2)} e^{-\omega_{kj}^{(2)} t_k} \\ b_{kj}^{(1)} e^{-\omega_{kj}^{(1)} t_k} + b_{kj}^{(2)} e^{-\omega_{kj}^{(2)} t_k} \end{array} \right\} + \left\{ \begin{array}{l} \bar{a}_{kj} \\ \bar{b}_{kj} \end{array} \right\} \\
&= \left\{ \begin{array}{l} a_{(k-1)j}^{(1)} e^{-\omega_{kj}^{(1)} t_k} + a_{(k-1)j}^{(2)} e^{-\omega_{kj}^{(2)} t_k} \\ b_{(k-1)j}^{(1)} e^{-\omega_{kj}^{(1)} t_k} + b_{(k-1)j}^{(2)} e^{-\omega_{kj}^{(2)} t_k} \end{array} \right\} + \left\{ \begin{array}{l} \bar{a}_{(k-1)j} \\ \bar{b}_{(k-1)j} \end{array} \right\}
\end{aligned} \tag{3.60}$$

where $\{\bar{a}_{nj}, \bar{b}_{nj}\}$ are the coefficients of the eigenfunction expansions for the known particular solutions $\bar{A}_{ek}(x)$ and $\bar{B}_{ek}(x)$, respectively,

$$\int_{-x_m}^{1} [\phi_j(x)]^2 \, dx \left\{ \begin{array}{l} \bar{a}_{nj} \\ \bar{b}_{nj} \end{array} \right\} = \int_{-x_m}^{1} \phi_j(x) \left\{ \begin{array}{l} \bar{A}_{en}(x) \\ \bar{B}_{en}(x) \end{array} \right\} dx.$$

and $\{a_{(k-1)j}^{(1)},\ ....,\ b_{(k-1)j}^{(2)}\}$ are known from the solution of period $(k-1)$, i.e., $[t_{k-1}, t_k)$.

Given

$$c_{11}c_{22} - c_{12}c_{21} = g_0(\lambda_j^2 + h_0 + g_L) + f_0\left(\lambda_j^2 + g_L\right) > 0 \tag{3.61}$$

and

$$\begin{aligned}
(Tr[C])^2 - 4Det[C] &= (c_{11} + c_{22})^2 - 4(c_{11}c_{22} - c_{12}c_{21}) \\
&= (c_{11} - c_{22})^2 + 4c_{12}c_{21} = (c_{11} - c_{22})^2 + f_0 h_0 > 0,
\end{aligned} \tag{3.62}$$

both $\omega_{kj}^{(1)}$and $\omega_{kj}^{(2)}$ are real (by (3.62)) and positive (by (3.61)). It follows from (3.59) that the transient components are dissipative and decay with time.

### 3.6.3 Numerical Results

The solution process above may be implemented to obtain an approximate LRO solution for our problem. Instead, we obtain a simpler solution by taking advantage of the fact that $f_0 \ll g_0$. Given that the example in Table 2.1 is of the LRO type, the eigenfunction solution of this section provides a mean to validate the numerical solutions discussed in the previous sections (but with the parameters in robustness index

$$R_b(t) = \frac{1}{b_h - b_\ell}\sqrt{\frac{1}{x_\ell - x_h}\int_{x_h}^{x_\ell}[b_e(x,t) - b_1(x,t)]^2 dx} \tag{3.63}$$

(as defined in (3.19)) re-set to take advantage of the orthogonality of the eigenfunctions. More specifically, we now take $x_h = -x_m$ instead of 0 but keep $x_\ell = 1$ to get

$$R_b(t) = \frac{1}{\bar{b}_h}\sqrt{\frac{1}{1 + x_m}\int_{-x_m}^{1}[b_e(x,t) - b_1(x,t)]^2 dx}. \tag{3.64}$$

While we may make use of the correct value $\tilde{b}_e(-x_m)$ for $\bar{b}_h$, it is just as appropriate to continue to use $\bar{b}_h = \bar{b}_1(0)$ as we have done herein.

For the steady state LRO and neglecting $f_0$ in $f_0 + g_0$, we have

$$a_1(x,t) = \bar{a}_1(x) \simeq \bar{A}_1(x) \equiv \frac{\bar{v}_L}{\mu_L^2} A_1(x), \tag{3.65}$$

where

$$A_1(x) = \begin{cases} \{1 - \frac{\cosh(\mu_L)}{\cosh(\mu_L(1+x_m))}\cosh(\mu_L(x + x_m))\} & (-x_m \le x \le 0) \\ \frac{\sinh(\mu_L x_m)}{\cosh(\mu_L(1+x_m))}\sinh(\mu_L(1-x)) & (0 \le x \le 1) \end{cases}, \tag{3.66}$$

We also have

$$\overline{u}_j = \frac{2}{1+x_m}\left\{\int_{-x_m}^{0}\left[1-\frac{\cosh(\mu_L)}{\cosh(\mu_L(1+x_m))}\cosh(\mu_L(x+x_m))\right]\phi_j(x)dx \right. \\ \left. + \int_0^1 \frac{\sinh(\mu_L x_m)}{\cosh(\mu_L(1+x_m))}\sinh(\mu_L(1-x))\phi_j(x)dx\right\} \tag{3.67}$$

where

$$\lambda_j = \frac{(2j+1)}{(1+x_m)}\frac{\pi}{2}, \qquad (j=0,1,2,...) \tag{3.68}$$

and

$$\phi_j(x) = sin(\lambda_j(1-x)), \qquad \mu_j^2 = \lambda_j^2 + h_0 + g_L \tag{3.69}$$

with

$$\mu_L^2 = \frac{g_0}{\alpha_0} + g_L \simeq h_0 + g_L, \tag{3.70}$$

here too we are neglecting $f_0$ on the second equation.

$$\bar{\lambda}_j^2 = \mu_j^2 - g_0 \tag{3.71}$$

Thus we have the following eigenfunction expansion:

$$a_1(x,t) \simeq \frac{\bar{v}_L}{\mu_L^2}\sum_{j=0}^{\infty}\bar{u}_j[1-e^{-\mu_j^2 t}]\phi_j(x) \tag{3.72}$$

the steady state LRO and neglecting $f_0$ gives us

$$\bar{b_1}(x) \simeq \frac{\bar{A}_1(x)}{\alpha_0} \simeq \frac{h_0}{g_0}\bar{A}_1(x) = \frac{h_0\bar{v}_L}{g_0\mu_L^2}A_1(x) \equiv \bar{B}_1(x), \tag{3.73}$$

$$b_1(x,t) \simeq \frac{h_0\bar{v}_L}{g_0\mu_L^2}\sum_{j=0}^{\infty} b_{1j}(t)\phi_j(x) \equiv B_1(x,t), \tag{3.74}$$

$$b_{1j}(t) = \bar{u}_j[1 - \frac{\mu_j^2 e^{-g_0 t} - g_0 e^{-\mu_j^2 t}}{\mu_j^2 - g_0}] \tag{3.75}$$

For the ectopic gradients (in LRO $e > 1$, in particular $e = 2$), we have

1. In the interval $0 = t_0 \le t \le t_1 = \tau \qquad v_L(x,t) = e\bar{v_L}H(-x)$

$$\begin{aligned} a(x,t) &\equiv a_e{}^{(0)}(x,t) \simeq \bar{A}_{e0}(x) + \hat{A}_{e0}(x,t) \equiv A_{e0}(x,t) \\ &= \frac{e\bar{v}_L}{\mu_L^2}[A_1(x) + \frac{\hat{A}_{e0}(x,t)}{e\bar{v}_L/\mu_L^2}] \\ &\equiv \frac{e\bar{v}_L}{\mu_L^2}\kappa_0\sum_{j=0}^{\infty}[\bar{u}_{0j} - \tilde{u}_{0j}e^{-\mu_j^2 t}]\phi_j(x), \end{aligned} \tag{3.76}$$

where $\bar{u}_{0j} = \tilde{u}_{0j} = \bar{u}_j \qquad$ and $\qquad \kappa_0 = 1$

and

$$\begin{aligned} b(x,t) &\equiv b_e{}^{(0)}(x,t) \simeq B_{e0}(x,t) \\ &= \frac{h_0 e\bar{v}_L}{g_0\mu_L^2}\sum_{j=0}^{\infty}[\bar{u}_{0j} - \tilde{w}_{0j}e^{-g_0 t}\frac{g_0}{\bar{\lambda}_j^2}\tilde{u}_{0j}e^{-\mu_j^2 t}]\phi_j(x) \end{aligned} \tag{3.77}$$

with $\tilde{w}_{0j} = \bar{u}_{0j} + \dfrac{g_0}{\bar{\lambda}_j^2}\tilde{u}_{0j} = \bar{u}_{0j}[1 + \dfrac{g_0}{\bar{\lambda}_j^2}] = \dfrac{\mu_j^2}{\bar{\lambda}_j^2}\bar{u}_{0j} = \dfrac{\mu_j^2}{\bar{\lambda}_j^2}\bar{u}_j$

therefore $B_{e0}(x,t) = \dfrac{h_0 e\bar{v_L}}{g_0\mu L^2}\sum_{j=0}^{\infty} b_{ej}^{(0)}(t)\phi_j(x)b_{ej}^{(0)} = [1 - \dfrac{\mu_j^2 e^{-g_0 t} - g_0 e^{-\mu_j^2 t}}{\bar{\lambda}_j^2}]\bar{u}_{0j}.$

We need to obtain $R_b(t_1)$ for the next time period

$$R_b(t_1) \approx \frac{1}{b_h}\sqrt{\frac{1}{1+x_m}\int_{-x_m}^{1}[B_{e0}(x,t)-B_1(x,t)]^2dx}$$
$$= \frac{1}{b_h}\frac{h_0\bar{v}_L}{g_0\mu_L^2}\sqrt{\frac{1}{2}\sum_{j=0}^{\infty}[eb_{ej}^{(0)}(t_1)-b_{1j}(t_1)]^2dx}$$
$$= \frac{h_0\bar{v_L}(e-1)}{g_0\mu_L^2 b_h\sqrt{2}}\sqrt{\sum_{j=0}^{\infty}[b_{1j}^2(t_1)]} \equiv r_b(t_1) \qquad (3.78)$$

2. For the general interval $t_i = i\tau \le t \le (i+1)\tau \equiv t_{i+1}$,

$$v_L(x,t) \equiv v_e^{(i)}(x,t) = \frac{v^{(i-1)}(x,t)}{1+cR_b(t-\tau)} = \frac{\kappa_{i-1}e\bar{v}_L H(-x)}{1+cR_b(t_i)}$$

Since $t_{i-1} \le t-\tau \le t_i$ , we get $R_b(t) = R_b(t_i)$.

Then we write $v_e^{(i)}(x,t) = \kappa_i e\bar{v}_L H(-x) \qquad (= \kappa_i v_e^{(0)}(x,t))$

$$\kappa_i = \frac{\kappa_{i-1}}{1+cR_b(t_i)} = \frac{1}{\prod_{l=0}^{i}[1+cR_b(t_l)]}$$

So $a(x,t) \equiv a_e^{(i)}(x,t)$ and $b(x,t) = b_e^{(i)}(x,t)$ are solutions for $v_e^{(i)}(x,t)$ in this interval.

$$b_e^{(i)}(x,t) = \frac{h_0 e\bar{v}_L\kappa_i}{g_0\mu_L^2}\sum_{j=0}^{\infty} b_{ej}^{(i)}(t)\phi_j(x)$$

$$b_{ej}^{(i)}(t) = \bar{u}_{ij} - \tilde{w}_{ij}e^{-g_0(t-t_i)} + \frac{g_0}{\bar{\lambda}_j^2}\tilde{u}_{ij}e^{\mu_j^2(t-t_i)}$$

with $\bar{u}_{ij} = \bar{u}_j$

$$\tilde{u}_{ij} = \bar{u}_{ij} - \frac{\kappa_{i-1}}{\kappa_i}\bar{u}_{i-1,j} + \frac{\kappa_{i-1}}{\kappa_i}\tilde{u}_{i-1,j}e^{\mu_j^2\tau} = (1 - \frac{\kappa_{i-1}}{\kappa_i})\bar{u}_j + \frac{\kappa_{i-1}}{\kappa_i}\tilde{u}_{i-1,j}e^{\mu_j^2\tau}$$

$$\tilde{w}_{ij} = \frac{\kappa_{i-1}}{\kappa_i}\tilde{w}_{i-1,j}e^{-g_0\tau} + (1 - \frac{\kappa_{i-1}}{\kappa_i})\bar{u}_j + \frac{g_0}{\overline{\lambda}_j^2}[\tilde{u}_{ij} - \frac{\kappa_{i-1}}{\kappa_i}\tilde{u}_{i-1,j}e^{\mu_j^2\tau}]$$

We have the values of $\bar{u}_j$ for all $j$, $\tilde{u}_{0j} = \bar{u}_{0j} = \bar{u}_j$ and $\tilde{w}_{0j} = \frac{\mu_j^2}{\overline{\lambda}_j^2}\bar{u}_j$.
Thus, we can compute the values for $\tilde{u}_{ij}$ and $\tilde{w}_{ij}$ recursively.

For the robustness index, we have

$$\begin{aligned} R_b(t_i) &= \frac{1}{b_h}\sqrt{\frac{1}{1+x_m}\int_{-x_m}^{1}[B_{ek}(x,t_i) - B_1(x,t)]^2 dx} \\ &= \frac{h_0\bar{v}_L}{\sqrt{2}b_h g_0 \mu_L^2}\sqrt{\sum_{j=0}^{\infty}[e\kappa_i b_{ej}^{(i)}(t_i) - b_{1j}(t_i)]^2} \end{aligned} \tag{3.79}$$

with $b_{ej}^{(i)}(t_i) = \bar{u}_j - \tilde{w}_{ij} + \frac{g_0}{\overline{\lambda}_j^2}\tilde{u}_{ij}$

and $b_{1j}(t_i) = \bar{u}_j[1 - \frac{\mu_j^2 e^{-g_0 t_i} - g_0 e^{-\mu_j^2 t_i}}{\mu_j^2 - g_0}] \approx \bar{u}_j$

For the case with No Feedback, we have

$$a_1(x,t) = \frac{\overline{v}_L}{\mu_L^2}\sum_{j=0}^{\infty}\overline{\mu}_j[1 - e^{-\mu_j^2 t}]\phi_j(x) \tag{3.80}$$

$$\mu_j^2 = \lambda^2 + h_0 + g_L, \qquad \mu_L^2 = \frac{g_0}{\alpha_0} + g_L \approx h_0 + g_L \tag{3.81}$$

$$\lambda_j = \frac{(2j+1)}{(1+x_m)}\frac{\pi}{2}, \qquad (j = 0, 1, 2, \dots) \tag{3.82}$$

$$\phi_j(x) = \sin(\lambda_j(1-x)) \tag{3.83}$$

$$\frac{\overline{v}_L}{\mu_L^2}\overline{u}_j\int_{-x_m}^{1}\phi_j^2(x)dx = \int_{-x_m}^{1}\overline{A}_1(x)\phi_j(x)dx \tag{3.84}$$

$$\overline{A}_1(x) = \begin{cases} \frac{\overline{v}_L}{\mu_L^2}\left(1 - \frac{\cosh(\mu_L)}{\cosh(\mu_L(1+x_m))}\right)\cosh(\mu_L(x+x_m)), & -x_m \le x \le 0 \\ \\ \frac{\overline{v}_L}{\mu_L^2}\left(\frac{\sinh(\mu_L x_m)}{\cosh(\mu_L(1+x_m))}\right)\sinh(\mu_L(1-x)), & 0 \le x \le 1 \end{cases} \tag{3.85}$$

Therefore

$$\begin{aligned} \overline{u}_j = \frac{2}{1+x_m}\Bigg\{ & \int_{-x_m}^{0}\left[1 - \frac{\cosh(\mu_L)}{\cosh(\mu_L(1+x_m))}\cosh(\mu_L(x+x_m))\right]\phi_j(x)dx \\ & + \int_0^1 \frac{\sinh(\mu_L x_m)}{\cosh(\mu_L(1+x_m))}\sinh(\mu_L(1-x))\phi_j(x)dx\Bigg\} \end{aligned} \tag{3.86}$$

<u>Note:</u>

1. $\int_{-x_m}^{1}\phi_j^2(x)dx = \int_{-x_m}^{1}\sin^2(\lambda_j(1-x))dx = \frac{1+x_m}{2}$

2. $\overline{B}_1(x) = \frac{\overline{A}_1(x)}{\alpha_0} \approx \frac{h_0}{g_0}\overline{A}_1(x)$ (steady state LRO $\overline{b}_1(x)$)

3. $\overline{B}_2(x) = 2\frac{h_0}{g_0}\overline{A}_1(x)$ ($\overline{v}_L \to 2\overline{v}_L$ ectopic gradient $e = 2$)

   $\Big[$We take $g_0 + f_0 \approx g_0$ so that $\alpha_0 = \frac{g_0+f_0}{h_0} \approx \frac{g_0}{h_0}\Big]$

4. $b_1(x,t) = \frac{\overline{v}_L}{\mu_L^2}\frac{h_0}{g_0}\sum_{j=0}^{\infty} b_{1j}(t)\phi_j(x)$ ($v_L = e\overline{v}_L H(-x), e = 1$)
   $b_{1j}(t) = \overline{u}_j\left[1 - \frac{\mu_j^2 e^{-g_0 t} - g_0 e^{-\mu_j^2 t}}{\overline{\lambda}_j^2}\right]$ ($j = 0, 1, 2, \dots$)
   $\overline{\lambda}_j^2 = \mu_j^2 - g_0 = \lambda_j^2 + h_0 + g_L - g_0$

5. $b_2(x,t) = 2b_1(x,t) \quad (v_L(x,t) = e\overline{v}_L H(-x), e = 2)$

6. $R_b(t) = \frac{1}{b_h}\sqrt{\frac{1}{1+x_m}\int_{-x_m}^{1}[b_2(x,t) - b_1(x,t)]^2 dx}$

$$= \frac{\overline{v}_L}{\mu_L^2}\frac{h_0}{g_0}\frac{1}{b_h\sqrt{1+x_m}}\sqrt{\int_{-x_m}^{1}\left[\sum_{j=0}^{\infty} b_{1j}(t)\phi_j(x)\right]^2 dx} = \frac{\overline{v}_L h_0}{\sqrt{2}\mu_L^2 g_0 b_h}\sqrt{\sum_{j=0}^{\infty} b_{1j}^2(t)}$$

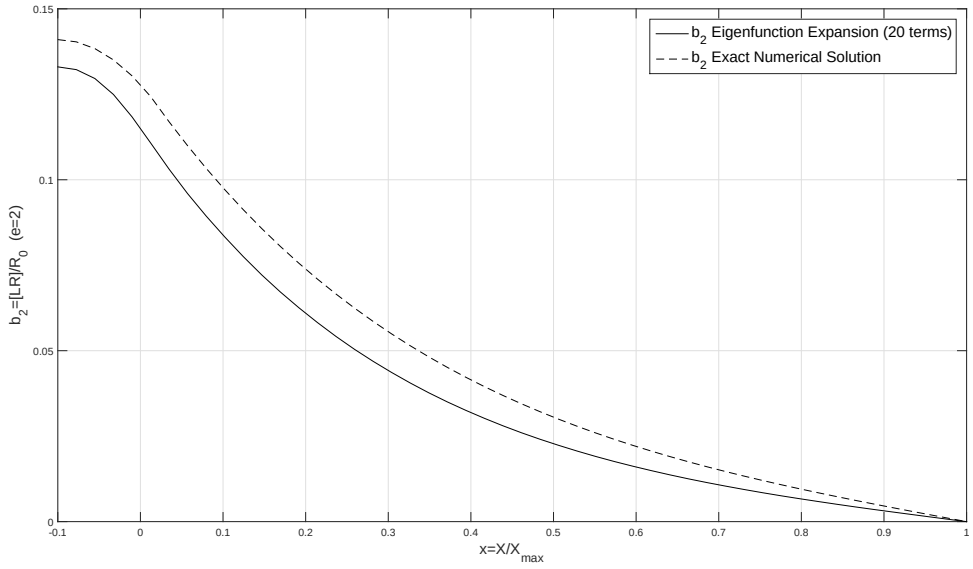


Figure 3.4: Comparison of ectopic (with no feedback) concentrations

Note that the results of Figure 3.4 serve to validate our numerical solutions for the steady state case (in LRO).

We also consider eigenfunction expansion with feedback in the transient phase (see Figure 3.5 below). For the eigenfunction expansion LRO case we have the following $R_b$ values:

$$
\begin{aligned}
R_b(t_1) &= 0.27318 \\
R_b(t_2) &= 0.15784 \\
R_b(t_3) &= 0.12959 \\
R_b(t_4) &= 0.11663 \\
R_b(t_5) &= 0.12332
\end{aligned} \tag{3.87}
$$

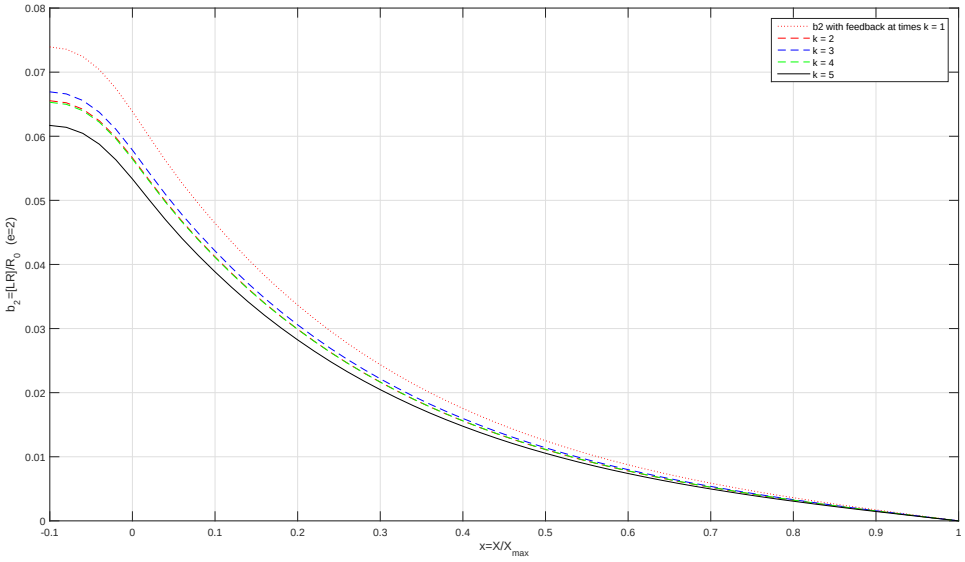


Figure 3.5: LRO Eigenfunction expansion with feedback in the transient phase

## 3.7 Concluding Remarks

In the proof of concept investigation examined in Chapter 2, we by-passed the actual agent responsible for down-regulating the ectopic signaling and implemented a negative feedback directly on the ligand synthesis rate (given the ultimate effect of the inhibition is equivalent to a reduction of ligand for binding with signaling receptors). In addition, we took the feedback to be effective as the development reaches a (quasi-) steady state. The work in this chapter complements that of the previous one by examining the same feedback mechanism

but now allowing it to be effective during the transient phase of the development, possibly repeated until a quasi-steady state of development is reached.

The transient phase feedback mechanism applied to the same illustrative example investigated in Chapter 2 shows some significant differences from the feedback in steady state process. The most obvious difference is that the new mechanism attains robustness for $c = 1$ (and $n = 1$) with $R_b$ well below 0.1 when the development reaches quasi-steady state whether or not there is a delay in the feedback process. In fact, $R_b$ is already below the robustness threshold of 0.2 even during the transient phase (see Table 3.1). In contrast, for the feedback in steady state approach with $c = 1$ and $n = 1$, the robustness index is $> 0.24$ which is well above the 0.2 threshold. With $n$ kept at 1, the latter mechanism would require $c = 2$ for $\bar{R}_b$ to decrease to 0.183... but still $> 0.1$ with $c = 4$. This advantage of the transient feedback is not surprising since the process allows for several adjustments before reaching steady state while the feedback in steady state effectively allows for only one feedback modification.

Thus it is reasonable to conclude that feedback in transient is more favorable (than feedback in steady state) to robust development of a biological organism that initiates (a spatially uniform nonlocal) feedback for adjusting the level of inhibition as it experiences environmental or genetic perturbations.

# Chapter 4

# Regulatory Feedbacks on Receptor and Non-receptor Synthesis Rates

## 4.1 Introduction

To explore the efficacy of the spatially uniform feedback approach to robust signaling gradients (investigated in Chapters 2 and 3), we apply the approach to the three robustness problems with Hill function type feedback investigated in [26]. In particular, we investigate the effects of the negative feedback on receptor synthesis rate, nonreceptors and a negative feedback on receptor synthesis rate, and feedback on both receptor (negative) and nonreceptor (positive) synthesis rates.

## 4.2 Feedback on Receptor Synthesis Rate

### 4.2.1 A Non-local Feedback

Excessive ligand concentration is known to down-regulate its own signaling receptor synthesis. In particular, Decapentaplegic represses the synthesis of its own receptor Tkv [27]. Another example is Wingless (Wg) repressing its signaling receptor DFz2 [6]. These and other experimental observations suggest a possible feedback mechanism for regulating abnormal effects of sustained genetic or epi-genetic changes on biological developments. To investigate this suggestion, down-regulation of Tkv by ectopic signaling Dpp gradient was modeled by a negative feedback of the Hill function type in [26] but was found to be ineffective as an instrument for robust development of the wing imaginal disc. A theoretical analysis of the model in [17] (and more recently in [28]) confirms the results of the numerical experiment and concludes that a spatially nonuniform feedback tends to distort the shape of the (prior to feedback) ectopic gradient as the feedback mechanism works to reduce its ectopicity nonuniformly, reducing receptor synthesis rate more where the ectopicity is higher. The conclusion in turn suggests that a spatially uniform feedback mechanism may be more effective for promoting robustness. To examine the merit of a spatially uniform feedback, we consider here the originally (normalized) spatially uniform receptor synthesis rate $\bar{v}_R$ being down-regulated to $v_R(t)$ by a negative feedback factor $\kappa^2(t)$ that is a function of the signaling robustness index $R_b(t)$,

$$v_R(t) = \kappa^2(t)\bar{v}_R, \tag{4.1}$$

Unlike the feedback instrument used in [37], the relation (4.1) effectively assumes the wild type synthesis rate $\bar{v}_R$ at any future time $t > 0$ to be unaffected by how the same synthesis rate at an earlier time has been changed by the negative feedback.

For a specific model, we take our alternative feedback instrument (to the Hill's function type) for down-regulating the receptor synthesis rate to be of the form

$$\kappa^2(t,\tau) = \frac{1}{1 + c\,[R_b(t)]^m} \tag{4.2}$$

where $c$ and $m$ are two parameters to be chosen for appropriate feedback strength similar to those for a Hill's function. Henceforth, the receptor synthesis rate (4.1) will become

$$v_R(t) = \kappa^2(t,\tau)\bar{v}_R = \frac{\bar{v}_R}{1 + c\,[R_b(t)]^m} \tag{4.3}$$

Two features of the feedback process in (4.3) should be noted. First, the feedback at any location does not depend on the ectopicity of the signaling gradient at that location, only on an average measure $R_b(t)$ of the excess over the span of the wing disc. It seems more reasonable (and likely) that signaling should be affected by some overall condition of the wing imaginal disc rather than being sensitive only to the local environment of individual cell. The other is the effect of the new feedback mechanism that only reduces the receptor synthesis rate by the same fraction $\kappa^2(t)$ throughout the wing imaginal disc. As such, the spatial variation of Dpp synthesis rate remains the same as in the absence of feedback.

As in the previous chapters, we work with the basic extracellular model of the Drosophila's wing imaginal disc. Let's recall the governing differential equations in dimensionless form:

$$\frac{\partial a_e}{\partial t} = \frac{\partial^2 a_e}{\partial x^2} - h_0 a_e r_e + f_0 b_e + v_e, \tag{4.4}$$

$$\frac{\partial b_e}{\partial t} = h_0 a_e r_e - (f_0 + g_0) b_e, \qquad \frac{\partial r_e}{\partial t} = v_R - h_0 a_e r_e + f_0 be - g_r r_e, \tag{4.5}$$

as before the Dpp and Tkv synthesis rates have been normalized to

$$v_e = \frac{eV_L/R_0}{D/X_{\max}^2} = e\bar{v}_L H(-x), \qquad v_R = \frac{\bar{V}_R/R_0}{D/X_{\max}^2} = \frac{k_R}{D/X_{\max}^2} \equiv g_r. \tag{4.6}$$

We have the following boundary conditions:

$$x = -x_m : \quad \frac{\partial a_e}{\partial x} = 0, \qquad x = 1 : \qquad a_e = 0, \tag{4.7}$$

all for $t > 0$, and the initial conditions

$$t = 0 : a_e = b_e = 0, \qquad r_e = 1. \tag{4.8}$$

For the investigation of the effects of our particular type of negative feedback on the receptor synthesis rate, we are interested in the modified signaling gradient (starting at $t = 0$) and the corresponding robustness index of the IBVP (4.4) - (4.8) but now with an enhanced ligand synthesis rate

$$v_L = e\bar{v}_L H(-x) \tag{4.9}$$

with an amplification factor $e > 1$ and a down-regulated receptor synthesis rate given by (4.3). In the presence of the feedback, the three ectopic gradients $\{a_e(x,t), b_e(x,t), r_e(x,t)\}$ of the new IBVP now depend on the robustness index $R_b(t)$ and are to be denoted by $\{a_R(x,t), b_R(x,t), r_R(x,t)\}$ which reduce to $\{a_e(x,t), b_e(x,t), r_e(x,t)\}$ when $c = 0$ (or $R_b(t) = 0$). The corresponding robustness index is determined by

$$R_b(t) = \frac{1}{b_h}\sqrt{\int_0^1 [b_R(x,t) - b_1(x,t)]^2 dx}. \tag{4.10}$$

### 4.2.2 Time Independent Steady State with Feedback

It has been shown in [23] that the extracellular model system without feedback has a unique steady state that is linearly stable with respect to a small perturbation from the steady state. The same is true for the case with negative feedback of the Hill function type [17, 28] on the receptor synthesis rate. In Chapter 2, we have obtained solutions for steady state gradients for a spatially uniform negative feedback $\kappa(R_b)$ on the ligand synthesis rate. Here, we examine the solution for the same extracellular model with the spatially uniform nonlocal feedback on the signaling receptor synthesis rate $\bar{V}_R$ of the type characterized by (4.3). Suppose the ectopic gradients down-regulated by negative feedback on receptor synthesis rate $\{a_R(x,t), b_R(x,t), r_R(x,t)\}$ tend to a time independent steady states $\{\bar{a}_R(x), \bar{b}_R(x), \bar{r}_R(x)\}$ as $t \to \infty$. In that case, we have also $R_b(t) \to \bar{R}_b$ and

$$\lim_{t\to\infty} \kappa^2(t;\tau) = \frac{1}{1 + c\left(\bar{R}_b\right)^m} \equiv \bar{\kappa}^2(\bar{R}_b) \tag{4.11}$$

with

$$\bar{R}_b = \lim_{t\to\infty} R_b(t) = \frac{1}{b_h}\sqrt{\int_0^1 [\bar{b}_R(x) - \bar{b}_1(x)]^2 dx} \tag{4.12}$$

and with $b_h$ appropriately taken to be $\bar{b}_1(0)$ or $B_1(0)$ in most cases.

With $\partial(\ )/\partial t = 0$, the governing equations and boundary conditions for the extracellular model become

$$\bar{a}_R'' - h_0 \bar{r}_R \bar{a}_R + f_0 \bar{b}_R + e\bar{v}_L H(-x) = 0 \tag{4.13}$$

$$h_0 \bar{a}_R \bar{r}_R - (f_0 + g_0)\bar{b}_R = 0, \qquad (g_r + h_0 \bar{a}_R)\bar{r}_R - f_0 \bar{b}_R = \bar{\kappa}^2 \bar{v}_R, \tag{4.14}$$

with

$$\bar{a}_R'(-x_m) = 0, \qquad \bar{a}_R(1) = 0, \tag{4.15}$$

where a prime indicates differentiation with respect to $x$, i.e., $(\ \ )' = d(\ \ )/dx$.

As in the case without feedback, we can solve (4.14) for $\bar{b}$ and $\bar{r}$ in terms of $\bar{a}$

$$\bar{b}_R(x) = \frac{\bar{\kappa}^2 \bar{a}_R(x)}{\alpha_0 + \zeta_0 \bar{a}_R(x)}, \qquad r_e(x) = \frac{\bar{\kappa}^2 \alpha_0}{\alpha_0 + \zeta_0 \bar{a}_R(x)}, \tag{4.16}$$

with $\alpha_0$ and $\zeta_0$ given by

$$\alpha_0 = \frac{f_0 + g_0}{h_0}, \qquad \zeta_0 = \frac{g_0}{g_r} \tag{4.17}$$

and use the results to eliminate these two quantities from the only ODE (4.13) to get a BVP for $\bar{a}_R$ alone:

$$\bar{a}_R'' - \frac{\bar{\kappa}^2 g_0 \bar{a}_R}{\alpha_0 + \zeta_0 \bar{a}_R} + e\bar{v}_L H(-x) = 0, \tag{4.18}$$

$$\bar{a}_R'(-x_m) = 0, \qquad \bar{a}_R(1) = 0. \tag{4.19}$$

where $\bar{\kappa}^2(\bar{R}_b)$ is given by (4.11). Existence of a unique solution for this problem and its monoticity can be proved in the same way as that for the problem without feedback carried out in [23].

### 4.2.3 Low Receptor Occupancy

For morphogen system in a state of *low receptor occupancy* prior to and after ligand synthesis enhancement so that

$$\zeta_0 \bar{a}_R \ll \alpha_0 \tag{4.20}$$

(including the special case where $c = 0$ and $e = 1$ so that $\bar{a}_R(x)$ reduces to $\bar{a}_1(x) = [\bar{a}_e(x,0)]_{e=1}$), we may approximate $\bar{a}_R(x)$ by $A_R(x) \equiv A_e(x, r_R)$ with the latter determined by the linearized model

$$A_R'' = \mu_R^2 A_R - e\bar{v}_L H(-x), \tag{4.21}$$

$$A_R'(-x_m) = 0, \quad A_R(1) = 0 \tag{4.22}$$

with

$$\mu_R^2 = \bar{\kappa}^2(\bar{R}_b)\mu_0^2 \simeq \bar{\kappa}^2(r_R)\frac{g_0}{\alpha_0}, \tag{4.23}$$

$$\bar{b}_e(x) \sim B_e(x, r_R) = B_R(x) = \frac{\bar{\kappa}^2(r_R)}{\alpha_0} A_R(x), \qquad \bar{r}_e(x) \sim \bar{\kappa}^2(r_R) \tag{4.24}$$

where the LRO approximation $r_R$ of $\bar{R}_b$ is calculated from (4.12) using $A_R(x)$ and $A_1(x,0)$ for $\bar{a}_R(x)$ and $\bar{a}_1(x) = [\bar{a}_e(x,0)]_{e=1}$, respectively, for an approximate solution of our problem.

The exact solution of (4.21)-(4.22), occasionally denoted by $A_R(x)$ is

$$A_R(x) = \begin{cases} \frac{e\bar{v}_L}{\bar{\kappa}^2(r_R)\mu_0^2}\{1 - \frac{\cosh(\mu_R)}{\cosh(\mu_R(1+x_m))}\cosh(\mu_R(x+x_m))\} & (-x_m \le x \le 0) \\ \frac{e\bar{v}_L}{\bar{\kappa}^2(r_R)\mu_0^2}\frac{\sinh(\mu_R x_m)}{\cosh(\mu_R(1+x_m))}\sinh(\mu_R(1-x)) & (0 \le x \le 1) \end{cases}, \quad (4.25)$$

with

$$\begin{aligned} \bar{b}_R(x) = \bar{b}_e(x, \bar{R}_b) \simeq B_e(x, r_R) &= \frac{\bar{\kappa}^2(r_R)}{\alpha_0}A_e(x; r_R) = \frac{\bar{\kappa}^2(r_R)}{\alpha_0}A_R(x) \\ &= \frac{e\bar{v}_L}{g_0}\frac{\sinh(\mu_R x_m)}{\cosh(\mu_R(1+x_m))}\sinh(\mu_R(1-x)) \qquad (0 \le x \le 1), \end{aligned} \quad (4.26)$$

where

$$\mu_R^2 = \bar{\kappa}^2(r_R)\mu_0^2 = \bar{\kappa}^2(r_R)\frac{g_0}{\alpha_0}. \quad (4.27)$$

It is expected to be an accurate approximation of the exact solution $\bar{a}_R(x; r_R)$ and reduces to the (approximate) wild-type ligand concentration $\bar{a}_1(x)$ when $c = 0$ and $e = 1$. For $e > 1$, the yet unknown robustness index $\bar{R}_b$ is to be determined by the LRO approximation of (4.12)

$$\bar{R}_b \sim r_R = \frac{1}{B_1(0)}\sqrt{\int_0^1 [B_e(x, r_R) - B_1(x)]^2 dx} \equiv C(r_R). \quad (4.28)$$

The relation (4.28) is an equation for $r_R$ $\left(\simeq \bar{R}_b\right)$ since the right hand side depends on $r_R$ through $B_R(x)$. It is to be solved for $r_R$ to complete the solution process.

Even without the explicit expression for $r_R$, we have the following proposition:

**Proposition 4.1.** *When both the wild-type and ectopic gradients are in a state of LRO, the negative feedback mechanism (4.3) on receptor synthesis rate does not lead to a robust development.*

*Proof.* The robustness index $r_b$ is positive when $e > 1$ and therewith $0 < \bar{\kappa}^2(r_b) < 1$. It follows from

$$B_e(0, r_R) = \frac{e\bar{v}_L}{g_0} \frac{\sinh(\mu_R x_m)}{\cosh(\mu_R(1 + x_m))} \sinh(\mu_R)$$

that the order of magnitude of $B_e(0, r_R)$ is not changed in any significant way by the presence of an integral feedback

$$\begin{aligned} \frac{B_e(0, r_R)}{B_1(0)} &= \frac{\sinh(\mu_R)}{\sinh(\mu_0)} \frac{\sinh(\mu_R x_m)}{\sinh(\mu_0 x_m)} \frac{\cosh(\mu_0(1 + x_m))}{\cosh(\mu_R(1 + x_m))} \\ &= O(e^{-\mu_0(1-\bar{\kappa})} e^{-\mu_0(1-\bar{\kappa})x_m} e^{\mu_0(1-\bar{\kappa})(1+x_m)}) = O(1) \end{aligned} \tag{4.29}$$

given $\mu_R^2 = \bar{\kappa}^2(r_R)\mu_0^2$ and $\mu_0^2 \simeq h_0 = O(10)$. While a more systematic calculation is possible, we have from the order of magnitude relation above

$$\frac{B_R(0)}{B_1(0)} = \frac{B_e(0, r_R)}{B_1(0)} = O(e), \qquad r_R = O\left(\sqrt{1 - e^{-2}}\right).$$

Hence negative feedback on receptor synthesis rate of the form (4.3) is not effective for attaining robust development at least for LRO gradients.

While the negative feedback (4.11) has little or no effects on the (up- or down-) regulaton of the magnitude of steady state signaling gradient, it does lead to a less convex modified ectopic signaling gradient since $\mu_R < \mu_0$ whenever $r_R > 0$. □

### 4.2.4 The General Case

For systems not in a state of LRO, we still can deduce results similar to that given in Proposition 4.1. From (4.18), we have

$$\bar{a}_R'' = \frac{\bar{\kappa}^2 g_0 \bar{a}_R}{\alpha_0 + \zeta_0 \bar{a}_R} - e\bar{v}_L H(-x)$$

subject to the two end conditions (4.19). This BVP generally requires some numerical method for an accurate solution. However, the structure of (4.18) can be seen to support the same conclusion for the moderate receptor occupancy case as well without computing the solution. For the same concentration level for the free ligand (which may be at different location $x$) in the range $(0 \leq x \leq 1)$, the gradient is less convex when there is negative feedback on receptor synthesis than when there is not.

As for the steepness of the gradient slope, we have from the first integral of (4.18),

$$\frac{1}{2}\left[\bar{a}_R'\right]^2 = \begin{cases} (e\bar{v}_L - \bar{\kappa}^2 g_r)(a_m - \bar{a}_R) + \frac{g_r^2}{\mu_0^2}\bar{\kappa}^2 \ln\left(\frac{\alpha_0+\zeta_0 a_m}{\alpha_0+\zeta_0 \bar{a}_R}\right) & (-x_m \leq x \leq 1) \\ \frac{1}{2}\left[s_1\right]^2 + \bar{\kappa}^2\left[g_r \bar{a}_R - \frac{g_r^2}{\mu_0^2}\ln\left(\frac{\alpha_0+\zeta_0 \bar{a}_R}{\alpha_0}\right)\right] & (0 \leq x \leq 1) \end{cases}, \quad (4.30)$$

with $s_1 = \bar{a}_R'(1) < 0$ given in terms of $a_m = \bar{a}_R(-x_m)$ and $a_0 = \bar{a}_R(0)$ by:

$$\frac{1}{2}\left[s_1\right]^2 = e\bar{v}_L(a_m - a_0) - \bar{\kappa}^2 g_r\left[a_m - \frac{g_r}{\mu_0^2}\ln\left(1 + \frac{\zeta_0}{\alpha_0}a_m\right)\right] \quad (4.31)$$

Upon integration, we obtain

$$\sqrt{2}(x_m + x) = \int_{\bar{a}_R}^{a_m} \frac{da}{\sqrt{\left(e\bar{v}_L - \bar{\kappa}^2 g_r\right)(a_m - a) + \bar{\kappa}^2 \frac{g_r^2}{\mu_0^2}\ln\left(\left(\alpha_0 + \zeta_0 a_m\right)/\left(\alpha_0 + \zeta_0 a\right)\right)}} \quad (x \leq 0)$$

$$1 - x = \int_0^{\bar{a}_R} \frac{da}{\sqrt{\left[s_1\right]^2 + 2\bar{\kappa}^2\left[g_r a - \frac{g_r^2}{\mu_0^2}\ln\left(\left(\alpha_0 + \zeta_0 a\right)/\alpha_0\right)\right]}} \quad (x \geq 0)$$

where $s_1 < 0$ is given in terms of $a_0$ and $a_m$ by (4.31) and the end conditions $\tilde{a}_R(1) = 0$ and $\tilde{a}_R(-x_m) = a_m$ have been used to fix the two constants of integration. The two remaining unknown constants $a_m$ and $a_0$ are then determined by specializing the integrals above to $x = -x_m$ and $x = 0$, respectively to get

$$\begin{aligned}\sqrt{2}x_m &= \int_{a_0}^{a_m} \frac{da}{\sqrt{\left(e\bar{v}_L - \bar{\kappa}^2 g_r\right)(a_m - a) + \bar{\kappa}^2 g_r^2 \ln\left(\left(\alpha_0 + \zeta_0 a_m\right)/\left(\alpha_0 + \zeta_0 a\right)\right)/\mu_0^2}} \\ 1 &= \int_0^{a_0} \frac{da}{\sqrt{\left[s_1\right]^2 + 2\bar{\kappa}^2[g_r a - g_r^2 \ln\left(\left(\alpha_0 + \zeta_0 a\right)/\alpha_0\right)]/\mu_0^2}}\end{aligned}$$

**Proposition 4.2.** *Negative feedback of the form (4.11) reduces the convexity of the free and signaling ligand gradient and increases the slope of the gradients (making it less negative).*

## 4.3 A Simple Iterative Algorithm for Steady State

### 4.3.1 An ODE Solution Process

The presence of the factor $\bar{R}_b$ in the ODE for $\bar{a}_R$ makes the solution of the BVP (4.18)-(4.19) much less straightforward. As $\bar{R}_b$ encapsulates the unknown concentrations of normal and ectopic signaling ligand-receptor complexes, it depends on the solutions of two BVP over the entire span of the solution domain through the integrated condition (4.32).

$$\bar{R}_b = \lim_{t\to\infty} R_b(t) = \frac{1}{b_h - b_\ell}\sqrt{\frac{1}{\left(x_\ell - x_h\right)^2}\int_{x_h}^{x_\ell} [\bar{b}_e(x) - \bar{b}_1(x)]^2 dx} \tag{4.32}$$

To the extent that there are reliable software for solving BVP in ODE, we re-configure the integro-differential equation problem for $\bar{a}_R$ as a BVP for a system of ODE. While a single pass algorithm is possible (as shown in Chapter 2), the problem is sufficiently simple to allow us to settle for an iterative solution scheme as formulated below.

For this purpose, we let $\bar{a}_1(x)$ and $\bar{a}_R(x)$ be the unknown free ligand concentration for a wild type ligand synthesis rate $\bar{v}_L H(-x)$ and an ectopic synthesis rate $e\bar{v}_L H(-x)$, respectively. The ectopic concentration $\bar{a}_R(x)$ is determined by the BVP (4.18)-(4.19) for $e > 1$ and $\bar{\kappa}^2$ as given in terms of $\bar{R}_b$ by (4.11). Results for specific calculations will be limited to the special case of $e = 2$ (to reflect to effect of temperature change engineered in the Lander Lab) and $m = 1$.

Having the solutions of the two BVP for $\bar{a}_R(x)$ and $\bar{a}_1(x)$ with $\bar{R}_b$ as a parameter, we can calculate the corresponding signaling gradients $\bar{b}_R(x;\bar{R}_b)$ and $\bar{b}_1(x)$ and then obtain $\bar{R}_b$ from the integral condition (4.32). To be concrete, we take $x_\ell = 1$, $x_h = 0$, and $b_\ell = 0$ so that

$$\bar{R}_b = \frac{1}{b_h}\sqrt{\int_0^1 [\bar{b}_e(x;\bar{R}_b) - \bar{b}_1(x)]^2 dx} \tag{4.33}$$

where

$$\bar{b}_R(x) = \bar{b}_e(x;\bar{R}_b) = \frac{\bar{\kappa}^2\bar{a}_R(x)}{\alpha_0 + \zeta_0\bar{a}_R(x)}, \qquad \bar{b}_1(x) = \frac{\bar{a}_1(x)}{\alpha_0 + \zeta_0\bar{a}_1(x)}. \tag{4.34}$$

As we have already mentioned, we take $b_h$ to be given by

$$b_h = B_1(0) = \frac{\bar{v}_L}{\alpha_0\mu_0^2}\frac{\sinh(\mu_0 x_m)\sinh(\mu_0)}{\cosh(\mu_0(1+x_m))} \;\simeq\; \bar{b}_1(0) \tag{4.35}$$

which is appropriate for systems of low (to moderate) receptor occupancy.

For an ODE oriented algorithm for the solution of our problem, we introduce a new function $R_2(x)$ by the IVP

$$R_2' = \frac{1}{b_h^2}[\bar{b}_R(x) - \bar{b}_1(x)]^2 = \frac{1}{b_h^2}\left(\frac{\bar{\kappa}^2\bar{a}_R(x)}{\alpha_0 + \zeta_0\bar{a}_R(x)} - \frac{\bar{a}_1(x)}{\alpha_0 + \zeta_0\bar{a}_1(x)}\right)^2 H(x), \tag{4.36}$$

$$R_2(-x_m) = 0, \tag{4.37}$$

to replace the integral relation (4.33). In actual illustrative examples, we will work with the special case of (4.11) with $m = 1$,

$$\bar{\kappa}^2 = \frac{1}{1 + c\bar{R}_b}, \tag{4.38}$$

where $c$ still to be specified. With the Heaviside function $H(x)$ on the right hand side of (4.36) and the stipulation of continuity on $R_2(x)$, the ODE and the auxiliary condition (4.37) for $R_2$ requires

$$R_2(1) = \bar{R}_b^2 \tag{4.39}$$

to be consistent with (4.33).

Note that $\bar{a}_1(x)$ may be solved separately and only once independent of any knowledge of $\bar{R}_b$. In theory, the two BVP for $\bar{a}_R(x)$ and $R_2(x)$ should be solved simultaneously since they both involve the unknown $\bar{R}_b$. The third order ODE system (4.18) and (4.36) are adequately augmented by three auxiliary conditions (4.19) and (4.37). Together, they determine $\bar{a}_R(x)$ and $R_2(x)$ up to the unknown parameter $\bar{R}_b$. The condition (4.39) then determines $\bar{R}_b$.

### 4.3.2 An Iterative Algorithm

While we can take an additional step to transform (4.39) into an ODE problem to result in a single pass algorithm for determining $\bar{R}_b$, it is rather straightforward to work with $R_2(x)$ as

defined by (4.36)-(4.37) to obtain an accurate approximation of $\bar{R}_b$ by the following iterative process:

1. Start with an initial guess $\bar{R}_0$, e.g., $\bar{R}_0 = 0$.
2. Having $\bar{R}_k$, solve the BVP for $\bar{a}_R(x)$ with $\bar{R}_b = \bar{R}_k$ and denote the solution and the corresponding signaling gradient by $\bar{a}_R^{(k)}(x)$ and $\bar{b}_R^{(k)}(x)$, respectively.
3. Use $\bar{b}_R^{(k)}(x)$ for $\bar{b}_R(x)$ in (4.36) and solve the IVP (4.36)-(4.37) to get $R_2^{(k)}(x)$.
4. Set $\bar{R}_{k+1} = R_2^{(k)}(1)$ and go to step 2 to repeat the process.

The four steps iterative solution process above may be taken in the form

$$\bar{R}_{k+1} = C(\bar{R}_k) \tag{4.40}$$

where

$$C(\bar{R}_k) = \frac{1}{b_h}\sqrt{\int_0^1 [\bar{b}_e(x;\bar{R}_k) - \bar{b}_1(x)]^2 dx} \tag{4.41}$$

can be calculated with $\bar{b}_e(x;\bar{R}_k) = \bar{b}_R^{(k)}(x)$ determined from (4.34) once we have the solution for $\bar{a}_e(x;\bar{R}_k) = \bar{a}_R^{(k)}(x)$. The sequence $\left\{\bar{R}_k\right\}$ can be shown to converge to give the following proposition:

**Proposition 4.3.** *Starting with $\bar{R}_0 = 0$, the iterative solution scheme (4.40) converges to a positive solution of (4.33).*

*Proof.* see [43] for the proof. □

As we shall see from an illustrative example in the next section, the iterative scheme converges rapidly for $c = 1$ but was found to require more iterations for $c \gg 1$. For larger values of $c$,

the sequence $\{\bar{R}_k\}$, though still bounded above and below and convergent, may alternately increase and decrease with successive iterations.

### 4.3.3 An Illustrative Example

To gain some insight to the iterative algorithm for the steady state robustness index $\bar{R}_b$, we apply it to the system characterized by the parameter values shown in Table 4.1. This system meets the condition (4.20) for a state of low receptor occupancy and is further confirmed to be so by comparison of the exact numerical solution with that of the linearized model. The steady state robustness index $\bar{R}_b$ is found after less than 10 iterations. For example, the $\bar{R}_b$ value for $c = 1$ given in Table 4.1 has a discrepancy of less than 0.2% between the $5^{th}$ and $6^{th}$ iterations.

Table 4.1 Numerical Solutions by the Iterative Algorithm

$$X_{\max} = 0.01\ cm, \qquad X_{\min} = 0.001\ cm, \qquad k_{on}R_0 = \ 0.01\,\mathrm{sec}./\mu M,$$
$$k_{deg} = 2 \times 10^{-4}/\,\mathrm{sec}., \qquad k_R = 0.001/\,\mathrm{sec}., \quad k_{off} = 10^{-6}/\,\mathrm{sec}., \qquad e = 2,$$
$$D = 10^{-7}\ cm^2/\,\mathrm{sec}., \qquad \bar{V}_L = 0.002\ \mu M/\,\mathrm{sec}., \qquad \bar{V}_R = 0.04\ \mu M/\,\mathrm{sec}.$$

| $c$ | $k$ | $\bar{R}_k$ | $r_R$ | $\bar{b}_e(0;\bar{R}_k)$ | $B_e(0,r_R)$ | $\bar{b}_1(0)$ | $B_1(0)$ |
|---|---|---|---|---|---|---|---|
| 0 | 1 | 0.3938 | 0.3943 | 0.11538 | 0.11664 | 0.05801 | 0.05832 |
| 0.5 | 5 | 0.3750 | 0.3739 | 0.1080 | 0.1094 | 0.05801 | 0.05832 |
| 1 | 5 | 0.3573 | 0.3567 | 0.1022 | 0.1038 | 0.05801 | 0.05832 |
| 2 | 7 | 0.3284 | 0.3284 | 0.09414 | 0.09571 | 0.05801 | 0.05832 |
| 4 | 10 | 0.2862 | 0.2871 | 0.08386 | 0.08551 | 0.05801 | 0.05832 |

While the quick convergence of the scheme for the particular example is gratifying, the biological implication of the resulting robustness index is not. The recorded final iterate $\bar{R}_k$ shown in the Table 4.1 for $c = 1$ is well above the acceptable level of 0.2, a rather modest requirement set arbitrarily in [26] for robustness. This is hardly surprising given that the explicit solution $B_e(x;r_b) \equiv B_R(x)$ for the LRO approximation of $\bar{b}_R(x)$ in (4.26) and the corresponding order of magnitude estimate of $r_b$ (the LRO approximation of $\bar{R}_k$),

are pretty much unaffected to the leading order by the chosen feedback instrument. These observations are further supported by comparing the accurate numerical solution for $\bar{b}_1(x)$ and $\bar{b}_e(x,0)$ with $\bar{b}_R(x) = \bar{b}_e(x,\bar{R}_b)$ (not shown in Table 4.1). The comparison shows that the latter is very much closer to $\bar{b}_e(x,0)$ than $\bar{b}_1(x)$. More specifically, we see from Table 4.1 that $\bar{b}_2(0;0)$ and $\bar{b}_R(0) = \bar{b}_2(0,\bar{R}_b)$ are nearly double the magnitude of $\bar{b}_1(0)$, confirming the ineffectiveness of the negative feedback $\bar{\kappa}^2(R_b)$ on the receptor synthesis rate.

In addition, increasing the value of the parameter $c$ to larger than 1 would not make the feedback $\bar{\kappa}^2(\bar{R}_b)$ significantly more effective. The effect of $c\bar{R}_b$ is only in the shape factor $\mu_R$ in the argument of the various *sinh* and *cosh* functions (see (4.26)). The expression $B_e(x;r_b)$ for LRO signaling gradient clearly shows that the general signaling gradient not in a state of LRO is not expected to be qualitatively different. In fact, graphs of $\bar{b}_R(x)$ in Figure 4.1 (and the exact solution for the LRO case) suggest that larger values of $c$ would only distort the shape of the gradients further and would not improve robustness. Therefore, it is necessary to look elsewhere for a more effective feedback instrument to promote robust development with respect to an enhanced Dpp synthesis rate. There are a number of such instruments available for this purpose. Here, we focus only on one of these, namely, the role of nonreceptors without or with nonlocal, spatially uniform feedback.

## 4.4 Effects of Nonreceptors

### 4.4.1 The Presence of Nonreceptors

As we have already mentioned, nonreceptors (such as heparan sulfate proteoglygans) are molecular substances that bind with signaling ligands such as Dpp in the wing imaginal disc but do not signal to induce cell differentiation. The effects of nonreceptors on the signaling Dpp gradients have been investigated theoretically by mathematical modeling, analysis and

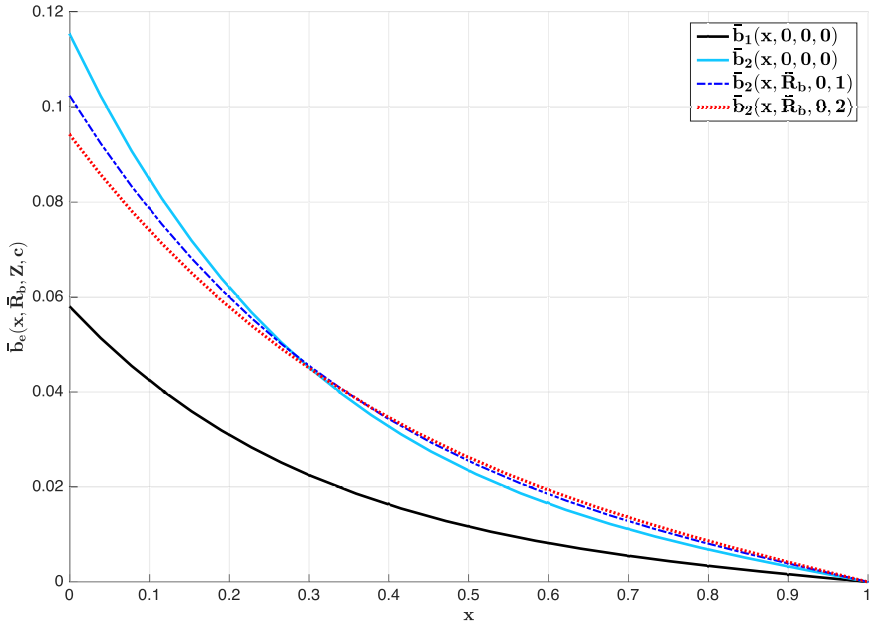


Figure 4.1: Spatially Uniform Negative Feedback on Receptor Synthesis Rate

numerical simulations in [26, 25, 28, 29, 42]. For our purpose, it suffices to take (as in [26] and elsewhere) the cell-surface bound non-receptor to be synthesized at a temporally uniform rate $\bar{V}_N$ so that we have a steady state nonreceptor concentration $N_0$ with

$$N_0 = \frac{\bar{V}_N}{j_N}, \qquad Z = \frac{N_0}{R_0} = \frac{\bar{V}_N/\bar{V}_R}{j_N/k_R}, \qquad \bar{v}_N = \frac{X_0^2}{D}\left\{\frac{\bar{V}_N}{N_0}\right\} = \frac{j_N}{D/X_0^2}, \tag{4.42}$$

where $j_N$ is the degradation rate constant for the unoccupied nonreceptors. Similar to receptors, (normalized) free nonreceptor concentration $n(x,t)$ is also bound reversibly to Dpp ligand to form normalized ligand-receptor complexes (or *bound nonreceptors* for brevity) of concentration $c(x,t)$,

$$\{c,n\} = \frac{1}{N_0}\{[LN],[N]\}, \tag{4.43}$$

with normalized "binding rate constant" $h_1 a$ (for binding between Dpp and nonreceptors), nonreceptor-mediated degradation rate constant $g_1$ (for degradation of Dpp-nonreceptor

complexes), dissociation rate constant $f_1$ (for dissociation rate of Dpp-nonreceptor complexes) and unoccupied nonreceptor degradation rate constant $g_n$:

$$\{h_1, g_1, f_1, g_n\} = \frac{X_0^2}{D}\{j_{on}R_0, j_{\deg}, j_{off}, j_N\}, \qquad \{\bar{h}_0, \bar{h}_1\} = \frac{X_0^2}{D}\{k_{on}N_0, j_{on}N_0\}. \tag{4.44}$$

In terms of these normalized quantities, we have the following IBVP for the five normalized unknowns $a$, $b, r, c$ and $n$ [42]:

$$\frac{\partial a_e}{\partial t} = \frac{\partial^2 a_e}{\partial x^2} - h_0 a_e r_e + f_0 b_e - Z h_1 a_e n_e + Z f_1 c_e + e\bar{v}_L H(-x), \tag{4.45}$$

$$\frac{\partial b_e}{\partial t} = h_0 a_e r_e - (f_0 + g_0) b_e, \qquad \frac{\partial r_e}{\partial t} = \bar{v}_R - h_0 a_e r_e + f_0 b_e - g_r r_e, \tag{4.46}$$

$$\frac{\partial c_e}{\partial t} = h_1 a_e n_e - (f_1 + g_1) c_e, \qquad \frac{\partial n_e}{\partial t} = \bar{v}_N - h_1 a_e n_e + f_1 c_e - g_n n_e, \tag{4.47}$$

with the boundary conditions

$$x = -x_m : \quad \frac{\partial a_e}{\partial x} = 0, \qquad\qquad x = 1 : \quad a_e = 0. \tag{4.48}$$

As before, the parameter $e$ is a measure of the ectopicity of the altered Dpp synthesis rate induced by a sustained genetic or epigenetic perturbation. We are interested in the effects of nonreceptors on the ectopic signaling gradients. To the extent that nonreceptors are ubiquitous during the development of the embryo, we take as initial conditions

$$t = 0 : \qquad a_e = b_e = c_e = 0, \quad r_e = 1, \quad n_e(x) = 1, \qquad (-x_m \le x \le 1) \tag{4.49}$$

at the onset of Dpp synthesis. By stipulating (4.49), we effectively assume a steady state concentration of nonreceptors at the instant of onset of Dpp synthesis. This assumption will be reconsidered later.

The IBVP defined by (4.45)-(4.49) constitutes a new mathematical model for morphogen activities in the presence of non-diffusive nonreceptors. It will be used to study the effects of such nonreceptor sites on the amplitude and shape of the various ligand concentration gradients and their robustness. Our ultimate goal is to see whether the presence of a sufficiently high concentration of nonreceptors should make the signaling morphogen gradient $[LR]$ insensitive to an enhanced Dpp synthesis rate.

### 4.4.2 Time-Independent Steady State

We denote by $\bar{a}_Z(x), \bar{b}_Z(x)$, $\bar{c}_Z(x), \bar{r}_Z(x)$, and $\bar{n}_Z(x)$ the time-independent steady state solution $a_e(x,t,Z)$, $b_e(x,t,Z)$, $c_e(x,t,Z)$, $r_e(x,t,Z)$ and $n_e(x,t,Z)$ of (4.45)-(4.49) when $e \neq 1$ (with $\left\{\bar{a}_1(x), \bar{b}_1(x), \bar{c}_1(x), \bar{r}_1(x), \bar{n}_1(x)\right\}$ defined only as the corresponding wildtype quantities, i.e., with $e = 1$ in the absence of non-receptors).

For this steady state solution, we have $\partial(\ )/\partial t = 0$ so that the governing differential equations and boundary conditions become

$$\bar{a}_Z'' - h_0 \bar{a}_Z \bar{r}_Z + f_0 \bar{b}_Z - h_1 Z \bar{a}_Z \bar{n}_Z + f_1 Z \bar{c}_Z + e\bar{v}_L H(-x) = 0 \tag{4.50}$$

$$h_0 \bar{a}_Z \bar{r}_Z - (f_0 + g_0)\bar{b}_Z = 0, \qquad (g_r + h_0 \bar{a}_Z)\bar{r}_Z - f_0 \bar{b}_Z = \bar{v}_R, \tag{4.51}$$

$$h_1 \bar{a}_Z \bar{n}_Z - (f_1 + g_1)\bar{c}_Z = 0, \qquad (g_n + h_1 \bar{a}_Z)\bar{n}_Z - f_1 \bar{c}_Z = \bar{v}_N, \tag{4.52}$$

with the end conditions

$$\bar{a}'_Z(-x_m) = 0, \qquad \bar{a}_Z(1) = 0. \tag{4.53}$$

We can solve (4.51) for $\bar{b}_Z$ and $\bar{r}_Z$ in terms of $\bar{a}_Z$ as before and (4.52) for $\bar{c}_Z$ and $\bar{n}_Z$ in terms of $\bar{a}_Z$ to get

$$\bar{b}_Z(x) = \frac{\bar{a}_Z(x)}{\alpha_0 + \zeta_0 \bar{a}_Z(x)}, \qquad \bar{r}_Z(x) = \frac{\alpha_0}{\alpha_0 + \zeta_0 \bar{a}_Z(x)}, \tag{4.54}$$

$$\bar{c}_Z(x) = \frac{\bar{a}_Z(x)}{\alpha_1 + \zeta_1 \bar{a}_Z(x)}, \qquad \bar{n}_Z(x) = \frac{\alpha_1}{\alpha_1 + \zeta_1 \bar{a}_Z(x)}, \tag{4.55}$$

with

$$\alpha_1 = \frac{f_1 + g_1}{h_1} = Z\bar{\alpha}_1, \quad \{\zeta_0,\ \zeta_1\} = \left\{ \frac{k_{\text{deg}}}{k_R}, \frac{j_{\text{deg}}}{j_N} \right\} = \left\{ \frac{g_0}{g_r}, \frac{g_1}{g_n} \right\}. \tag{4.56}$$

The results are then used to obtain from (4.50) a BVP for $\bar{a}_Z(x) \equiv \hat{a}_e(x, Z)$ alone:

$$\bar{a}''_Z - \frac{g_0 \bar{a}_Z}{\alpha_0 + \zeta_0 \bar{a}_Z} - \frac{Z g_1 \bar{a}_Z}{\alpha_1 + \zeta_1 \bar{a}_Z} + e\bar{v}_L H(-x) = 0. \tag{4.57}$$

Evidently, $\bar{a}_Z(x)$ varies with $Z$ (and hence occasionally denoted by $\bar{a}_e(x, Z)$) and is not the same as $\bar{a}_e(x)$ unless $Z = 0$, i.e., $\bar{a}_e(x) = \bar{a}_e(x, 0)$. Even if $e = 1$, $\bar{a}_1(x, Z)$ is different from the wildtype free morphogen concentration $\bar{a}_1(x)$ as specified at the start of this subsection. Existence, uniqueness and monotonicity of the BVP above have already been proved in [42].

### 4.4.3 Low Receptor and Non-receptor Occupancy (LRNO)

For the signaling gradient to provide positional information that differentiates cell fates, the normalized concentration $b = [LR]/R_0$ should not be nearly uniform. Positional indifference

except for a steep gradient near the imaginal disc edge is less likely to occur if diffusion is relatively fast and receptors and nonreceptors are abundant (for binding with most available ligands) so that $\alpha_0 + \zeta_0 \hat{a}(x) \simeq \alpha_0$ and $\alpha_1 + \zeta_1 \hat{a}(x) \simeq \alpha_1$. In that case, the gradient system is said to be in a state of *low receptor and nonreceptor occupancy* (LRNO) and the ODE (4.57) can be linearized. With the corresponding approximate steady state solution denoted by $\{A_Z, B_Z, C_Z, N_Z, R_Z\}$, we have for this LRNO state case

$$A_Z'' = \mu_Z^2 A_Z - e\bar{v}_L H(-x), \qquad \mu_Z^2 = \mu_0^2 + Z\mu_1^2 \tag{4.58}$$

$$A_Z'(-x_m) = 0, \qquad A_Z(1) = 0 \tag{4.59}$$

with

$$\mu_0^2 = \frac{g_0}{\alpha_0} = \frac{k_{\deg}}{k_{\deg} + k_{off}} \frac{x_{max}^2}{D} k_{on} R_0, \tag{4.60}$$

$$Z\mu_1^2 = \frac{g_1}{\alpha_1} Z = \frac{j_{\deg}}{j_{\deg} + j_{off}} \frac{x_{max}^2}{D} j_{on} N_0. \tag{4.61}$$

The complementary solutions of the linear ODE (4.58) are the exponential functions $e^{-\mu x}$ and $e^{\mu x}$. The slope of

$$\bar{b}_Z(x) \simeq B_Z(x) = \frac{A_Z(x)}{\alpha_0} \simeq \frac{\bar{a}_Z(x)}{\alpha_0 + \zeta_0 \bar{a}_Z(x)}$$

is then determined by the parameter $\mu_Z$. If $\mu_Z \gg 1$, the signaling gradient would be too steep and nearly vanishing except for a narrow interval adjacent to the *Dpp* source (as seen from the corresponding wildtype solution (4.62)-(4.63)).

$$A_e(x) = \begin{cases} \frac{e\bar{v}_L}{\mu_0^2}\{1 - \frac{\cosh(\mu_0)}{\cosh(\mu_0(1+x_m))}\cosh(\mu_0(x+x_m))\} & (-x_m \le x \le 0) \\ \frac{e\bar{v}_L}{\mu_0^2}\frac{\sinh(\mu_0 x_m)}{\cosh(\mu_0(1+x_m))}\sinh(\mu_0(1-x)) & (0 \le x \le 1) \end{cases} \tag{4.62}$$

$$\bar{b}_e(x) \simeq B_e(x) = \frac{A_e(x)}{\alpha_0}, \qquad \bar{r}_e(x) \simeq R_e(x) = 1. \tag{4.63}$$

Hence, we have the following operational definition of a meaningful biological signaling gradient (or a biological gradient for brevity) useful for cell differentiation:

**Definition 4.4.** A signaling morphogen gradient is a biological gradient if (i) the dimensionless binding rate constants $h_0$ and $h_1^* = Zh_1$ are $O(1)$, ii) $\alpha_0 \gg \zeta_0 \bar{a}_Z(0)$, and iii) $\alpha_1 \gg \zeta_1 \bar{a}_Z(x)$ so that

$$\alpha_0 + \zeta_0 \bar{a}_Z(x) \simeq \alpha_0, \qquad \alpha_1 + \zeta_1 \bar{a}_Z(x) \simeq \alpha_1, \qquad \mu_Z^2 = O(1). \tag{4.64}$$

The first two conditions in (4.64) ensure (a state of LRNO and) the adequacy of (4.58) as an approximation of the original nonlinear BVP. For the Drosophila wing imaginal disc, we have $f_0 \ll g_0$ and $f_1 < g_1$ so that $g_0/\alpha_0 \simeq h_0$ and $Zg_1/\alpha_1 \simeq h_1^*$. In that case, we have $\mu_Z^2 = \mu_0^2 + Z\mu_1^2 = O(h_0) + O(h_1^*)$. The last condition in (4.64) then ensures that the gradient is sufficiently differentiating and hence biologically meaningful. With both $\zeta_0$ and $\zeta_1$ typically less than unity (and often $\ll 1$) in a Drosophila wing imaginal disc, we expect the first two conditions of (4.64) to hold for moderate values of $\bar{v}_L$. This makes it possible to linearize the BVP for $\bar{a}_Z(x)$ and work with (4.58)-(4.59) for the determination of the approximating LRNO state $A_Z(x) \equiv A_e(x, Z)$. The explicit solution for that linear problem should offer considerable insight to the effects of nonreceptors on the wing imaginal disc development. The exact solution for the new problem is the following:

$$A_e(x, Z) = \begin{cases} \frac{e\bar{v}_L}{\mu_Z^2}\{1 - \frac{\cosh(\mu_Z)}{\cosh(\mu_Z(1+x_m))}\cosh(\mu_Z(x + x_m))\} & (-x_m \le x \le 0) \\ \frac{e\bar{v}_L}{\mu_Z^2}\frac{\sinh(\mu_Z x_m)}{\cosh(\mu_Z(1+x_m))}\sinh(\mu_Z(1-x)) & (0 \le x \le 1) \end{cases}, \tag{4.65}$$

with

$$\bar{b}_Z(x) \sim B_Z(x) = \frac{A_Z(x)}{\alpha_0} \left( = \frac{A_e(x,Z)}{\alpha_0} \right) \tag{4.66}$$
$$= \frac{e\bar{v}_L}{\alpha_0 \mu_Z^2} \frac{\sinh(\mu_Z x_m)}{\cosh(\mu_Z(1+x_m)))} \sinh(\mu_Z(1-x)) \qquad (x \geq 0)$$

and

$$B_Z(0) = \frac{A_Z(0)}{\alpha_0} = \frac{e\bar{v}_L}{\alpha_0 \mu_Z^2} O(1) = \frac{eB_1(0)}{1 + \frac{h_1}{h_0} Z} O(1) \tag{4.67}$$

where $B_1(0) = [B_Z(0) = B_e(0,Z)]_{e=1,Z=0}$ (given $f_k \ll g_k$ for both $k = 0$ and 1). For an adequately high nonreceptor synthesis rate relative to that for receptors, we have $Z \gg 1$ so that $B_Z(0) = O(B_1(0)/Z)$. We have then the following result for the biologically realistic case of $f_k \ll g_k$, $k = 0$,1:

**Proposition 4.5.** *In the presence of an adequately high non-receptor synthesis rate and high binding rate to nonreceptors relative to that for receptors so that $h_1 Z/h_0 \geq e$, the amplitude of the ectopic signaling gradient at $x = 0$ may be reduced to the magnitude of the wildtype.*

*Proof.* Upon rewriting (4.67) as

$$\bar{b}_Z(0) \sim B_Z(0) = \frac{e\bar{v}_L/g_0}{1 + \frac{h_1}{h_0} Z} O(1) = \frac{eB_1(0)}{1 + \frac{h_1}{h_0} Z} O(1)$$

we have

$$\bar{b}_Z(0) = O(B_1(0))$$

since $1 + h_1 Z/h_0 > e$ keeping in mind $B_1(0) = [B_Z(0) = B_e(0,Z)]_{e=1,Z=0}$. □

We can also calculate the LRNO approximation $\bar{r}_b$ of our adopted measure of robustness $\bar{R}_b$ from (4.28) to get

$$\bar{r}_b = \frac{1}{B_1(0,0)}\sqrt{\int_0^1 [B_e(x,Z) - B_1(x,0)]^2 dx}$$

where neither $B_e(x,Z)$ nor $B_1(x,0)$ depends of $\bar{r}_b$ (as there is no feedback instrument of any kind operating in the present model). For typical values of $\mu_0$ (around 3 for our examples) and the typical ectopicity $e = 2$ on the enhanced Dpp synthesis rate of interest, we have a good approximation

$$\bar{r}_b \sim \sqrt{\int_0^1 [2\gamma(Z)e^{-\mu_Z x} - e^{-\mu_0 x}]^2 dx}, \tag{4.68}$$

where

$$\gamma(Z) = \frac{1}{1 + Zh_1/h_0}, \qquad \mu_Z^2 = \mu_0^2\left(1 + Z\frac{\mu_1^2}{\mu_0^2}\right) \sim h_0\left(1 + Z\frac{h_1}{h_0}\right)$$

since $f_k$ is known to be $\ll g_k$ for Dpp in the wing imaginal disc. (Note that the factor 2 in (4.68) would be replaced by the ectopicity factor $e$ in the general case.)

While it is gratifying to see the reduction of ectopic signaling gradient toward robustness, there is a negative consequence of a sufficiently large $Z$ value. With

$$\mu_Z^2 = \mu_0^2 + Z\mu_1^2 = \mu_0^2\,(1 + h_1 Z/h_0) \gg \mu_0^2$$

since we must have $e/h_1 Z/h_0 = O(1)$ or smaller for Proposition 4.5 to apply, $B_Z(x)$ (proportional to $\sinh(\mu_Z(1-x))$) is effectively (or close to) a boundary layer adjacent to $x = 0$. We have then the following negative result validating the corresponding finding in [26]:

**Proposition 4.6.** *For a sufficiently high nonreceptor synthesis rate, the signaling gradient for a LRNO state of the wing imaginal disc is not sufficiently differentiating and hence not suitable for normal biological development.*

### 4.4.4 The General Case

Accurate numerical results for $\bar{b}_Z(x)$ and $\bar{R}_b$ have been obtained for different (uniform) nonreceptor synthesis rates (as characterized by the parameter $Z$). Some typical results are reported in Table 4.2 for the same ligand system as in Table 4.1. In addition to the parameter values given in Table 4.1, we now have additional parameters associated with the nonreceptors. For these, we assigned the following values in the illustrating examples:

$$j_{\deg} = k_{\deg}, \quad j_{on} = k_{on}, \quad j_{off} = 10k_{off}, \quad j_N = 10k_R$$

Similar to the uniform receptor synthesis rate $\bar{V}_R$, the uniform nonreceptor synthesis rate $\bar{V}_N$ is also not involved explicitly in computing the various solutions. It only appears in the ratio $Z = N_0/R_0 = \left(\bar{V}_N/j_N\right) / \left(\bar{V}_R/k_R\right)$ which is to be varied to indicate the level of the nonreceptor concentration.

It is evident from the results in Table 4.2 that $\bar{r}_b = \bar{r}_b(Z)$ and $B_Z(0) = B_e(0;Z)$ are quite accurate approximations of the corresponding numerical solutions for $\bar{R}_b(Z)$ and $\bar{b}_Z(0) = \bar{b}_e(0;Z)$ of the new model for the illustrative example. As such, the effects of nonreceptors are pretty much delineated by the LRNO approximate solution.

Table 4.2

$(g_1 = 0.2; \quad h_1 = 10, \quad f_1 = 0.01, \quad g_n = 10; \quad v_L = 0.05, \quad e = 2)$

| $Z$ | $\bar{R}_b$ | $\bar{r}_b$ | $\bar{b}_2(0,Z)$ | $B_2(0;Z)$ | $\bar{b}_1(0,0)$ | $B_1(0,0)$ |
|---|---|---|---|---|---|---|
| 0 | 0.3943 | 0.3948 | 0.11517 | 0.11643 | 0.05790 | 0.05821 |
| 1 | 0.0714 | 0.0725 | 0.07398 | 0.07471 | 0.05790 | 0.05821 |
| 2 | 0.1298 | 0.1290 | 0.05597 | 0.05642 | 0.05790 | 0.05821 |

From either the LRNO solution or the numerical solutions for the original nonlinear BVP, we see that the presence of an adequate concentration of nonreceptor would bring $\bar{b}_Z(0) = \bar{b}_e(0;Z)$ close to the wildtype solution $\bar{b}_1(0)$ $(= \left[\bar{b}_e(0;Z)\right]_{e=1,Z=0}$, not to be confused with $\left[\bar{b}_Z(0)\right]_{Z=1} = \left[\bar{b}_e(0;Z)\right]_{Z=1})$. This is also the case between $\bar{b}_Z(x)$ and $\bar{b}_1(x)$ but these two gradients do not coincide for any $Z > 0$ since the presence of nonreceptors generally renders $\bar{b}_Z(x)$ steeper and more convex than $\bar{b}_1(x)$ as shown in Figure 4.2 (even if it does not severely distort the slope and convexity of the wild-type gradients nonuniformly as the Hill function type feedback).

Furthermore, beyond an optimal level of $\bar{V}_N$, still higher receptor synthesis rate becomes deleterious as it would reduce the ectopic gradient concentration below the wildtype gradient $\bar{b}_1(x,0)$ and worsen the corresponding shape difference, possibly to an unacceptable level of robustness. For the illustrative example, the optimal $Z$ value that gives the smallest $\bar{R}_b$ is for $Z = 1.134...$ with an $\bar{R}_b = 0.0670...$ which is insignificantly below $\bar{R}_b = 0.0714...$ for $Z = 1$ but both are significantly below $\bar{R}_b = 0.1298...$ for $Z = 2$ (even if the latter is still below robustness threshold). For that reason, we do not calculate the solution for higher $Z$ values for this example.

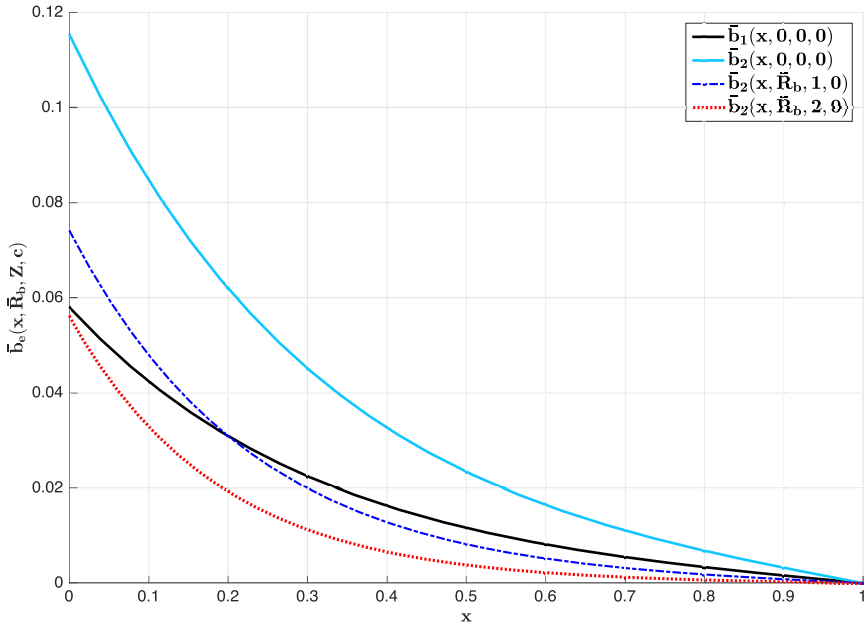


Figure 4.2: Effects of Nonreceptors

## 4.5 Non-receptors and Feedback

### 4.5.1 Nonreceptors and a Negative Feedback on Receptor Synthesis

So far we have seen that, by itself, negative feedback on receptor synthesis rate does not lead to a robust signaling Dpp gradient. Such a negative feedback generally reduces the signaling gradient slope steepness and flattens its curvature. That this negative feedback generally works against a robust signaling gradient is consistent with the finding in [26] (for a negative feedback of the Hill's function type). The situation is somewhat different with the presence of nonreceptors. An adequate concentration of nonreceptors would down regulate the concentration of the Dpp-Tkv complexes (which would otherwise be enhanced by sustained abnormal pertubations) so that $b_Z(x)$ is closer to the level of the wildtype

concentration. At the same time, the rate of nonreceptor synthesis needed to accomplish this may be sufficiently high that the corresponding gradient shape distortion results in an unacceptable robustness index of $R_b > 0.2$ (only for $c \geq 2$ in our illustrating example).

That a high concentration of nonreceptors would steepen the signaling gradient slope and rendering it more convex suggests a role for the negative feedback on receptor synthesis. Since the two instruments affect the slope and convexity in opposite direction, adding a negative feedback on receptor synthesis to a gradient system with a relatively high concentration of nonreceptors would ameliorate the shape distortion caused by nonreceptors and strive toward a robust signaling gradient. Here, we extend the previous model to examine the effects of adding (to the model with nonreceptors) the same nonlocal and spatially uniform negative feedback (4.11) on receptor synthesis rate. Similar to the findings in [26] for a Hill function type feedback, the presence of an $\bar{R}_b$-induced negative feedback will be seen to also ameliorate the excessive changes in slope and convexity induced by the presence of nonreceptors and to drive the signaling gradient toward the shape of the wild type signaling gradient.

Consider then the model (4.45)-(4.49) but now with a negative feedback of the form (4.3) on the receptor synthesis rate. In steady state, the problem can again be reduced similarly to a BVP for the corresponding free morphogen concentration denoted by $\bar{a}_{RZ}(x) \equiv \bar{a}_e(x; \bar{R}_b, Z)$:

$$\bar{a}''_{RZ} - \frac{\bar{\kappa}^2(\bar{R}_b) g_0 \bar{a}_{RZ}}{\alpha_0 + \zeta_0 \bar{a}_{RZ}} - \frac{Z g_1 \bar{a}_{RZ}}{\alpha_1 + \zeta_1 \bar{a}_{RZ}} + e\bar{v}_L H(-x) = 0. \tag{4.69}$$

$$\bar{a}'_{RZ}(-x_m) = 0, \qquad \bar{a}_{RZ}(1) = 0, \tag{4.70}$$

For this new problem, the steady state signaling gradient and unoccupied receptor gradient, $\bar{b}_{RZ}(x) \equiv \bar{b}_e(x, \bar{R}_b, Z)$ and $\bar{r}_{RZ}(x) \equiv \bar{r}_e(x, \bar{R}_b, Z)$, are given in terms of $\bar{a}_{RZ}(x)$ by

$$\bar{b}_{RZ}(x) = \frac{\bar{\kappa}^2(\bar{R}_b)\bar{a}_{RZ}}{\alpha_0 + \zeta_0 \bar{a}_{RZ}}, \qquad \bar{r}_{RZ}(x) = \frac{\bar{\kappa}^2(\bar{R}_b)\alpha_0}{\alpha_0 + \zeta_0 \bar{a}_{RZ}}. \tag{4.71}$$

$$\bar{c}_{RZ}(x) = \frac{\bar{a}_{RZ}(x)}{\alpha_1 + \zeta_1 \bar{a}_{RZ}(x)}, \qquad \bar{n}_{RZ}(x) = \frac{\alpha_1}{\alpha_1 + \zeta_1 \bar{a}_{RZ}(x)}, \tag{4.72}$$

where $\bar{\kappa}^2(\bar{R}_b)$ is given by (4.11)-(4.12) with $\bar{b}_R(x)$ replaced by $\bar{b}_{RZ}(x)$.

**Low Receptor and Nonreceptor Occupancy**

When both receptors and nonreceptors are in a state of low occupancy, we may linearize the ODE (4.69) to get

$$A''_{RZ} - \mu^2_{RZ} A_{RZ} + e\bar{v}_L H(-x) = 0, \tag{4.73}$$

for the LRNO free Dpp concentration $A_{RZ}$ with

$$\begin{aligned} \mu^2_{RZ} &\equiv \mu^2_R + Z\mu^2_1 = \bar{\kappa}^2(\bar{r}_b)\mu^2_0 + Z\mu^2_1 \\ &= \frac{\mu^2_0}{1 + c\bar{r}_b} + Z\mu^2_1 = \mu^2_R + Z\mu^2_1, \end{aligned} \tag{4.74}$$

having taken $m = 1$ in (4.11) as before. Here $\bar{\kappa}^2$ is consistently taken to be in terms of the LRNO approximation $\bar{r}_b$ of the robustness index $\bar{R}_b$.

The ODE (4.73) is augmented by the two end conditions (4.70) to form a two point BVP for $A_{RZ}(x)$. The exact solution for $A_{RZ}$ is

$$A_{RZ}(x) = \begin{cases} \frac{e\bar{v}_L}{\mu^2_{RZ}} \{1 - \frac{\cosh(\mu_{rZ})}{\cosh(\mu_{RZ}(1+x_m))} \cosh(\mu_{RZ}(x + x_m))\} & (-x_m \le x \le 0) \\ \frac{e\bar{v}_L}{\mu^2_{RZ}} \frac{\sinh(\mu_{RZ} x_m)}{\cosh(\mu_{RZ}(1+x_m))} \sinh(\mu_{RZ}(1 - x)) & (0 \le x \le 1) \end{cases}, \tag{4.75}$$

with

$$\bar{b}_{RZ}(x) \sim B_{RZ}(x) = \frac{\bar{\kappa}^2(\bar{r}_b)}{\alpha_0} A_{RZ}(x)$$
$$= \frac{\bar{\kappa}^2(\bar{r}_b) e\bar{\nu}_L}{\alpha_0 \mu_{RZ}^2} \frac{\sinh(\mu_{RZ} x_m)}{\cosh(\mu_{RZ}(1+x_m))} \sinh(\mu_{RZ}(1-x)) \qquad (0 \le x \le 1) \tag{4.76}$$

$$\bar{\kappa}^2(\bar{r}_b) = \frac{1}{1+c\bar{r}_b} \tag{4.77}$$

where $\mu_{RZ}$ is as given in (4.74). From the expression

$$\alpha_0 \bar{b}_{RZ}(0) \sim \bar{\kappa}^2(\bar{r}_b) A_{RZ}(0) = \frac{e\bar{v}_L}{\mu_{RZ}^2} \frac{\bar{\kappa}^2(\bar{r}_b) \sinh(\mu_{RZ} x_m)}{\cosh(\mu_{RZ}(1+x_m)))} \sinh(\mu_{RZ}),$$

we get for biologically typical values of $\mu_0^2$ and $\mu_1^2$ and sufficiently large value of $Z$ (so that $\mu_{RZ}^2 > 1$) $\bar{b}_{RZ}(0) \sim B_{RZ}(0)$ with

$$B_{RZ}(0) = \frac{\bar{\kappa}^2(\bar{r}_b)}{\alpha_0} A_{RZ}(0) = \frac{\bar{\kappa}^2(\bar{r}_b)}{\alpha_0} A_e(0; \bar{r}_b, Z)))$$
$$\sim \frac{\bar{\kappa}^2(\bar{r}_b) e\bar{v}_L}{\alpha_0 \mu_{RZ}^2} O(1) = \frac{e\bar{v}_L / g_0}{1 + Z\,(1+c\bar{r}_b)\,(h_1/h_0)} O(1). \tag{4.78}$$

In the absence of nonreceptors so that $Z = 0$, we already learned from a previous section that the only effect on robustness by a nonlocal spatially uniform negative feedback on receptor synthesis rate in steady state is a leveling and flattening of the shape of (the otherwise) ectopic signaling gradient without changing its magnitude. This negative effect on robustness is seen again from (4.76), (4.77) and (4.78) with $Z = 0$. On the other hand, the introduction of nonreceptors without a negative feedback on receptor synthesis would reduce the magnitude of the signaling gradient by a factor $1 + Z(1 + c\bar{r}_b)\,(h_1/h_0)$. Hence, an appropriate concentration of nonreceptors (e.g., $Z = 1$ in the normalized model) would

reduce the ectopicity to an acceptable level. However, a still higher concentration of nonreceptors would further reduce the gradient concentration and increase deviation from normal gradient in the opposite direction. Hence, there is an optimal $Z$ that would minimize the ectopicity of the signaling gradient

Presence of nonreceptors also induces a change of wildtype shape factor $\mu_0^2$ to $\mu_Z^2 = \mu_0^2 + Z\mu_1^2$ that would steepen the slope and increase the convexity of the ectopic signaling gradient shape. As such the presence of nonreceptors alone affect robustness both positively and negatively. However, in the presence of a moderate (steady state) concentration of nonreceptors, the role of the same effect on the gradient shape by a negative feedback on receptor synthesis rate now takes on the role of promoting robustness instead. The wildtype shape factor $\mu_0^2$ having been increased to $\mu_0^2 + Z\mu_1^2$ with the introduction of nonreceptors (and thereby steepening the shape of the gradients) is now ameliorated by the negative feedback on receptor synthesis rate given:

$$\mu_{RZ}^2 = \bar{\kappa}^2\mu_0^2 + Z\mu_1^2 = \frac{\mu_0^2}{1 + c\bar{r}_b} + Z\mu_1^2 < \mu_0^2 + Z\mu_1^2 = \mu_Z^2.$$

Whether we work with the LRNO approximation or not, the new shape factor $\mu_{RZ}^2$ (see (4.74)) is smaller than $\mu_Z^2 = \mu_0^2 + Z\mu_1^2$.

Furthermore, the benefits toward robustness from $c > 0$ is more than through the factor $(1 + c\bar{r}_b)^{-1}$ multiplying $\mu_0^2$; it also benefits from the same factor multiplying $Z$ on the right-hand side of (4.78) leading to a smaller $Z$ needed to attain the same reduction on the magnitude of the signaling gradient. We have then the following proposition when the system is in an LRNO state:

**Proposition 4.7.** *In the presence of an appropriate non-receptor synthesis rate, the (steady state limit of a) spatially uniform nonlocal negative feedback (4.11) on receptors reduces the*

*signaling gradient concentration and ameliorates the distortion of signaling gradient shape induced by the presence of nonreceptors.*

The mathematically rigorous results for $\bar{r}_b$ when the systems is in a state of LRNO are recorded in Table 4.3 below for different feedback strengths for the illustrative example to show their accuracy as approximations of the corresponding numerical solutions for the exact model.

Table 4.3

$(g_0 = g_1 = 0.2;\ \ h_0 = h_1 = 10,\ g_r = 1,\ \ g_n = 10;\ \ f_0 = 0.001,\ f_1 = 0.01, v_L = 0.05,\ \ e = 2)$

| $Z$ | $c$ | $k$ | $\bar{R}_k$ | $\bar{r}_b$ | $\bar{b}_{RZ}(0)$ | $B_{RZ}(0)$ | $\bar{b}_1(0)$ |
|---|---|---|---|---|---|---|---|
| 0 | 0 | 0 | 0.3943 | 0.3948 | 0.11517 | 0.11642 | 0.05790 |
| 0 | 1 | 5 | 0.3557 | 0.3569 | 0.10222 | 0.10364 | 0.05790 |
| 0 | 2 | 8 | 0.3269 | 0.3285 | 0.09407 | 0.09555 | 0.05790 |
| 1 | 0 | 0 | 0.0714 | 0.0725 | 0.07398 | 0.07471 | 0.05790 |
| 1 | 1 | 5 | 0.0619 | 0.0626 | 0.07550 | 0.05484 | 0.05790 |
| 1 | 2 | 8 | 0.0560 | 0.0566 | 0.06894 | 0.05407 | 0.05790 |
| 2 | 0 | 0 | 0.1298 | 0.1290 | 0.05597 | 0.05642 | 0.05790 |
| 2 | 1 | 5 | 0.1471 | 0.1461 | 0.05778 | 0.06657 | 0.05790 |
| 2 | 2 | 8 | 0.1683 | 0.1672 | 0.04463 | 0.05807 | 0.05790 |

**The General Case**

Accurate numerical results for $\bar{b}_{RZ}(x)$ and $\bar{R}_b$ of the original nonlinear BVP have also been obtained for different (spatially uniform) nonreceptor synthesis rates through the parameter $Z$. Some typical results are reported in Table 4.3 for the same wing imaginal disc as the ones for Tables 4.1 and 4.2.

The numerical results in Table 4.3 support our expectation that the LRNO solution constitutes an accurate approximation of the corresponding exact solution for the original nonlinear problem (4.69)-(4.70). For such cases, the effects of the $\bar{R}_b$-based (nonlocal spatially uniform) negative feedback (of the $\bar{R}_b$-based nonlocal type) on receptor synthesis rate are

pretty much delineated by the LRNO approximate solution. More specifically, our type of negative feedback on receptor synthesis rate in the presence of an adequate nonreceptor synthesis rate serves to ameliorate the ectopicity of the signaling gradient substantially by reducing gradient magnitude without distorting the wildtype gradient shape resulting in an acceptable value of the robustness index. The results in Table 4.3 also show that too high a concentration of non-receptors ($Z \geq 2$ in our example) would cause an excessive reduction of signal morphogen concentration and too severe a shape distortion to result in an unacceptable $\bar{R}_b$. With too high a non-receptor synthesis rate, more intense negative feedback on receptor synthesis rate may reduce ectopicity only a little or not at all, at least for the illustrating example. The corresponding graphs of $\bar{b}_{RZ}(x) = \bar{b}_e(x, \bar{R}_b, Z)$ for different $Z$ and $c$ in Figure 4.3 clearly show why robustness eventually deteriorates with increasing nonreceptor concentration.

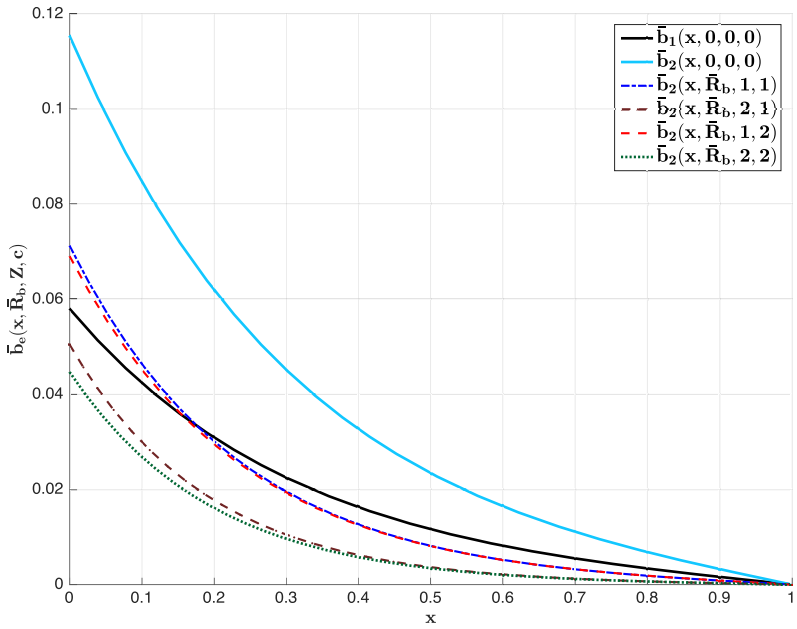


Figure 4.3: Effects of Negative Feedback on Receptor Synthesis for $Z > 0$

The findings above for the effects of nonreceptors with our $\bar{R}_b$-based negative feedback on receptor synthesis rate are generally consistent with the numerical experiments for the Hill function type negative feedback of [26]. Together, they suggest a substantive role for the down-regulation of signaling receptor synthesis rate in promoting robustness even if robustness cannot be attained with a feedback on receptor synthesis rate alone.

### 4.5.2 Feedback on Receptor and Nonreceptor Synthesis Rates

Up to now, models involving nonreceptors examine only the effects of synthesizing nonreceptors at a prescribed rate when the ligand synthesis rate becomes ectopic. In actual developments, genetic or epigenetic perturbations typically begin in the midst of wild-type development and the synthesis of signaling-inhibiting nonreceptors needed to counter the enhanced ligand synthesis for a robust development is stimulated by some kind of feedback mechanism. The existence of both inhibiting nonreceptors and the associated feedback process are well documented for the BMP family ligands that includes the Dpp ligand (see [45, 32] and elsewhere). Known nonreceptor type inhibitors include noggin, chordin, dally, follistatin, sog *and* various heparan sulfate proteoglycans. They are ubiquitous during wing imaginal disc and other biological developments, some prior to the onset of ectopic ligand synthesis [30, 48, 35, 46, 18, 3, 15, 44, 5]. A more biologically realistic model should allow for *i*) possible presence of nonreceptors prior to the onset of genetic or epi-genetic perturbations, and *ii*) a ($\bar{R}_b$-based) feedback process on non-receptor concentration for stimulation of an adequate synthesis rate of the signaling inhibiting non-receptors.

#### The Model

Since some form of feedback is needed to trigger additional signaling-inhibiting agents for robust developments, we pursue here one such feedback mechanism suggested by the simu-

lation results of [26], namely a positive feedback on nonreceptor synthesis rate to generate more inhibitors to limit signaling. Consistent with the $\bar{R}_b$-based feedback mechanism investigated here, we incorporate in the model (4.45)-(4.49) a positive feedback on nonreceptor synthesis rate of the form

$$V_N = \bar{V}_N + \hat{V}_N \left[R_b(t)\right]^s \tag{4.79}$$

with the model in the previous section corresponding to $\hat{V}_N = 0$ while the case $\hat{V}_N > 0$ offers a positive feedback instrument for generating more nonreceptors to inhibit ectopic signaling. As the system approaches steady state, $V_N(t)$ tends to a time independent synthesis rate:

$$V_N(t) \to \bar{V}_N + \hat{V}_N \left[\bar{R}_b\right]^s. \tag{4.80}$$

In susbsequent development, we limit our discussion to the special case of $s = 1$ (as we did in setting $m = 1$ for the negative feedback on receptor synthesis rate).

With the steady state positive feedback (4.80), the steady state system (4.69)-(4.71) is modified to read

$$\bar{a}''_{RN} - \frac{\bar{\kappa}^2(\bar{R}_b) g_0 \bar{a}_{RN}}{\alpha_0 + \zeta_0 \bar{a}_{RN}} - \frac{\bar{\kappa}_N^2(\bar{R}_b) g_1 \bar{a}_{RN}}{\alpha_1 + \zeta_1 \bar{a}_{RN}} + e\bar{v}_L H(-x) = 0, \tag{4.81}$$

$$\bar{a}'_{RN}(-x_m) = 0, \qquad \bar{a}_{RN}(1) = 0, \tag{4.82}$$

where

$$\bar{\kappa}^2(\bar{R}_b) = 1 + c\bar{R}_b, \qquad \bar{\kappa}_N^2(\bar{R}_b) = Z + \sigma \bar{R}_b, \tag{4.83}$$

(given $s = 1$) with

$$Z = \frac{\bar{V}_N/j_N}{\bar{V}_R/k_R}\,, \qquad \sigma = \frac{\hat{V}_N/j_N}{\bar{V}_R/k_R}. \tag{4.84}$$

The ectopic solution $\bar{a}_{RN}(x) = \bar{a}_e(x, \bar{R}_b, c, Z, \sigma)$ is equal to the wildtype solution $\bar{a}_1(x) = \bar{a}_e(x, \bar{R}_b, 0, 0, 0)$ for $e = 1$. The other related gradients are given by

$$\bar{b}_{RN}(x) = \frac{\bar{\kappa}^2(\bar{R}_b)\bar{a}_{RN}}{\alpha_0 + \zeta_0\bar{a}_{RN}}, \qquad \bar{r}_{RN}(x) = \frac{\bar{\kappa}^2(\bar{R}_b)\alpha_0}{\alpha_0 + \zeta_0\bar{a}_{RN}} \tag{4.85}$$

$$\bar{c}_{RN}(x) = \frac{\bar{\kappa}_N^2(\bar{R}_b)\bar{a}_{RN}}{\alpha_1 + \zeta_1\bar{a}_{RN}}, \qquad \bar{n}_{RN}(x) = \frac{\bar{\kappa}_N^2(\bar{R}_b)\alpha_1}{\alpha_1 + \zeta_1\bar{a}_{RN}} \tag{4.86}$$

For a particular wing imaginal disc at its early stages of development, it is clear from the model that robust development depends on 1) the nonreceptor synthesis rate prior to ectopic ligand synthesis characterized by the parameter $Z$, and 2) sensitivity to feedback on receptor and nonreceptor synthesis rates characterized by the parameters $c$ and $\sigma$, respectively. Numerical solutions for the relevant nonlinear BVP of our model have been obtained for our illustrating example and reported in Table 4.4 for some typical combinations of values for the parameters $Z,\ c$ and $\sigma$.

Table 4.4

$(g_0 = g_1 = 0.2;\ \ h_0 = h_1 = 10,\ g_r = 1,\ \ g_n = 10;\ \ f_0 = 0.001,\ f_1 = 0.01)$

| $Z$ | $c$ | $\sigma$ | $\bar{R}_k$ | $\bar{b}_2(0, \bar{R}_b, Z, c, \sigma)$ | $\bar{b}_2(0)$ | $\bar{b}_1(0)$ |
|---|---|---|---|---|---|---|
| 0 | 0 | 0 | 0.3943 | 0.1152 | 0.1152 | 0.0580 |
| 0 | 1 | 0 | 0.3557 | 0.1022 | 0.1152 | 0.0580 |
| 0 | 2 | 0 | 0.3269 | 0.0941 | 0.1152 | 0.0580 |
| 0 | 0 | 1 | 0.2569 | 0.1000 | 0.1152 | 0.0580 |
| 0 | 1 | 1 | 0.2284 | 0.0917 | 0.1152 | 0.0580 |
| 0 | 0 | 2 | 0.2003 | 0.0936 | 0.1152 | 0.0580 |
| 0 | 1 | 2 | 0.1576 | 0.0845 | 0.1152 | 0.0580 |
| 1 | 0 | 0 | 0.0714 | 0.0740 | 0.1152 | 0.0580 |
| 1 | 1 | 0 | 0.0619 | 0.0755 | 0.1152 | 0.0580 |
| 1 | 2 | 0 | 0.0560 | 0.0689 | 0.1152 | 0.0580 |
| 1 | 0 | 1 | 0.0679 | 0.0723 | 0.1152 | 0.0580 |
| 1 | 1 | 1 | 0.0608 | 0.0697 | 0.1152 | 0.0580 |
| 2 | 0 | 0 | 0.1298 | 0.0560 | 0.1152 | 0.0580 |
| 2 | 1 | 0 | 0.1471 | 0.0578 | 0.1152 | 0.0580 |
| 2 | 2 | 0 | 0.1683 | 0.0446 | 0.1152 | 0.0580 |
| 2 | 0 | 1 | 0.1529 | 0.0522 | 0.1152 | 0.0580 |
| 2 | 1 | 1 | 0.1774 | 0.0454 | 0.1152 | 0.0580 |

**Low Receptor and Nonreceptor Occupancy**

When both receptors and nonreceptors are in a state of low occupancy, we may linearize the ODE (4.69) to get

$$A''_{RN} - \mu^2_{RN} A_{RN} + e\bar{v}_L H(-x) = 0,$$

subject to the two end conditions (4.70) and with

$$\mu^2_{RN} = \mu^2_R + \mu^2_N = \bar{\kappa}^2(\bar{r}_b)\mu^2_0 + \bar{\kappa}^2_N(\bar{r}_b)\mu^2_1 = \frac{\mu^2_0}{1 + c\bar{r}_b} + \mu^2_1 \left(Z + \sigma\bar{r}_b\right), \tag{4.87}$$

where $m$ and $s$ in (4.11) and (4.80), respectively, have been taken to be 1 and $\bar{r}_b$ is the LRNO approximation of $\bar{R}_b$.

The exact solution for $A_{RN}(x) \equiv A_e(x, \bar{r}_b, Z, c, \sigma)$ is

$$A_{RN}(x) = \begin{cases} \frac{e\bar{v}_L}{\mu_{RN}^2}\{1 - \frac{\cosh(\mu_{RN})}{\cosh(\mu_{RN}(1+x_m))}\cosh(\mu_{RN}(x+x_m))\} & (-x_m \le x \le 0) \\ \frac{e\bar{v}_L}{\mu_{RN}^2}\frac{\sinh(\mu_{RN}x_m)}{\cosh(\mu_{RN}(1+x_m))}\sinh(\mu_{RN}(1-x)) & (0 \le x \le 1) \end{cases} \tag{4.88}$$

In the range $(0 \le x \le 1)$, we have

$$\begin{aligned} \bar{b}_{RN}(x) \sim B_{RN}(x) &= \frac{\bar{\kappa}^2(\bar{r}_b)}{\alpha_0}A_{RN}(x) \\ &= \frac{\bar{\kappa}^2(\bar{r}_b)e\bar{v}_L\sinh(\mu_{RN}x_m)}{\alpha_0\mu_{RN}^2\cosh(\mu_{RN}(1+x_m))}\sinh(\mu_{RN}(1-x)) \quad (0 \le x \le 1) \end{aligned} \tag{4.89}$$

where $\mu_{RN}^2$ is as given in (4.87). From the expression for

$$\begin{aligned} \alpha_0\bar{b}_{RN}(0) &= \bar{\kappa}^2(\bar{R}_b)\bar{a}_{RN}(0) \\ &\sim \bar{\kappa}^2(\bar{r}_b)A_{RN}(0) = \frac{e\bar{v}_L}{\mu_{RN}^2}\frac{\bar{\kappa}^2(\bar{r}_b)\sinh(\mu_{RN}x_m)}{\cosh(\mu_{RN}(1+x_m)))}\sinh(\mu_{RN}). \end{aligned} \tag{4.90}$$

we obtain

$$\begin{aligned} \bar{b}_{RN}(0) \;\sim\; B_{RN}(0) &= \frac{\bar{\kappa}^2(\bar{r}_b)}{\alpha_0}A_{RN}(0) = \frac{\bar{\kappa}^2(\bar{r}_b)e\bar{v}_L}{\alpha_0\mu_{RN}^2}O(1) \\ &= \frac{e\bar{v}_L/g_0}{1 + (1+c\bar{r}_b)\,(Z+\sigma\bar{r}_b)\,(h_1/h_0)}O(1) \end{aligned} \tag{4.91}$$

given $f_k \ll g_k$ for both $k = 0$ and 1. Correspondingly, we have

$$\frac{\bar{b}_{RN}(0)}{\bar{b}_1(0)} \;\sim\; \frac{B_{RN}(0)}{B_1(0)} = \frac{e}{1 + (1+c\bar{r}_b)\,(Z+\sigma\bar{r}_b)\,(h_1/h_0)}O(1). \tag{4.92}$$

Evidently, the presence on non-receptors (through a non-receptor synthesis rate) leads to a substantial reduction of the amplitude of the signaling gradient, easily offset the ectopicity factor caused by the enhanced ligand synthesis rate even for moderate values of the parameters of $Z$ and $\sigma$. Let's note two general effects of non-receptors:

1. Without non-receptors (corresponding to $Z = \sigma = 0$), negative feedback has no effect on the amplitude of the LRNO signaling gradient $B_{RN}(x)$.

2. In contrast, the dimensionless gradient shape parameter $\mu_{RN}$ is substantially affected by feedback on both receptor and non-receptor synthesis rate as evident from (4.87) taken in the form

$$\mu_{RN}^2 = \frac{\mu_0^2}{1 + c\bar{r}_b} + \mu_1^2 \left(Z + \sigma\bar{r}_b\right) \simeq \frac{h_0}{1 + c\bar{r}_b} + h_1 \left(Z + \sigma\bar{r}_b\right) \tag{4.93}$$

with the $\bar{\kappa}^2(\bar{R}_b)$ negative feedback on receptor synthesis rate offering a mechanism for ameliorating the shape distortion caused by a concentration of nonreceptors.

## 4.6 Feedback During the Transient Phase

Given the limited effectiveness of the steady state solution, we are led to investigate improved effectiveness of starting feedback during the transient phase of the development. After experimenting with different approaches as to when to apply the feedback adjustment, we have concluded that most likely a biological organism initiates an adjustment once the robustness index crosses a certain threshold. For our numerical results below, we implement the feedback during transient at the instant when the robustness index crosses the value 0.2.

### 4.6.1 Numerical Results

The following figures show the transient solutions of the three problems investigated in this chapter for several sets of parameter values:

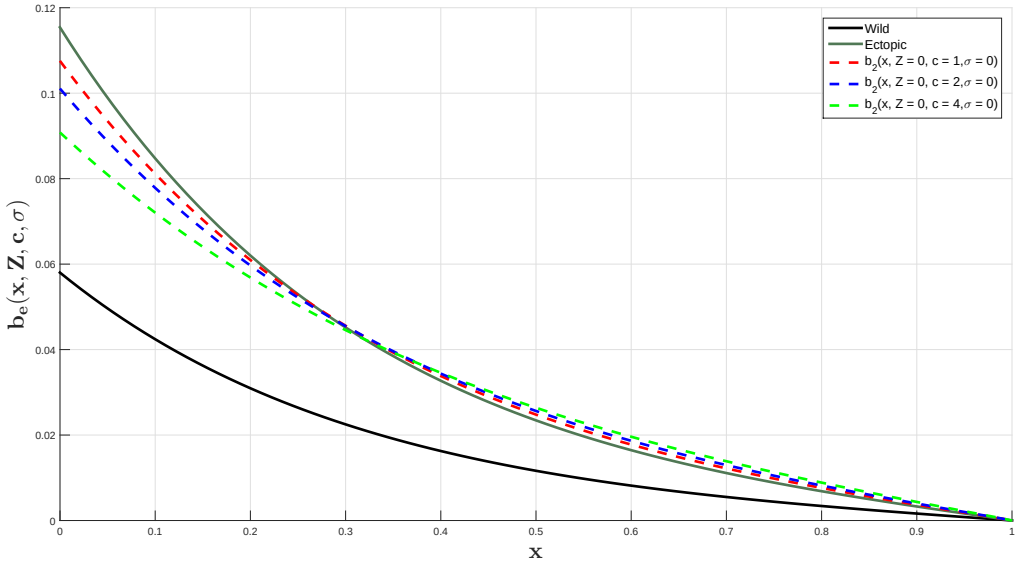


Figure 4.4: Negative Feedback on Receptor Synthesis Rate for Various $c$ Values (Transient)

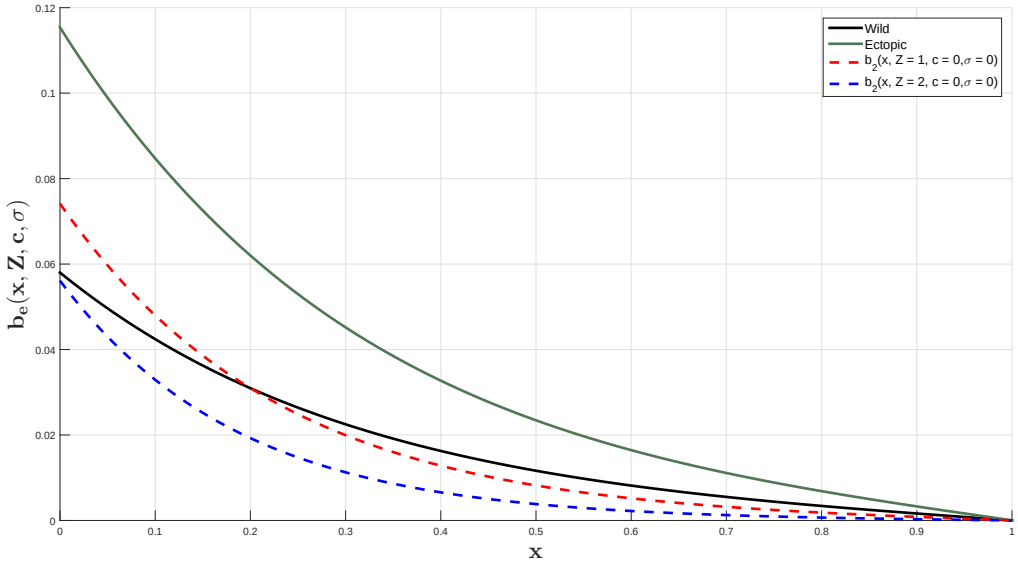


Figure 4.5: Effects of Non-receptors in Transient Phase

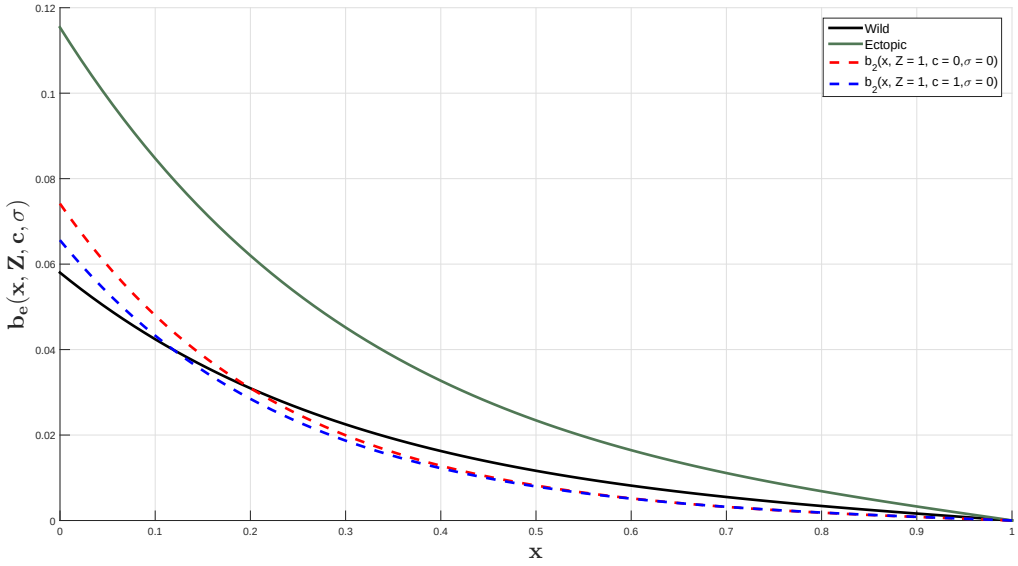


Figure 4.6: Non-receptors and Negative Feedback on Receptors (Transient)

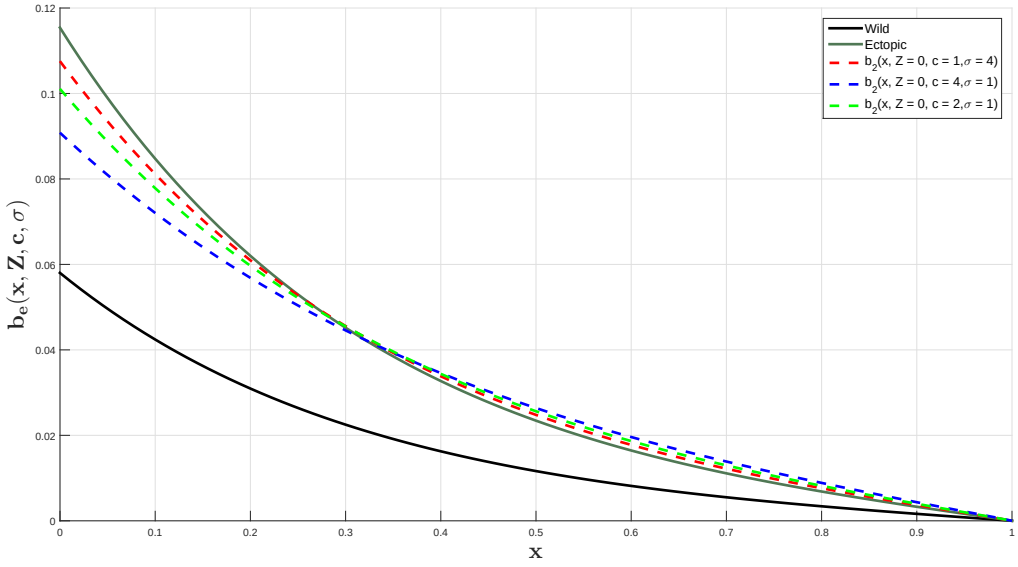


Figure 4.7: Feedback on Both Non-receptor and Receptor Synthesis Rates (Transient)

In Table 4.5 below we display the results of transient counterparts to the steady state ones shown in Table 4.4. We see that, though for some combinations of parameters, we have similar results, for others there is a drastic difference in fact favoring steady state approach over the transient. This could be due the fact that feedback during the transient phase

over-adjusts the ectopicity. Thus a more careful investigation is needed to determine the most optimal instance for applying the feedback adjustments.

Table 4.5 (Transient Feedback)

$(g_0 = g_1 = 0.2;\quad h_0 = h_1 = 10,\ g_r = 1,\quad g_n = 10;\quad f_0 = 0.001,\ f_1 = 0.01)$

| $Z$ | $c$ | $\sigma$ | $\bar{R}_k$ | $\bar{b}_2(0, \bar{R}_b, Z, c, \sigma)$ | $\bar{b}_2(0)$ | $\bar{b}_1(0)$ |
|---|---|---|---|---|---|---|
| 0 | 0 | 0 | 0.3939 | 0.1154 | 0.1152 | 0.0580 |
| 0 | 1 | 0 | 0.3718 | 0.1075 | 0.1152 | 0.0580 |
| 0 | 2 | 0 | 0.3512 | 0.1011 | 0.1152 | 0.0580 |
| 0 | 0 | 1 | 0.3939 | 0.1154 | 0.1152 | 0.0580 |
| 0 | 1 | 1 | 0.3718 | 0.1075 | 0.1152 | 0.0580 |
| 0 | 0 | 2 | 0.3939 | 0.1154 | 0.1152 | 0.0580 |
| 0 | 1 | 2 | 0.3718 | 0.1075 | 0.1152 | 0.0580 |
| 0 | 1 | 4 | 0.3718 | 0.1075 | 0.1152 | 0.0580 |
| 0 | 4 | 1 | 0.3138 | 0.0908 | 0.1152 | 0.0580 |
| 0 | 2 | 1 | 0.3512 | 0.1011 | 0.1152 | 0.0580 |
| 1 | 0 | 0 | 0.0712 | 0.0741 | 0.1152 | 0.0580 |
| 1 | 1 | 0 | 0.0504 | 0.0656 | 0.1152 | 0.0580 |
| 1 | 2 | 0 | 0.0573 | 0.0588 | 0.1152 | 0.0580 |
| 1 | 0 | 1 | 0.0677 | 0.0695 | 0.1152 | 0.0580 |
| 1 | 1 | 1 | 0.0697 | 0.0612 | 0.1152 | 0.0580 |
| 2 | 0 | 0 | 0.2367 | 0.0386 | 0.1152 | 0.0580 |

From the numerical results obtained, we conclude that the cases that are more interesting to be investigated further appear to be for $Z = 0$. The reason for this is that any non-receptors present in the organism must have been there to ensure proper wild type gradients. Any non-receptors needed to down-regulate the ectopic signaling gradient due to $e > 1$ starting at $t = 0$ should be induced by feedback.

## 4.7 Concluding Remarks

Though the conventional Hill function type negative feedback on receptor synthesis rate proves to be ineffective for the purpose of attaining robustness [28, 17, 26], we have shown that a spatially uniform feedback process based on a spanwise average of excess signaling can play such a role. With a simple iterative algorithms developed for the solution of specific integro-differential equation system for such a feedback mechanism, the results obtained for steady state gradient systems confirm that at least one feedback mechanism can be effective for ensuring robustness and suggest that many other effective feedback mechanisms are possible and should be investigated.

Given the limited effectiveness of the steady state solution, we investigate improved effectiveness of starting feedback during the transient phase of the development.

Overall, we have learned from this chapter that a spatially uniform negative feedback on receptor synthesis rate, though not at all useful, by itself, for promoting robustness (similar to the Hill function type approach), is necessary for attaining robustness in conjunction with a positive feedback on non-receptor synthesis rate with or without pre-existing concentration of non-receptors prior to the onset of ectopic ligand synthesis. Most results from the transient phase appear to be somewhat similar to that of the steady state approach.

# Chapter 5

# Conclusion

In this dissertation, we investigate feedback mechanisms for robust signaling gradients in biological tissue patterning. The findings of [26] served as a motivation for us to examine a new spatially uniform feedback mechanism distinctly different from the conventional spatially nonuniform Hill function approach. In Chapter 2, as a first step in our investigation, we applied the new feedback mechanism to the ligand synthesis rate. The results obtained in Chapter 2 confirmed that such feedback mechanism can be effective for ensuring robustness.

In Chapter 3, we complemented the investigation of feedback in steady state (the one in Chapter 2) by examining the effects of one or more feedback adjustments during the transient phase of the biological development. At the end of our examination, we concluded that feedback in transient is more favorable (than feedback in steady state) to robust development of a biological organism.

In Chapter 4, we investigated the feedback controls applied directly to the inhibiting agent, rather than by-passing it as we did in Chapters 2 and 3. Among the possible agents for achieving robustness that appear biologically realistic, nonreceptors appear to be ubiquitous for down-regulating signaling. Such down-regulation has already been observed and

investigated theoretically in [28, 29]. Hence, we examined the efficacy of our new feedback mechanism on the system that also includes nonreceptors. The main results obtained from Chapter 4 are: a spatially uniform negative feedback on receptor synthesis rate, though not at all useful, by itself, for promoting robustness (similar to the Hill function type approach), is needed for attaining robustness in conjunction with a positive feedback on non-receptor synthesis rate with or without pre-existing concentration of non-receptors prior to the onset of ectopic ligand synthesis. Implementation of the feedback during transient stages of the biological development produced similar results.

To the extent that spatially uniform feedback studied in this dissertation appears to hold more promise in ensuring the robustness of signaling gradients, it naturally paves the way to additional relevant investigations of other regulatory processes for Dpp gradient in wing imaginal disc as well as of other morphogen gradient systems based on similar (spatially uniform) feedback instruments.

Below are some additional possible spatially uniform feedback controls on a number of known regulatory processes that may promote robust signaling and should be investigated.

1. Positive Feedback on Ligand Degradation: It has been observed that introduction of polypeptide *noggin* (encoded by the *NOG gene*) binds and inactivates members of the transforming growth factor-beta (TGF-beta) superfamily signaling proteins, such as *bone morphogenetic proteins* (BMP). At the same time, an ectopic concentration of BMP causes significant up-regulation of Sox9 and Noggin expression [30, 45, 48]. By-passing the processes of ligand up-regulating noggin expression, we could model this reduction of available BMP molecules very crudely by a negative feedback on ligand synthesis rate. A somewhat more biologically realistic feedback process would be a positive feedback on the degradation rate constant $k_L$ as the reduction of ligand pertain to its concentration (and not its synthesis rate). For such a model, we would keep

the ligand synthesis rate for both the wild type and perturbed system unaffected by the robustness index but now with a positive feedback on the (free) ligand degradation rate.

2. Negative Feedback on the Signaling Complex Binding Rate: It is also known that over-expression of Dad (*Daughters against dpp*) blocks Dpp signaling activity (as seen from a lack of dpp target gene *optomotor blind* (omb)) and there is a negative feedback circuit in which Dpp induces expression of its own antagonist, Dad [40, 32]. (A similar observation has been made on the BMP antagonist Chordin [35, 46].) One important signaling activity that affects signaling gradient is the binding rate of the ligand with its signaling receptor.

3. Other Known Signaling Inhibiting Processes: Other possible feedback controls may come from modeling the following experimental observations:

    - Dpp represses the synthesis of its own receptor Tkv which in turn enhances Dpp destruction [27].
    - Wingless (Wg) represses its signaling receptor DFz2 but Dpp signaling mediated by DFz2 leads to stabilization of Wg rather than degradation [6].
    - Positive feedback on receptor-mediated degradation rate [7].
    - Dlp (Dally-like) has opposite effects at high and low levels of Wingless. Dlp promotes low-level Wingless activity but reduces high-level Wingless activity [18].

In reality, robust signaling gradients in the presence of genetic and epigenetic changes are likely to be the consequences of a combination of different feedback activities including those mentioned above. Understanding how robustness is attained is important to help explain the presence of elaborate regulatory schemes in morphogen systems. Feedback as a mean for promoting and attaining robustness of biological developments constitutes a rich area for theoretical and empirical research.

# Bibliography


[1] T. Akiyama, K. Kamimura, C. Firkus, S. Takeo, O. Shimmi, and H. Nakato. Dally regulates dpp morphogen gradient formation by stabilizing dpp on the cell surface. *Developmental Biology*, 313(1):408–419, 2008.

[2] H. Amann. On the existence of positive solutions of nonlinear elliptic boundary value problems. *Indiana University Mathematics Journal*, 21(2):125–146, 1971.

[3] H. Amthor, B. Christ, F. Rashid-Doubell, C.F. Kemp, E. Lang, and K. Patel. Follistatin regulates bone morphogenetic protein-7 (bmp-7) activity to stimulate embryonic muscle growth. *Developmental biology*, 243(1):115–127, 2003.

[4] M. Bernfield, M. Götte, P.W. Park, O. Reizes, M.L. Fitzgerald, J. Lincecum, and M. Zako. Functions of cell surface heparan sulfate proteoglycans. *Annual review of biochemistry*, 68(1):729–777, 1999.

[5] B. Biehs, V. Francois, and E. Bier. The drosophila short gastrulation gene prevents dpp from autoactivating and suppressing neurogenesis in the neuroectoderm. *Genes & Development*, 10(22):2922–2934, 1996.

[6] K.M. Cadigan, M.P. Fish, E.J. Rulifson, and R. Nusse. Wingless repression of drosophila frizzled 2 expression shapes the wingless morphogen gradient in the wing. *Cell*, 93(5):767–777, 1998.

[7] M.V. Cubellis, T.-C. Wun, and F. Blasi. Receptor-mediated internalization and degradation of urokinase is caused by its specific inhibitor pai-1. *The EMBO Journal*, 9(4):1079, 1990.

[8] A. Eldar, D. Rosin, B.Z. Shilo, and N. Barkai. Self-enhanced ligand degradation underlies robustness of morphogen gradients. *Dev. Cell*, 5:635–646, 2003.

[9] A. Eldar, B.Z. Shilo, and N. Barkai. Elucidating mechanisms underlying robustness of morphogen gradients. *Current opinion in genetics & development*, 14(4):435–439, 2004.

[10] E.V. Entchev, A. Schwabedissen, and M. Gonzalez-Gaitan. Gradient formation of the TGF-$\beta$ homolog Dpp. *Cell*, 103(6):981 – 91, 2000.

[11] M. Freeman. Feedback control of intracellular signaling in development. *Nature*, 408(6810):313–331, 2000.

[12] A.J. Giráldez, R.R. Copley, and S.M. Cohen. Hspg modification by the secreted enzyme notum shapes the wingless morphogen gradient. *Developmental cell*, 2(5):667–676, 2002.

[13] J.B. Gurdon and P.Y. Bourillot. Morphogen gradient interpretation. *Nature*, 413(6858):797, 2001.

[14] B. Houchmandzadeh, E. Wieschaus, and S. Leibler. Establishment of developmental precision and proportions in the early drosophila embryo. *Nature*, 415(6873):798–802, 2002.

[15] S.I. Iemura, T.S. Yamamoto, C. Takagi, H. Uchiyama, T. Natsume, S. Shimasaki, H. Sugino, and N. Ueno. Direct binding of follistatin to a complex of bone-morphogenetic protein and its receptor inhibits ventral and epidermal cell fates in early xenopus embryo. *Proceedings of the National Academy of Sciences*, 95(16):9337–9342, 1998.

[16] N.T. Ingolia. Topology and robustness in the drosophila segment polarity network. *PLoS biology*, 2(6):e123, 2004.

[17] M. Khong and F.Y.M. Wan. Negative feedback in morphogen gradients. *Frontiers Of Applied Mathematics*, pages 29–52, 2007.

[18] J. Kreuger, L. Perez, A.J. Giraldez, and S.M. Cohen. Opposing activities of dally-like glypican at high and low levels of wingless morphogen activity. *Developmental cell*, 7(4):503–512, 2004.

[19] T. Kushner, A. Simonyan, and F.Y.M. Wan. A new approach to feedback for robust signaling gradients. *Studies in Applied Mathematics*, 133(1):18–51, 2014.

[20] A. Lander, Q. Nie, B. Vargas, and F. Wan. Size-normalized robustness of dpp gradient in drosophila wing imaginal disc. *Journal of mechanics of materials and structures*, 6(1):321–350, 2011.

[21] A.D. Lander, W.-C. Lo, Q. Nie, and F.Y.M. Wan. The measure of success: constraints, objectives, and tradeoffs in morphogen-mediated patterning. *Cold Spring Harbor Perspectives in Biology*, 1(1):a002022, 2009.

[22] A.D. Lander, Q. Nie, and F.Y.M. Wan. Do morphogen gradients arise by diffusion? *Developmental cell*, 2(6):785–796, 2002.

[23] A.D. Lander, Q. Nie, and F.Y.M. Wan. Spatially distributed morphogen production and morphogen gradient formation. *Math. Biosci. Eng. (MBE)*, 2:239 – 262, 2005.

[24] A.D. Lander, Q. Nie, and F.Y.M Wan. Internalization and end flux in morphogen gradient formation. *Journal of Computational and Applied Mathematics*, 190(1):232–251, 2006.

[25] A.D. Lander, Q. Nie, and F.Y.M. Wan. Membrane-associated non-receptors and morphogen gradients. *Bulletin of Mathematical Biology*, 69:33–54, 2007.

[26] A.D. Lander, F.Y.M. Wan, and Q. Nie. Multiple paths to morphogen gradient robustness. *CCBS Preprint, University of California, Irvine*, 2005.

[27] T. Lecuit and S.M. Cohen. Dpp receptor levels contribute to shaping the dpp morphogen gradient in the drosophila wing imaginal disc. *Development*, 125(24):4901–4907, 1998.

[28] J. Lei, F.Y.M. Wan, A.D. Lander, and Q. Nie. Robustness of signaling gradient in drosophila wing imaginal disc. *Discrete and continuous dynamical systems. Series B*, 16(3):835, 2011.

[29] J. Lei, D. Wang, Y. Song, Q. Nie, and F.Y.M. Wan. Robustness of morphogen gradients with "bucket brigade" transport through membrane-associated non-receptors. *Discrete and continuous dynamical systems. Series B*, 18(3), 2013.

[30] D.A. Lim, A.D. Tramontin, J.M. Trevejo, D.G. Herrera, J.M. García-Verdugo, and A. Alvarez-Buylla. Noggin antagonizes bmp signaling to create a niche for adult neurogenesis. *Neuron*, 3(28):713–726, 2000.

[31] Y. Lou, Q. Nie, and F.Y.M. Wan. Effects of sog on dpp-receptor binding. *SIAM journal on applied mathematics*, 65(5):1748–1771, 2005.

[32] Y. Ogiso, K. Tsuneizumi, N. Masuda, M. Sato, and T. Tabata. Robustness of the dpp morphogen activity gradient depends on negative feedback regulation by the inhibitory smad, dad. *Development, growth & differentiation*, 53(5):668–678, 2011.

[33] J. Pentek, L. Parker, A. Wu, and K. Arora. Follistatin preferentially antagonizes activin rather than bmp signaling in drosophila. *Genesis*, 47(4):261–273, 2009.

[34] N. Perrimon and A.P. McMahon. Negative feedback mechanisms and their roles during pattern formation. *Cell*, 97(1):13–16, 1999.

[35] Y. Sasai, B. Lu, H. Steinbeisser, and E.M. De Robertis. Regulation of neural induction by the chd and bmp-4 antagonistic patterning signals in xenopus. *Nature*, 376(6538):333–336, 1995.

[36] D.H. Sattinger. Monotone methods in nonlinear elliptic and parabolic boundary value problems. *Indiana University Mathematics Journal*, 21(11):979–1000, 1972.

[37] A. Simonyan and F.Y.M. Wan. Transient feedback and robust signaling gradients. *International journal of numerical analysis and modeling*, 13(2):179–204, 2016.

[38] J. Smoller. *Shock Waves and Reaction-Diffusion Equations*. Springer Verlag New York, 2000.

[39] A.A. Teleman and S.M. Cohen. Dpp gradient formation in the drosophila wing imaginal disc. *Cell*, 103(6):971–980, 2000.

[40] K. Tsuneizumi, T. Nakayama, Y. Kamoshida, T.B. Kornberg, et al. Daughters against dpp modulates dpp organizing activity in drosophila wing development. *Nature*, 389(6651):627–631, 1997.

[41] G. von Dassow, E. Meir, E.M. Munro, and G.M. Odell. The segment polarity network is a robust developmental module. *Nature*, 406:188–192, 2000.

[42] F.Y.M. Wan. Cell-surface bound nonreceptors and signaling morphogen gradients. *Studies in Applied Mathematics*, 133(2):151–181, 2014.

[43] F.Y.M. Wan, C. Sanchez-Tapia, and A. Simonyan. Regulatory feedbacks on receptor and non-receptor synthesis for robust signaling. Under Preparation.

[44] X.P. Wang, M. Suomalainen, C.J. Jorgez, M.M. Matzuk, S. Werner, and I. Thesleff. Follistatin regulates enamel patterning in mouse incisors by asymmetrically inhibiting bmp signaling and ameloblast differentiation. *Developmental cell*, 7(5):719–730, 2004.

[45] B.K. Zehentner, A. Haussmann, and H. Burtscher. The bone morphogenetic protein antagonist noggin is regulated by sox9 during endochondral differentiation. *Development, growth & differentiation*, 44(1):1–9, 2002.

[46] J.L. Zhang, L.Y. Qiu, A. Kotzsch, S. Weidauer, L. Patterson, M. Hammerschmidt, W. Sebald, and T.D. Mueller. Crystal structure analysis reveals how the chordin family member crossveinless 2 blocks bmp-2 receptor binding. *Developmental cell*, 14(5):739–750, 2008.

[47] S. Zhou. *Extracellular diffusion creates the Dpp morphogen gradient of the Drosophila wing disc*. PhD thesis, University of California, Irvine, 2011.

[48] L.B. Zimmerman, J.M. De Jesus-Escobar, and R.M. Harland. The spemann organizer signal noggin binds and inactivates bone morphogenetic protein 4. *Cell*, 86:599–606, 1996.